Volume 69A
Number 1
Jan.–Feb. 1965

Physics and Chemistry

U.S. DEPARTMENT OF COMMERCE

SECTION A

JOURNAL OF RESEARCH

NATIONAL BUREAU OF STANDARDS

Journal of Research

of the

National Bureau of Standards

A. Physics and Chemistry

Jan.–Feb. • 1965

VOLUME • 69A

NUMBER • 1

Editor: C. W. Beckett

Associate Editors: D. D. Wagman
J. M. Richardson

Publication dates:
Feb. 1, Apr. 1, June 1, Aug. 1, Oct. 1, Dec. 1, 1965

JOURNAL OF RESEARCH

The National Bureau of Standards Journal of Research reports research and development in the fields of activity shown at right. Also included from time to time are survey articles on topics closely related to the Bureau's scientific and technical program.

The Journal is published in four separate sections as follows:

A. Physics and Chemistry

Contains papers of interest primarily to scientists working in these fields. Issued six times a year. Annual subscription: domestic, $4.00; foreign, $4.75. Single copy, 70d.

B. Mathematics and Mathematical Physics

Presents studies and compilations designed mainly for the mathematician and the theoretical physicist. Issued quarterly. Annual subscription: domestic, $2.25; foreign, $2.75. Single copy, 75c.

C. Engineering and Instrumentation

Reports research and development results of interest chiefly to the engineer and the applied scientist. Issued quarterly. Annual subscription: domestic, $2.25; foreign, $2.75. Single copy, 75c.

D. Radio Science (formerly Radio Propagation)

Published in cooperation with U.S. National Committee of URSI. Presents papers in radio propagation, communications, and radio science generally. Issued monthly. Annual subscription: domestic, $9.00; foreign, $11.50. Single copy, $1.00.

The National Bureau of Standards is a principal focal point in the Federal Government for assuring maximum application of the physical and engineering sciences to the advancement of technology in industry and commerce. Its responsibilities include development and maintenance of the national standards of measurement, and the provision of means for making measurements consistent with those standards; determination of physical constants and properties of materials; development of methods for testing materials, mechanisms, and structures, and making such tests as may be necessary, particularly for government agencies; cooperation in the establishment of standard practices for incorporation in codes and specifications; advisory service to government agencies on scientific and technical problems; invention and development of devices to serve special needs of the Government; assistance to industry, business and consumers in the development and acceptance of commercial standards and simplified trade practice recommendations; administration of programs in cooperation with United States business groups and standards organizations for the development of international standards of practice; and maintenance of a clearinghouse for the collection and dissemination of scientific, technical, and engineering information.

Institute for Basic Standards. Electricity. Metrology. Heat. Radiation Physics. Mechanics. Applied Mathematics. Atomic Physics. Physical Chemistry. Laboratory Astrophysics.* Radio Standards Laboratory: Radio Standards Physics; Radio Standards Engineering.** Office of Standard Reference Data.

Institute for Materials Research. Analytical Chemistry. Polymers. Metallurgy. Inorganic Materials. Reactor Radiations. Cryogenics.** Office of Standard Reference Materials.

Central Radio Propagation Laboratory.** Ionosphere Research and Propagation. Troposphere and Space Communications. Radio Systems. Upper Atmosphere and Space Physics.

Institute for Applied Technology. Textiles and Apparel Technology Center. Building Research. Industrial Equipment. Information Technology. Performance Test Development. Instrumentation. Transport Systems. Office of Technical Services. Office of Weights and Measures. Office of Engineering Standards. Office of Industrial Services.

*JILA Group, Joint Institute for Laboratory Astrophysics of the University of Colorado.
**Located at Boulder, Colo.

U.S. DEPARTMENT OF COMMERCE
Luther H. Hodges, Secretary

NATIONAL BUREAU OF STANDARDS
A. V. Astin, Director

Order all publications from the Superintendent of Documents
U.S. Government Printing Office, Washington, D.C., 20402

Use of funds for printing this publication approved by the Director of the Bureau of the Budget (June 19, 1961).

JOURNAL OF RESEARCH of the National Bureau of Standards—A. Physics and Chemistry
Vol. 69A, No. 1, January–February 1965

Heat of Decomposition of Sodium and Potassium Chlorate

Alexis A. Gilliland and Donald D. Wagman

(September 29, 1964)

The heats of decomposition of sodium and potassium chlorate into their respective chlorides have been determined in a bomb calorimeter. The processes may be represented by the equations:

$$NaClO_3(c) = NaCl(c) + 3/2\ O_2(g)$$
$$\Delta H°\ (25\ °C) = -45.76 \pm 0.17\ kJ/mole$$
$$= -10.94 \pm 0.04\ kcal/mole$$
$$KClO_3(c) = KCl(c) + 3/2\ O_2(g)$$
$$\Delta H°\ (25\ °C) = -38.25 \pm 0.30\ kJ/mole$$
$$= -9.16 \pm 0.07\ kcal/mole.$$

Combination of these data with the heats of formation of NaCl(c) and KCl(c) gives -87.33 ± 0.07 kcal/mole and -95.23 ± 0.10 kcal/mole for the standard heats of formation of $NaClO_3(c)$ and $KClO_3(c)$, respectively, at 25° C.

1. Introduction

This investigation was carried out in the Thermochemistry Section of the National Bureau of Standards, as part of a program currently in progress on the determination of the thermodynamic properties of the "light element" compounds. Although sodium and potassium chlorate are well known, considerable uncertainty exists in the values of the heats and free energies of formation.

2. Materials

The sodium chlorate and potassium chlorate were reagent-grade materials which were twice recrystallized from water. They were dried at 120 °C, ground, and stored in a desiccator over magnesium perchlorate. Tests for chloride ion in the recrystallized samples were negative.

The benzoic acid was NBS Standard Sample 39h. Samples of the same material were used for both the calibration and decomposition experiments.

The oxygen was freed from traces of combustible materials and of carbon dioxide by passing it successively though (1) a tube packed with copper oxide and heated to 600 °C, and (2) an absorber containing Ascarite. No attempt was made to remove traces of nitrogen.

3. Units of Energy and Molecular Weights

The unit of energy is the joule; for conversion to the conventional thermochemical calorie, one calorie is taken as 4.1840 J.

All atomic weights were taken from the 1961 International Table of Atomic Weights [1].[1]

[1] Figures in brackets indicate the literature references at the end of this paper.

4. Apparatus and Procedure

The calorimeter was of the Dickinson isothermal-jacket type which has been previously described [2, 3]. The temperature of the calorimeter jacket was controlled within ±0.002 °C at about 25 °C by means of a thermostat. The calorimeter temperatures were measured by means of a platinum resistance thermometer and a Mueller-type bridge; timing of the experiments was made by reference to the NBS standard second signals.

The bomb was of the NBS twin-valve type, similar to that which has been described [3]; its volume was 365.9 ml. It was modified slightly for the $NaClO_3$ and $KClO_3$ decomposition experiments in that two crucibles were used, one being mounted about 1 mm directly above the other. The sample of chlorate was weighed into the upper crucible, while the benzoic acid pellet, approximately 0.5 g, was weighed into the lower crucible. Ignition was accomplished by means of an electrically heated iron-wire fuse which was placed in contact with the benzoic acid pellet. Care had to be taken to ensure that the iron-wire fuse was not shorted out by contact with either of the platinum crucibles. One milliliter of water was placed in the bomb, which was then sealed, flushed with oxygen, and filled with oxygen to a pressure of 30 atm at 25 °C.

The details of the calorimetric procedure have been described [3, 4]. The heat evolved by burning the benzoic acid was sufficient to decompose the $NaClO_3$ and $KClO_3$ samples, leaving a mass of fused NaCl or KCl in the crucible. In each case the combustion products were analyzed, to determine how completely the chlorate had decomposed to the chloride. The total mass of carbon dioxide was determined by collecting the dry gas in a weighed absorption tube containing Ascarite. The material remaining

in the bomb was washed into a flask, and the amount of chloride ion determined by titration with standard $AgNO_3$, using fluorescein as the indicator [5]. The reaction went to completion, except for two cases indicated in the tables.

The calorimeter system was calibrated by a series of combustion experiments with benzoic acid, NBS Standard Sample 39h. The mass of benzoic acid (about 0.52 g) was chosen because it was sufficient for the $NaClO_3$ and $KClO_3$ decomposition experiments, and it was desirable to duplicate as nearly as possible the initial and final calorimeter temperatures.

5. Results and Calculations

The results of the calibration experiments with benzoic acid are given in table 1, where ΔRc is the corrected rise in temperature of the calorimetric system [6], (as measured on the particular thermometer and bridge), m_s is the mass of benzoic acid corrected to weigh in vacuo, q_i is the ignition energy from combustion of the iron-wire fuse, and q_N is the energy evolved by the formation of nitric acid from traces of nitrogen in the bomb. The quantity WC is the Washburn correction [6, 7] applied here to convert the reactants and products from their thermodynamic standard states into the actual conditions of the bomb process. The quantity Δe is the deviation in energy equivalent of the actual calorimeter system from that of the "standard" system, which in this instance was taken to include 0.515 g of benzoic acid.

TABLE 1

Expt. No.	ΔR_c	q_i	q_N	m_s	WC	E_s
	Ohm	*J*	*J*		*J*	*J/ohm*
1	0.101535	34.0	4.4	0.51560	9.2	134,597
2	.101860	33.1	5.8	.51708	9.3	134,557
3	.101796	35.3	4.2	.51665	9.3	134,536
4	.101121	34.8	4.6	.51361	9.2	134,638
5	.101531	34.4	4.4	.51557	9.2	134,598
6	.101369	35.3	6.0	.51461	9.2	134,587
7	.101957	34.0	5.2	.51759	9.3	134,565
Mean						134,583
Standard deviation of the mean						±25

The heat of combustion of benzoic acid for the standard bomb process, $-\Delta E_B(25\ °C)$ was taken as 26434.0 J/g. This value was corrected to give $-\Delta E°(25\ °C) = 26413.3$ J/g for the heat of combustion at constant volume, for the reactants and products in their thermodynamic standard states.

The energy equivalent of the "standard" calorimetric system for the temperature interval of 24 to 25 °C is obtained by:

$$E_s(25\ °C) = \frac{(26{,}413.3\ m_s + q_i + q_n + \mathrm{WC}) - \Delta e}{\Delta Rc}.$$

The results of the experiments on the decomposition of $NaClO_3$ are given in table 2, for $KClO_3$ in table 3. The value obtained for the standard

TABLE 2

Expt. No.	ΔRc	Δe	q_i	q_N	q_{BA}	WC	$NaClO_3$	$-\Delta E°$ (25 °C)
	Ohm	*J/ohm*	*J*	*J*	*J*	*J*	*Mole*	*kJ/mole*
1	0.110907	26.2	33.6	4.9	13,613.2	24.2	0.0251582	49.805
2	.110380	26.6	33.6	4.9	13,609.7	23.9	.02400*	49.412
3	.111061	26.6	33.1	1.3	13,635.3	24.5	.0255067	49.222
4	.111263	26.6	43.3	1.3	13,648.0	25.0	.0255270	49.332
5	.110561	26.5	44.3	1.3	13,545.3	24.6	.0255452	49.594
6	.111243	26.6	42.7	1.3	13,642.5	24.7	.0255149	49.500
Mean								49.478
Standard deviation of the mean								±0.168

*By analysis.

TABLE 3

Expt. No.	ΔRc	Δe	q_i	q_N	q_{BA}	WC	$KClO_3$	$-\Delta E°$ (25 °C)
	Ohm	*J/ohm*	*J*	*J*	*J*	*J*	*Mole*	*kJ/mole*
1	0.107426	19.1	34.8	4.9	13,593.6	20.9	0.0190032	42.377
2	.107643	20.0	36.4	4.9	13,583.3	21.5	.0199302	42.288
3	.107543	20.1	35.0	4.9	13,565.9	21.9	.0200348	42.311
4	.108517	20.5	36.8	4.9	13,766.3	20.9	.0187698	41.434
5	.105985	18.0	35.1	4.9	13,514.1	19.2	.0164333	42.122
6	.108117	23.6	34.8	4.9	13,585.4	22.8	.02172*	41.668
7	.109033	22.5	35.1	4.9	13,751.3	22.1	.0207571	41.571
Mean								41.967
Standard deviation of the mean								±0.300

*By analysis.

constant-volume process at 25 °C is given by the relationship:

$$-\Delta E^\circ(25\ ^\circ C)=\frac{(Es+\Delta e)\Delta Rc-q_i-q_n-q_{BA}-\mathrm{WC}}{\text{mole } NaClO_3}$$

and may be represented by the equation:

$$NaClO_3(c)=NaCl(c)+3/2\ O_2(g)$$

$$\Delta E^\circ(25\ ^\circ C)=-49.48\pm0.17\ \text{kJ/mole}. \qquad (1)$$

For $KClO_3$, the same relationship applies for the standard constant-volume process and for the equation:

$$KClO_3(c)=KCl(c)+3/2\ O_2(g)$$

$$\Delta E^\circ(25\ ^\circ C)=-41.97\pm0.30\ \text{kJ/mole}. \qquad (2)$$

The results of eqs (1) and (2) were corrected to constant pressure at 25 °C, with $R=8.3143$ J/deg mole;

$$\Delta H^\circ(25\ ^\circ C)=\Delta E^\circ+P\Delta V=\Delta E^\circ+\Delta nRT$$

for eq (1) $\Delta H^\circ(25\ ^\circ C)=-45.76\pm0.28$ kJ/mole,

$=-10.94\pm0.07$ kcal/mole,

for eq (2) $=-38.25\pm0.42$ kJ/mole,

$=-9.16\pm0.10$ kcal/mole.

The uncertainty intervals for the measured heats have been taken as twice the overall standard deviation of the mean, based on the sum of the variances from the calibration and reaction experiments and reasonable estimates for other errors.

The heat of formation of NaCl(c) has been taken as −98.232 kcal/mole [8] and the heat of formation of KCl(c) has been taken as −104.175 kcal/mole [8]. From these values and the heats of decomposition corresponding to eqs (1) and (2) the following values have been obtained:

$NaClO_3(c)$, $\Delta Hf^\circ(25\ ^\circ C)=-87.29\pm0.07$ kcal/mole;

$KClO_3(c)$, $\Delta Hf^\circ(25\ ^\circ C)=-95.02\pm0.10$ kcal/mole.

6. Discussion

The heat of decomposition of $KClO_3(c)$ has been measured by Thomsen [10]; Frankland [11]; Hofmann and Marin [12]; Wöhler and Schuff [13]; and Vorob'ev, Privalova, and Huang Li-Tao [14]. Thomsen obtained the decomposition by burning H_2 in O_2 in the presence of $KClO_3$, while Hofmann and Marin produced decomposition in a bomb by burning paraffin oil. Vorob'ev et al., produced decomposition by electrical heating of a bomb containing $KClO_3$ to which MnO_2 had been added to facilitate decomposition. No details of Wöhler and Schuff's procedure are available.

Thomsen [10] and Berthelot [9] determined the heat of formation of $HClO_3(aq)$ by measuring the heat of reaction of $SO_2(aq)$ with $HClO_3(aq)$ to form $H_2SO_4(aq)+HCl(aq)$. These data yield values of ΔHf° for $HClO_3(aq)=-32.5$ and -27.4 kcal/mole, respectively. Taking the heat of neutralization of $HClO_3(aq)$ to be the same as that for $HNO_3(aq)$ (see Thomsen [10]) and the heat of solution of $KClO_3(c)$ to be +9.9 kcal [16] we obtain −102.5 and −97.4 kcal/mole for the heat of formation of $KClO_3(c)$. The results of the various investigations on $KClO_3$ are compared with present work in table 4.

The only measurements on $NaClO_3(c)$ are those of Vorob'ev et al., who reported a heat of decomposition of −12.5 kcal/mole. From this we compute the heat of formation to be −88.94 kcal/mole, whereas the value obtained here is −87.38 kcal/mole.

TABLE 4

Decomposition of $KClO_3(c)$, kcal/mole

Investigator	$\Delta H_{decomp}(25\ ^\circ C)$	$\Delta Hf^\circ(25\ ^\circ C)$
Berthelot		−97.4
Thomsen	−9.71	−94.67
Thomsen		−102.5
Frankland	−4.3	−100.8
Hofmann et al	−11.2	−93.0
Wöhler et al	−10.2	−94.0
Vorob'ev et al	−11.6	−97.69
This work	−9.16	−95.25

Brönsted [15], from EMF data, obtained for the following reaction:

$$NaClO_3(c)+KCl(c)\rightarrow NaCl(c)+KClO_3(c)$$
$$\Delta H=-1.52\ \text{kcal/mole}.$$

Using the recently selected values for NaCl(c) and KCl(c) [17], −98.27 and −104.39 kcal/mole, we obtain:

$$\Delta Hf^\circ KClO_3(c)-\Delta Hf^\circ\ NaClO_3(c)=-7.64\ \text{kcal/mole}.$$

The result of our present investigation yields −7.73 kcal/mole for this difference.

The consistency of the present results may also be demonstrated by calculation of the heat of formation of ClO_3^- (aq) ion from the heats of solution of the chlorates [16] and the values of ΔHf° for $Na^+(aq)$ and $K^+(aq)$ [17], −57.39 and −60.32 kcal/mole, respectively. We calculate the following:

$$NaClO_3(c)\rightarrow NaClO_3(aq,\ \text{inf diln})$$
$$\Delta H^\circ=5.191\ \text{kcal/mole}$$
$$\Delta Hf^\circ ClO_3^-(aq)=-24.71\ \text{kcal/mole}$$
$$KClO_3(c)\rightarrow KClO_3(aq,\ \text{inf diln})$$
$$\Delta H^\circ=9.89\ \text{kcal/mole}$$
$$\Delta Hf^\circ ClO_3^-(aq)=-24.81\ \text{kcal/mole}.$$

This agreement is well within the uncertainties of the various combined experimental data.

7. References

[1] A. E. Cameron and E. Wichers, J. Am. Chem. Soc. **84,** 4175 (1962).
[2] J. R. Eckman and F. D. Rossini, BS J. Research **3,** 597 (1929) RP111.
[3] E. J. Prosen and F. D. Rossini, J. Res. NBS **27,** 289 (1941) RP1420.
[4] W. H. Johnson, E. J. Prosen, and F. D. Rossini, J. Res. NBS **35,** 141 (1945) RP1665.
[5] I. M. Kolthoff, Chem. Revs. **16,** 87 (1935).
[6] E. J. Prosen, Chapter 6 in Experimental Thermochemistry, F. D. Rossini, ed. (Interscience Publishers, Inc., New York, N.Y., 1956).
[7] E. W. Washburn, BS J. Research **10,** 525 (1933) RP546.
[8] F. D. Rossini, D. D. Wagman, W. H. Evans, S. Levine, and I. Jaffe, Selected values of chemical thermodynamic properties, NBS Circ. 500. (U.S. Government Printing Office, Washington 25, D.C., 1952).
[9] M. Berthelot, Ann. chim. Phys. [5] **10,** 377 (1877).
[10] J. Thomsen, Thermochemische Untersuchungen. Band II, p. 138 [Verlag J. A. Booth Leipzig (1882–1886)].
[11] E. Frankland, Phil. Mag. [4] **32,** 182 (1866).
[12] K. Hofmann and P. Marin, Sitzber preuss. Akad. Wiss. Physik. Math Klasse **1932,** 448.
[13] L. Wöhler and W. Schuff, Z. anorg. Chem. **209,** 33 (1932).
[14] A. F. Vorob'ev, N. M. Privalova and Huang Li-Tao, Vestn. Mosk. Univ., Ser. II, Khim. **18,** (6) 27 (1963).
[15] J. N. Brönsted, Z. phys. Chem. **80,** 206 (1912).
[16] V. B. Parker Thermal properties of aqueous uniunivalent electrolytes, NBS Monograph No. 82 (1964).
[17] W. H. Evans (private communication).

(Paper 69A1–320)

JOURNAL OF RESEARCH of the National Bureau of Standards—A. Physics and Chemistry
Vol. 69A, No. 1, January–February 1965

Application of Precise Heat-Capacity Data to the Analysis of the Temperature Intervals of the NBS (1955) and the International Practical Temperature Scales in the Region of 90 °K

George T. Furukawa and Martin L. Reilly

(September 4, 1964)

A method is presented for analyzing the temperature intervals of the NBS (1955) temperature scale and the International Practical Temperature Scale (IPTS). Values of dT/dR as a function of resistance are derived from equations of dQ/dR and dQ/dT, obtained from precise heat-capacity data (better than ± 0.02 percent) by the method of least squares. An adjusted temperature scale is obtained by integration of the values of dT/dR relative to a reference temperature and the corresponding resistance of the thermometer. The results of the adjusting process in the neighborhood of the oxygen point (90.18 °K) are discussed and compared with the existing temperature scales. The derived temperature scale was found to be similar to the scales maintained by the Pennsylvania State University (PSU), the Physico-Technical and Radio-Technical Measurements Institute (PRMI), and the National Physical Laboratory (NPL) from the upper limits of these scales, near 90 °K, down to 50 °K. The adjusting method presented is limited by the uncertainty of formulation of dQ/dR and dQ/dT and the derived temperature scale is limited by the accumulated uncertainty in the integral of dT/dR.

1. Introduction

The International Practical Temperature Scale (IPTS) [1] [1] is defined between −183 and 630 °C in terms of the resistance of platinum thermometers of specified characteristics, four fixed points (the triple point of water and the normal boiling points of oxygen, water, and sulfur), and two interpolation formulas (quadratic above and quartic below 0 °C). In the region from 10 to 90 °K a provisional temperature scale has been maintained at the National Bureau of Standards in terms of a set of platinum resistance thermometers. The thermometers now being used to maintain the NBS provisional scale are "two generations" removed from the original thermometers that were compared directly with a helium-gas thermometer in 1939 [2]. The present NBS provisional temperature scale is designated NBS (1955) and is defined to be 0.01 deg lower than the NBS (1939) scale [2].

Since 1939, other laboratories have also established independent temperature scales between 10 and 90 °K, based on gas thermometry and maintained by means of platinum resistance thermometers. They are California Institute of Technology in Pasadena, Calif. [3], Pennsylvania State University in University Park, Pa. [4], Physico-Technical and Radio-Technical Measurements Institute in Moscow (U.S.S.R.) [5], and National Physical Laboratory in Teddington (U.K.) [6]. (Henceforth, the temperature scales established by the above laboratories will be referred to as CIT, PSU, PRMI, and NPL scales, respectively.) These temperature scales have been shown to be in agreement within 0.02 deg over most of the 10 to 90 °K range after adjustments are made to the common oxygen-point value [3, 7].

Prior to 1939, results of comparison of platinum-resistance thermometers with a helium-gas thermometer were reported between 14 and 90 °K by Henning and Otto [8] and between 15 and 83 °K by Keesom and Bijl [9]. No accurate comparison of these temperature scales can be made with existing scales.

Although the NBS (1955) scale was designed to join the IPTS smoothly, the results of heat-capacity measurements made at NBS and elsewhere have consistently indicated irregularities in the region where the two temperature scales join, and in certain other regions of the NBS (1955) scale, that cannot be attributed to measurement errors. Since the heat-capacity determinations are concerned with temperature differences, any short-range variations in the "size of the degree" given by the resistance (R)-temperature (T) relation of the thermometer can be detected. If these variations occur gradually over a broad temperature range, the present techniques used in heat-capacity determinations alone will not indicate any irregularities in the temperature scale.

A pattern of well defined irregularities has been found to exist in the relative deviations of the experimental data from an equation composed of a linear combination of Debye and Einstein heat-capacity functions which have been fitted to the data by the method of least squares. A composite deviation plot for 11 independent sets of NBS data each fitted by such an equation is shown in figure 1. (A set of

[1] Figures in the brackets indicate the literature references given at the end of this paper.

data consists of the measurements of energy increments and the corresponding thermometer resistances from about 15 to 380 °K obtained in the heat-capacity determinations on the empty vessel or on the vessel with sample and analyzed as a single set.) Three different calorimetric apparatus were used over the period of time in which these experimental data were obtained and a different capsule-type platinum resistance thermometer was used with each apparatus. The thermometers were calibrated at the NBS, the first (L–18) in 1943, the second (769894) in 1950, and the third (1057849) in 1953. Deviation curves of the data from simpler equations, such as a single Debye heat-capacity function or a cubic equation, exhibit irregularities at the same temperatures as shown in figure 1. The similarity of the irregularities observed in different measurements and equations used in analyzing the data indicate that the temperature scales as represented by NBS (1955)—IPTS scales do not have uniform temperature intervals with respect to the thermodynamic temperature scale, particularly in the region of the oxygen point.

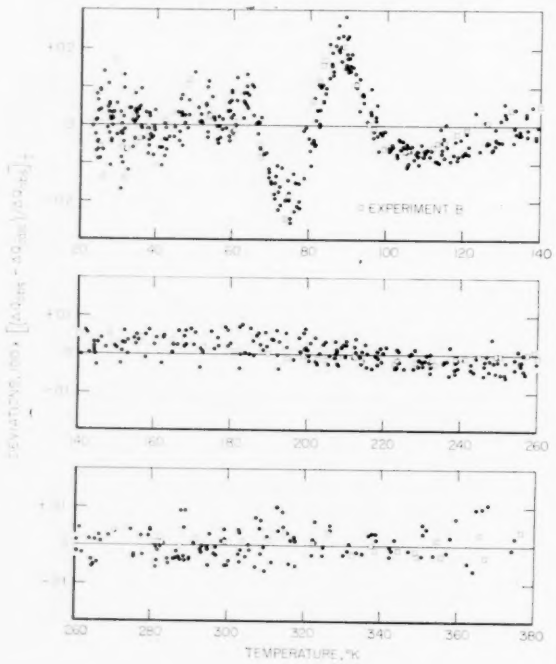

FIGURE 1. *Composite of the deviations (percent),*

$100\times[(\Delta Q\ (observed)-\Delta Q\ (calculated))/\Delta Q\ (observed)]_T$,

for eleven (11) heat-capacity determinations in which three different thermometers (L–18, 769894, and 1057849) were used.

The values of ΔQ (calculated) were obtained from equations containing a series of Debye and Einstein function terms with characteristic temperatures arbitrarily selected and coefficients determined by fitting to ΔQ (observed) using the least squares method. A typical experiment (experiment *B*, used in smoothing the temperature scale) is shown distinct from other data by open squares.

The resistance-temperature relation of the IPTS begins to exhibit relatively large curvature below about 120 °K. The IPTS formulation introduces an incorrect slope at the oxygen point and the IPTS above this temperature is distorted from that of the thermodynamic temperature scale. The change in resistance with temperature at the oxygen point $(1/R_0)(dR/dT)_{O_2}$, for the IPTS formulation is about 4.348×10^{-3}/deg for 12 thermometers in use in the low-temperature calorimetry laboratory at NBS. (In the expression $(1/R_0)(dR/dT)_{O_2}$, R_0 is the thermometer resistance at 0 °C and the subscript $_{O_2}$ indicates the oxygen point.) The values for $(1/R_0)(dR/dT)_{O_2}$ on the NBS (1955) scale for these thermometers are within about $\pm0.001\times10^{-3}$/deg of the above value, which indicates that the scales appear to join satisfactorily at 90.18 °K. The difference between the values of $(1/R_0)(dR/dT)_{O_2}$ from the gas thermometer comparison and the IPTS formulation cannot be obtained for the thermometer (L–6) used to represent the NBS (1939) scale [2]. The thermometer was apparently not calibrated on the IPTS. The PRMI scale [5] is based on a group of four platinum thermometers constructed from a platinum wire designated UX–6. This scale has not been adjusted to join with the IPTS and its value for $(1/R_0)(dR/dT)_{O_2}$ is approximately 4.342×10^{-3}/deg. Using the IPTS calibration constants ($\alpha=0.0039251$, $\delta=1.4899$, and $\beta=0.1127$) given for the UX–6 group standard [10], $(1/R_0)(dR/dT)_{O_2}$ calculates to be 4.350×10^{-3}/deg, which is 0.008×10^{-3}/deg higher than the PMRI scale value. (Variations in the slope of this magnitude (0.2 percent) are easily detected in precision calorimetry.) The resistance-temperature relation of platinum has also an inflection point at about 87 °K; the slope is, therefore, the highest at this temperature. Under these circumstances, the smooth joining of the NBS (1955) scale or any of the other scales mentioned above with the present IPTS would be expected to yield a temperature scale whose intervals are not consistent with those of the thermodynamic scale.

In the present paper the locations of the irregularities in the temperature scales are pointed out and a method is presented for adjusting the NBS (1955) scale and the IPTS, using very precise heat-capacity data.

2. Method

The heat capacity of a system is defined by

$$C=dQ/dT=\lim_{\Delta T\to0}(\Delta Q/\Delta T), \tag{1}$$

so that in principle the heat capacity can be determined from precise measurements of the temperatures, T, and the energy increments, ΔQ, introduced. Except for systems that have transitions at unique temperatures, the heat capacity should be a smooth function of the thermodynamic temperature scale.

The resistance of platinum is also a smooth function of the temperature. (For the heat data obtained between 15 and 380 °K on the systems under discussion and for the platinum resistance thermometer, a smooth function is defined and restricted to the following properties: (a) continuous derivatives, (b) monotonic increasing with not more than two inflection points, and (c) sigmoidal configuration of the heat-capacity curve.) The heat capacity can be expressed alternatively by

$$C=dQ/dT=(dQ/dR)(dR/dT), \tag{2}$$

which shows that the heat capacity can be calculated from corresponding values of dQ/dR and dR/dT. The values of dQ/dR can be obtained as a function of the resistance R (or the temperature T) of the thermometer from observed values of ΔQ and the associated resistances. The values of dR/dT corresponding to the resistance R (or the temperature T) can be obtained from the calibration of the thermometer used in the measurements. The problem is, however, that the values of dR/dT for the NBS (1955)—IPTS scales do not yield smooth, "well-behaved" values of dQ/dT expected. In addition, the accuracy of dR/dT is limited in the NBS (1955) scale range because of the tabular nature of the scale. These irregularities of dQ/dT will appear at the same temperatures as found in the data analyses as shown in figure 1, where the observed thermometer resistances are converted to temperatures and the values of ΔQ and T analyzed.

The method presented in this paper for adjusting the temperature scales involve the relation:

$$dT/dR=(dQ/dR)/(dQ/dT), \tag{3}$$

whereby the above process (eq (2)) is reversed and values of dT/dR are obtained from the smooth values of dQ/dR and dQ/dT. Smoothed values of dQ/dR are obtained as a function of the resistance R of the thermometer from the observations of ΔQ's and the corresponding resistances. Smoothed values of dQ/dT are obtained in the usual manner by fitting equations to the observed ΔQ's and temperatures, obtained by converting the thermometer resistance to temperatures. The dQ/dT values from the fitted equations are taken to be correct and the irregularities in the dQ/dT are disregarded because they should not exist. The values of dT/dR are obtained in accordance with eq (3) as a function of the resistance from corresponding values of dQ/dR and dQ/dT. The values of dT/dR are then integrated relative to a reference temperature (for example, 90.18 or 273.15 °K) and the corresponding thermometer resistance to obtain an adjusted temperature scale. (Henceforth, the values of dT/dR (or dR/dT) obtained from the heat-capacity data will be referred to as derived dT/dR. The temperature scale obtained by integration of dT/dR will be described by the same adjective.)

The method has several limitations with strong dependence on accurate formulation of dQ/dT as a function of the temperature. The "kinks" shown in figure 1 must be smoothed out properly without gain or loss of enthalpy change or degrees between two fixed points. A linear combination of Einstein and Debye heat-capacity functions was found from experience to yield the most suitable heat-capacity-like equation. The equations of dQ/dT were analyzed by examining the higher derivatives for smoothness and the required configuration in accordance with the specifications previously given. Although the functional form of dQ/dT meets the requirements set forth and is obtained by fitting the data over a broad range of temperature, other equally acceptable expressions of dQ/dT may be obtained. Inasmuch as each set of data that have been analyzed contain a fairly large number of observations, it is expected that any variations in dQ/dT resulting from additional observations would be smaller than the irregularities in the NBS (1955)—IPTS scales. Also, the differences between the given equations and any other formulation of dQ/dT that meets the requirements of smoothness and configuration should not exceed the deviations shown in figure 1. The shape of the functional form is very much dependent upon the distribution of the temperatures of the experimental points. At this time no investigation has been made on the most suitable distribution of experimental data. Since the energy introduced can be determined accurately, the accuracy of dQ/dR was limited in the data analyzed only by the resistance measurements. Below about 40 °K the relative accuracy of dQ/dR decreased because of the small changes of resistance that were measured. The accuracy could be improved by using a thermometer of higher dR/dT. The values of dQ/dR increase very rapidly with decrease in temperature below about 25 °K, because the thermometer resistance begins to decrease more rapidly with decrease in temperature than the heat capacity. (See insert, fig. 5.) Thus, an accurate formulation of dQ/dR was not favorable below about 25 °K. The method permits smoothing of the temperature scale about a reference temperature by integration of the values of dT/dR, but the range of temperature is limited by the accumulation of the uncertainty in the integral of dT/dR.

Since the temperature intervals of the NBS (1955)—IPTS scales are already close to those of the thermodynamic scale, the derived temperature scale obtained by integration should not deviate drastically from the original NBS–IPTS scales as long as the values of dT/dR obtained are sufficiently precise. The values of dT/dR, dQ/dR, and dQ/dT do not change rapidly with temperature, therefore the possible uncertainty (a few hundredths of a degree) between the thermodynamic temperature scale and the NBS (1955) scale and IPTS should not have significant effect on the integrated temperature scale. (See sec. 3.) The heat data used in the smoothing process were precise to about ± 0.02 percent or better rom 40 to 380 °K. Below 40 °K the data were less precise because of the decreasing sensitivity of the thermometer.

3. Analysis of the Heat Data and Results of the Smoothing Process

The measured quantities in the determination of heat capacity (C) are series of thermometer resistances (R) or the converted temperatures (T) before and after the introduction of precisely known energy increments (ΔQ). If

$$C=dQ/dT=f(T) \tag{4}$$

and

$$dQ/dR=f(R) \tag{5}$$

then

$$\Delta Q=\int_{T_1}^{T_2} C\,dT=\int_{T_1}^{T_2} f(T)\,dT \tag{6}$$

and

$$\Delta Q=\int_{R_1}^{R_2} f(R)\,dR. \tag{7}$$

The experimental data were analyzed in accordance with eqs (6) and (7). The function $f(T)$ was formulated as a linear combination of Debye and Einstein heat-capacity functions

$$dQ/dT=f(T)=\sum_{i=1}^{9} a_i D(\theta_i/T)+\sum_{j=1}^{10} a_j E(\omega_j/T) \tag{8}$$

with the characteristic temperature for each term arbitrarily selected and the corresponding coefficient determined by the method of least squares from the observed data. The characteristic temperatures used were: θ_i=50, 100, 150, 200, 250, 300, 400, 500, and 700 and ω_j=100, 150, 200, 250, 300, 400, 500, 700, 900, and 1100. The function $f(R)$ was obtained as smoothed tabular values at regularly spaced intervals of resistance. The table was based on three partially overlapping polynomials of the form

$$dQ/dR=f(R)=\sum_{n=-4}^{4} a_n R^n, \tag{9}$$

fitted to the data by the method of least squares. A high speed digital computer at the NBS was used in the calculations.

The heat-capacity data from six different sets of measurements that were obtained recently and considered to be the most precise were analyzed. These data are part of those shown in the composite plot of figure 1. The same capsule-type thermometer No. 769894, (α=0.00392536, δ=1.49$_{30}$, β=0.11014, and R_0=25.54772 ohms) was used with the same calorimeter vessel that was fabricated principally of copper and assembled with "silver solder" and tin-lead solder. The inner surface of the vessel was covered with pure tin and the outer surface gold plated. (For details of the calorimeter design and measurement procedures, see references [11, 12].) Of these data, three sets were from completely independent measurements on the empty vessel and the other three sets were from measurements on the vessel containing samples. The measurements on the empty vessel were made immediately after each measurement with the sample. Henceforth, these sets of experiments will be identified alphabetically, the capital letter representing the vessel-plus-sample measurements and the lower case letter the corresponding empty-vessel measurements. The letter A corresponds to the measurements obtained with $BeO{\cdot}Al_2O_3$, B with Al_4C_3, and C with $LiAlH_4$. The functions $f(T)$ and $f(R)$ were obtained over the complete temperature range of each set of measurements (fig. 1). The analysis of the calorimeter vessel-plus-sample data was complicated since the heat capacity of the sample was superimposed on that of the vessel. Deviations (percent),

$$100\times[(\Delta Q_{\text{obs}}-\Delta Q_{\text{calc}})/\Delta Q_{\text{obs}}]_T$$

of each set of measurements from their respective functions $_f(T)$ are shown in figure 2. The corresponding deviations,

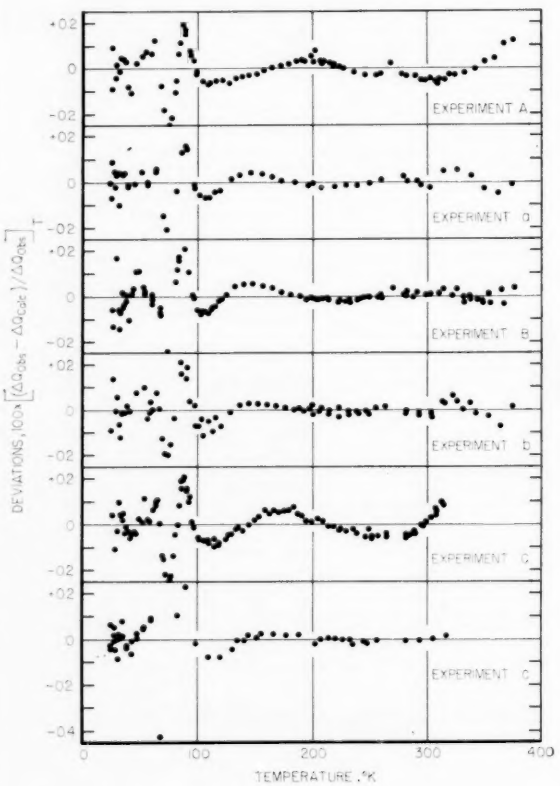

FIGURE 2. *The deviations (percent),*

$$100\times[(\Delta Q\ (observed)-\Delta Q\ (calculated))/\Delta Q\ (observed)]_T,$$

for each of the six (6) sets of measurements obtained using thermometer No. 769894.

These were the measurements analyzed to smooth the NBS (1955)—IPTS scales. The values of ΔQ (calculated) were obtained from $f(T)$ at the appropriate experimental temperatures.

$$100\times[(\Delta Q_{obs}-\Delta Q_{calc})/\Delta Q_{obs}]_R,$$

of these same sets of measurements from functions $f(R)$ are shown in figure 3. The subscripts T and R indicate the methods (eqs (6) and (7), respectively) by which ΔQ (calculated) was obtained.

In figures 4 and 5 are shown the plots of $f(T)$ and $f(R)$ for the data analysed. The three measurements of the empty vessel (a,b,c) are coincident on the scale shown in the plots. The plots are given to show the broad range of magnitudes of values of dQ/dT and dQ/dR of each set of data. The magnitudes of dQ/dT and dQ/dR of the different sets of measurements are sufficiently diverse to permit detecting whether or not an irregular characteristic or "kink" common to these sets of measurements is additive. In particular, any "kink" in the heat-capacity curve of the empty vessel should be exhibited in figures 1 and 2 as a regular pattern of relative deviation inversely proportional in magnitude to the magnitude of dQ/dT. The deviations of figures 1 and 2 disclose regular proportional errors of about the same magnitude. Calibration errors in any bridge or potentiometer settings will be revealed as a fixed pattern in the relative deviation recurring whenever that dial position is used throughout the temperature range of measurements. The lack of a repeating irregularity in the deviation plots of figures 1 and 2 and the lack of repeating or large irregularities in the deviation plots of the analysis of ΔQ versus R of figure 3 discount the existence of any such large calibration errors in the above instruments.

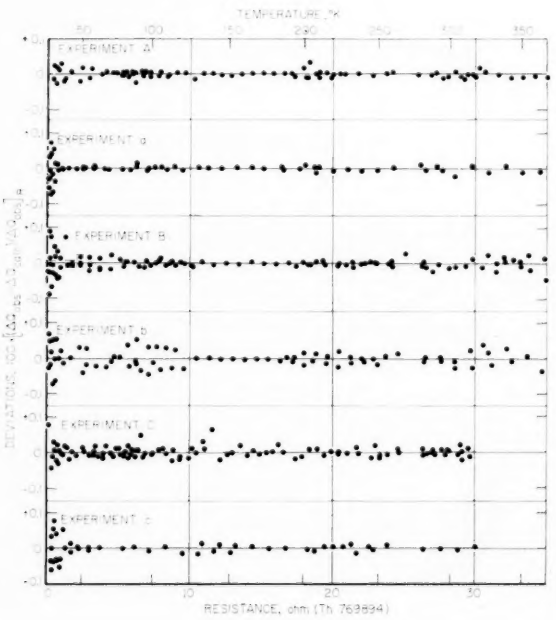

FIGURE 3. *The deviations (percent),*

$$100\times[(\Delta Q\ (observed)-\Delta Q\ (calculated))/\Delta Q\ (observed)]_R,$$

for each of the six (6) sets of measurements obtained using thermometer No. 769894.

These were the measurements analyzed to smooth the NBS (1955)—IPTS scales. The values of ΔQ (calculated) were obtained from $f(R)$ at the appropriate experimentally observed resistances.

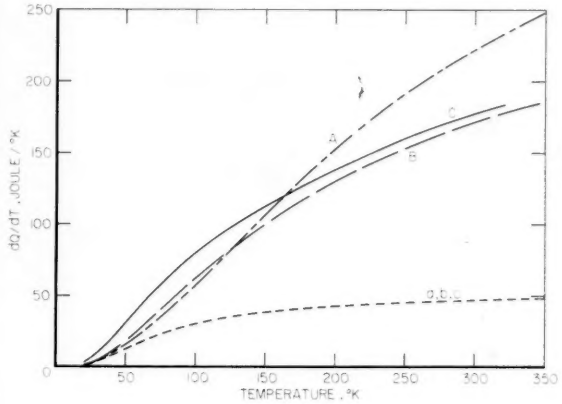

FIGURE 4. *Comparison of the smoothed heat capacities* f(T) *of experiments used in smoothing the NBS (1955)—IPTS scales.*

The heat capacities of the empty vessel (experiments a, b, and c) are virtually coincident.

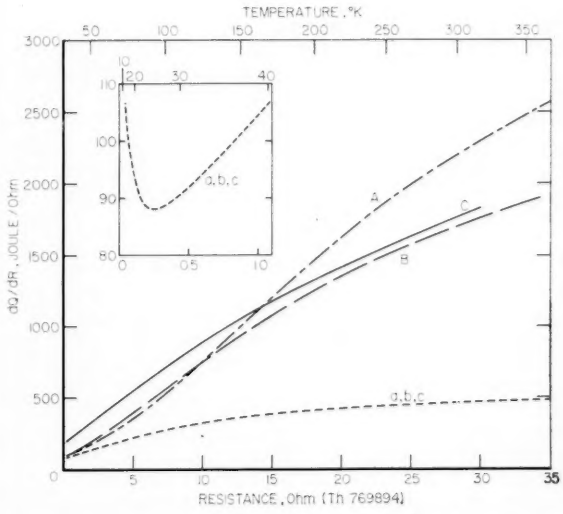

FIGURE 5. *Comparison of the values of* f(R) *of experiments used in smoothing the NBS (1955)—IPTS scales.*

The values of $f(R)$ of the empty vessel (experiments a, b, and c) are virtually coincident.

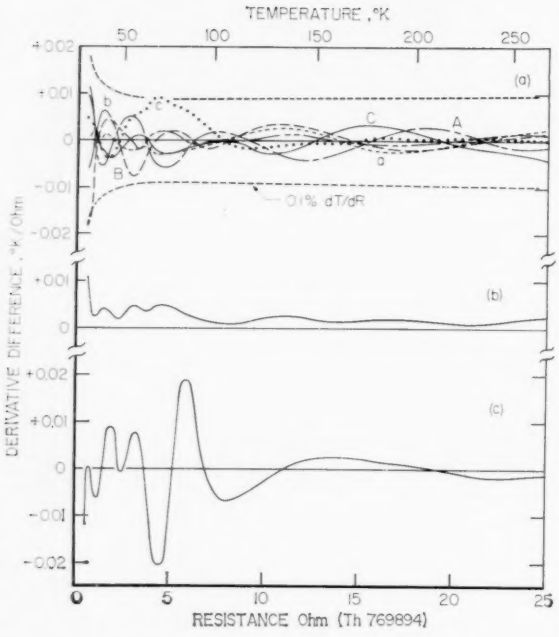

FIGURE 6. (a) *Deviation from their mean of* dT/dR *determined from each of the six experimental measurements.*
(b) *Root-mean-square deviation from the mean of the six sets of* dT/dR.
(c) *Difference in* dT/dR *between derived scale and NBS (1955)—IPTS scales (base line).*

Figure 6a shows the deviations of the dT/dR obtained from each set of measurements from their mean. The root-mean-square (rms) deviation from their mean plotted in figure 6b shows that the agreement in the derived dT/dR is best in the neighborhood of the oxygen point. The rms deviation increases to about 0.02 percent at temperatures above and 0.04 percent below the oxygen point, respectively. The deviation of the mean derived dT/dR from the dT/dR of the NBS (1955)—IPTS scales shown in figure 6c is similar to the

$$100\times[(\Delta Q_{\text{obs}}-\Delta Q_{\text{calc}})/\Delta Q_{\text{obs}}]_T$$

plots shown in figures 1 and 2. The apparently high (or low) values shown in figures 1 and 2 of ΔQ (observed) over those of ΔQ (calculated) arise from values of ΔT that are too small (or too large) corresponding to the observed ΔR. Since the ΔT corresponding to the ΔR has been adjusted accordingly in the derived values of dT/dR, the configuration of figures 1, 2, and 6a should be very similar.

In figure 7 the mean derived dR/dT (reciprocal of dT/dR (obtained) is compared with those of the NBS (1955)—IPTS scales in the neighborhood of the oxygen point. The shape of the derived dR/dT is considerably different from that of the NBS (1955)—IPTS scales. The inflection point at 90.18 °K of the dT/dR of the NBS (1955)—IPTS scales has been displaced in the derived dT/dR to around 110 °K. This should yield a temperature scale more compatible with the heat-capacity measurements. The general configurational relation between the curves in the interval 75 to about 95 °K is very similar to that reported by Borovick-Romanov [5] for the PRMI and NBS (1955) scales and the IPTS using UX–3 and UX–6 platinum thermometers.

Figure 8a shows between 30 and 220 °K the deviation of the temperatures derived by integration of dT/dR relative to the oxygen point of each set of measurements from their mean. The rms deviation of the derived temperature scales given in figure 8b shows that the agreement is best between about 60 and 150 °K. Beyond these temperatures the rms deviation is about 0.01 deg. The divergence below the oxygen point of the temperature scale derived from experiment c is shown to be unusually high. This is considered to be due to the temperatures at which the experimental data were taken.

Figure 8c shows the deviation of the mean derived temperature scale from NBS (1955)—IPTS scales. The average of the deviations of the PSU, PRMI, and NPL scales from the NBS (1955) scale is also shown.

As a part of the program of the International Committee on Weights and Measures, the National Physical Laboratory and the Physico-Technical and Radio-Technical Measurements Institute intercompared platinum resistance thermometers that were calibrated on the NBS (1955), PSU, PRMI, and NPL temperature scales. These data made available to us through J. L. Riddle (NBS), were used freely in comparing them with the derived temperature scale. Both the NPL data and the PRMI data on the resistance thermometers representing each of the scales were assumed to have been observed at the same temperatures. For convenience of the subsequent discussion the PSU, PRMI, and NPL temperature scales will be referred to collectively as non-NBS temperature scales. The derived temperature scale was found to track the average of the non-

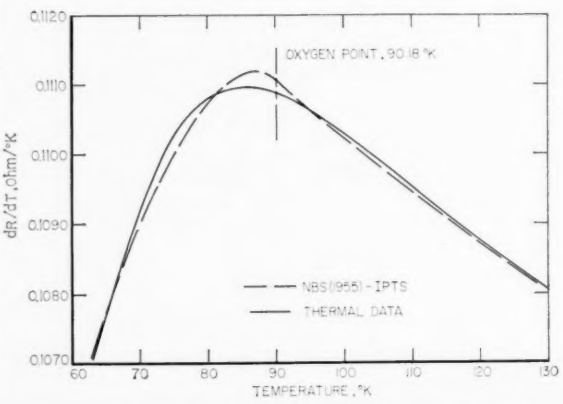

FIGURE 7. *Comparison of the derived values of* dR/dT *with those of the NBS (1955)—IPTS scales.*

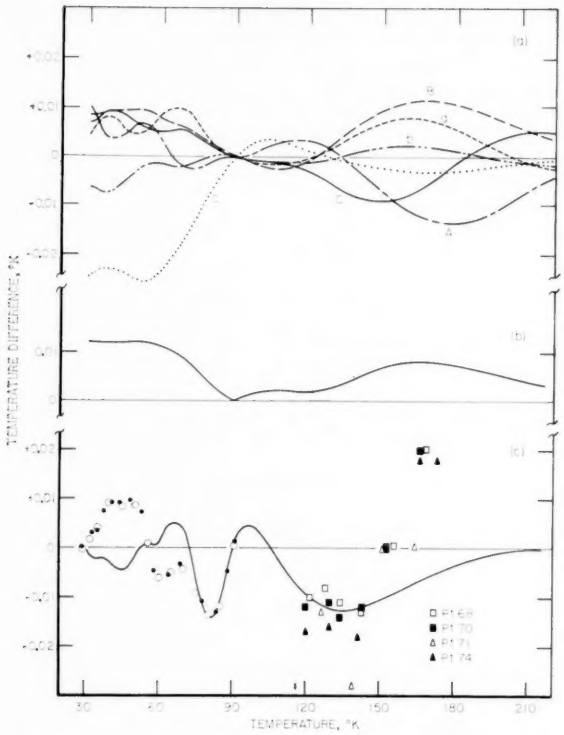

FIGURE 8. *(a) Deviations from their mean of the temperature scales derived from each of the six (β) experiments.*

The temperature scales were obtained by integration relative to the oxygen point (90.18 °K).

(b) *Root-mean-square deviation from their mean of the six derived temperature scales.*
(c) *Deviations from the NBS (1955)—IPTS scales of the mean derived temperature scale.*

The symbols ○ and ● indicate, respectively, the mean of the deviations of the PSU, PRMI, and NPL temperature scales from the NBS (1955) scale as observed at NPL and PRMI. The symbols □, ■, △, and ▲ indicate deviations from the IPTS of the helium-gas thermometer reported by Keesom and Dammers [13] for platinum thermometers designated Pt 68, 70, 71, and 74, respectively.

NBS scales closely from the oxygen point down to about 75 °K. From 75 down to about 55 °K the configuration is similar, but the maximum deviation is about 0.01 deg. Below 55 °K, the shape is different and the deviation is as large as 0.014 deg.

In the region above the oxygen point, a portion of the data on the intercomparison of the IPTS with a helium-gas thermometer obtained by Keesom and Dammers [13] is plotted in figure 8c. In the region of about 120 to 140 °K, these data are in fair agreement with the derived scale. Above about 140 °K, there is considerable divergence.

The deviations shown below 55 °K and above 140 °K in the comparisons given in figure 8c are considered to be due to the inability of the method presented to account for any long-range, gradual variations in the NBS (1955)—IPTS scales. Therefore, the deviations of the observations shown in 8c are not indicative of any variations in the data.

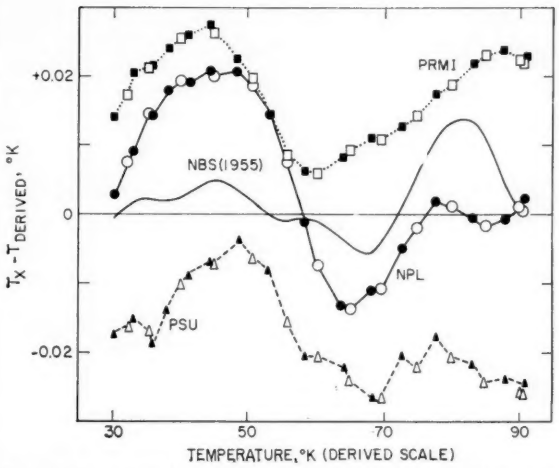

FIGURE 9. *Deviations of the NBS (1955), PSU, PRMI, and NPL temperature scales from the derived temperature scale.*

The open and filled symbols indicate, respectively, the data obtained at NPL and PRMI.

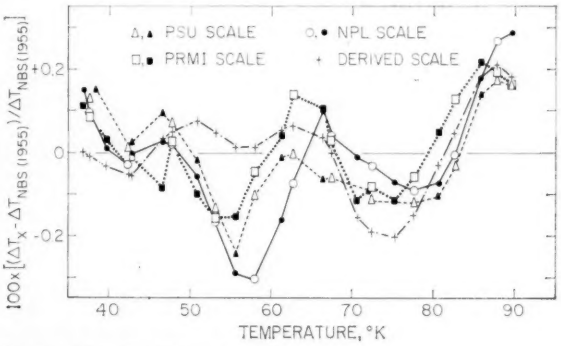

FIGURE 10. *Deviations (percent),*

$$100\times[(\Delta T_x - \Delta T_{NBS(1955)})/\Delta T_{NBS(1955)}],$$

of PSU, PRMI, NPL, and the derived temperature scales.

The subscript x indicates any of the above temperature scales. The values of ΔT were obtained from the same data obtained at the NPL and PRMI for the comparison of the NBS (1955), PSU, PRMI, and NPL temperature scales. The abscissa for the points plotted is the mean temperature of the two temperature used to obtain ΔT.

The deviations of the NBS (1955) and the non-NBS temperature scales from the derived scale are shown from 30 to 90 °K in figure 9. Except for the displacement of the scales, due to the use of numerically different values for the oxygen point, the PSU scale is in excellent agreement with the derived scale from 90 down to about 55 °K, the NPL scale down to 70 °K, and the PRMI scale down to 75 °K. The NBS (1955) scale is shown to be relatively divergent from each of the non-NBS temperature scales. The NBS (1955) and the derived scale are in good agreement below 70 °K.

A comparison of the "size of the degree", or effectively the values of dT/dR used to obtain the derived temperature scale, is made with those of other scales in figure 10. The differences in the

successive temperatures obtained for the various temperature scales are compared with the differences in the corresponding successive temperatures on the NBS (1955) scale by the relation:

$$100 \times [(\Delta T_x - \Delta T_{\text{NBS}})/\Delta T_{\text{NBS}}], \qquad (10)$$

where the subscript x represents any of the other temperature scales. The configuration of the relation given by eq (10) for the derived scale is similar to those of the non-NBS scales over the entire temperature range shown in figure 10. This similarity indicates that the derived and non-NBS temperature scales are closely alike. It is remarkable that the derived temperature scale agrees closely with the non-NBS scales.

4. Conclusions

The temperature intervals of the NBS (1955)—IPTS scales were adjusted, utilizing values of dT/dR that were derived from six independent sets of heat-capacity data. These data were fitted by the method of least squares to equations representing dQ/dT and dQ/dR which differ over a broad range in the magnitude of their values. The rms deviations of the values of dT/dR obtained from the six sets of data are from 0.01 to 0.02 percent above 90 °K and increase to about 0.04 percent at 70 °K and lower. Comparison of the derived temperature scale, obtained by integrating the values of dT/dR relative to the oxygen point, with the mean of the non-NBS temperature scales indicates agreement to better than 0.01 deg from 90 down to about 55 °K with slightly larger deviations at lower temperatures and falls well within the range of the existing scales. Between 60 to 90 °K, the deviation of the "size of the degree" of the derived scale from the mean value of the non-NBS scales is comparable or smaller than the spread of the values of the non-NBS scales. Below 60 °K, slightly larger deviations were obtained.

Because of the lack of data, no accurate comparison can be made of the derived temperature scale above the oxygen point.

The method described for adjusting the temperature scales using precise heat-capacity data is limited to a short range near the reference temperature because of the accumulation of the uncertainty in the integral of dT/dR. An accurate formulation of the values of dQ/dR and dQ/dT is essential to the success of the method. A large number of properly distributed, highly precise heat-capacity data is a prerequisite. Accurate formulation of dQ/dR is complicated below about 25 °K because of its rapid increase with decrease in temperature. The relative precision at the lower temperatures would be better if a thermometer of higher dR/dT is used.

A method for adjusting the temperature scale is demonstrated in this paper using the laboratory data that had accumulated in the past few years. The heat-capacity data from the measurements of the vessel plus sample had complicated shapes because of the superposition of the heat capacity of the sample on that of the vessel. Systematic measurements on systems having values of dQ/dT with a simple shape should yield more accurate equations for the values of dQ/dT.

5. References

[1] H. F. Stimson, J. Res. NBS **65A,** 139 (1961).
[2] H. J. Hoge and F. G. Brickwedde, J. Res. NBS **22,** 351 (1939).
[3] D. M. Yost, C. S. Garner, D. W. Osborne, T. R. Rubin, and H. Russell, Jr., J. Am. Chem. Soc. **63,** 3488 (1941).
[4] G. W. Moessen, J. G. Aston, and R. G. Ascah, Temperature, Its Measurement and Control in Science and Industry, Vol. **3,** pt 1, p. 91 (Reinhold Publishing Corp., New York, 1962).
[5] A. S. Borovick-Romanov, P. G. Strelkov, M. P. Orlova, and D. N. Astrov, Temperature, Its Measurement and Control in Science and Industry, Vol. **3,** pt 1, p. 113 (Reinhold Publishing Corp., New York, 1962).
[6] C. R. Barber, Brit. J. Appl. Phys. **13,** 235 (1962).
[7] C. R. Barber, Temperature, Its Measurement and Control in Science and Industry, Vol. **3**, pt. 1, p. 345 (Reinhold Publishing Corp., New York, 1962).
[8] F. Henning and J. Otto, Physik. Zeitschr. **37,** 601 (1936).
[9] W. H. Keesom and A. Bijl, Physica **3,** 418 (1936).
[10] D. I. Sharevskaya, P. G. Strelkov, A. S. Borovik-Romanov, D. N. Astrov, and M. P. Orlova, Temperature, Its Measurement and Control in Science and Industry, Vol. **3,** pt. 1, p. 351 (Reinhold Publishing Corp., New York, 1962).
[11] G. T. Furukawa, M. L. Reilly, and J. H. Piccirelli, J. Res. NBS **68A,** 381 (1964).
[12] A. R. Glasgow, Jr., G. S. Ross, A. T. Horton, D. Enagonio, H. D. Dixon, and C. P. Saylor; and G. T. Furukawa, M. L. Reilly, and J. M. Henning, Anal. Chem. Acta **17,** 54 (1957).
[13] W. H. Keesom and B. G. Dammers, Physica **2,** 1080 (1935).

(Paper 69A1–321)

JOURNAL OF RESEARCH of the National Bureau of Standards—A. Physics and Chemistry
Vol. 69A, No. 1, January–February 1965

Heat Capacity and Thermodynamic Properties of Beryllium Aluminate (Chrysoberyl), $BeO \cdot Al_2O_3$, From 16 to 380 °K*

George T. Furukawa and William G. Saba

(October 6, 1964)

The heat capacity of beryllium aluminate (chrysoberyl), $BeO \cdot Al_2O_3$, was determined from 16 to 380 °K and the thermodynamic properties calculated from 0 to 380 °K.

1. Introduction

As a part of the program at the National Bureau of Standards to provide accurate thermodynamic data on the "light-element" compounds, the heat capacities of the compounds of the BeO–Al_2O_3 system are being investigated. Thermodynamic data on these compounds should be of interest in high-temperature research and ceramic technology. Although numerous heat-capacity data on BeO and Al_2O_3 have been published [1],[1] no low-temperature heat-capacity data have been found in the literature on any of the mixed-oxide compounds of Be and Al. In this paper, the results of the heat-capacity measurements in the range 16 to 380 °K on beryllium aluminate (chrysoberyl), $BeO \cdot Al_2O_3$, are given. (Henceforth, the name chrysoberyl will be used synonymously with $BeO \cdot Al_2O_3$. Whenever the name beryllium aluminate is used, the chemical formula will be given also for identifying the compound of the BeO–Al_2O_3 system to which the reference is made.) Heat-capacity measurements now being made on the compound $BeO \cdot 3Al_2O_3$ will be reported in a future paper.

Beryllium oxide (BeO) and aluminum oxide (Al_2O_3) form two congruently melting mixed-metal oxide compounds, $BeO \cdot Al_2O_3$ and $BeO \cdot 3Al_2O_3$. Lang et al. [2] reported 1870° ±10 °C and 1910° ±10 °C, respectively, for the melting points of these compounds. Fedoseev [3] reported in addition the compound $3BeO \cdot Al_2O_3$ with an incongruent melting point of 1980 °C. Foster and Royal [4] found $BeO \cdot Al_2O_3$ and $BeO \cdot 3Al_2O_3$ to exhibit very similar optical properties, but distinctive x-ray diffraction patterns. Chrysoberyl occurs in nature in various shades of green, brown, and yellow, or red by transmitted light, with an orthorhombic, dipyramidal crystal structure, space group Pmnb (a_0=5.47 Å, b_0=9.39 Å, and c_0=4.42 Å; all ±1 percent) [5]. The compounds $BeO \cdot 3Al_2O_3$ and $3BeO \cdot Al_2O_3$ have not been found in nature. The gem variety of chrysoberyl that is red by transmitted light is known as alexandrite and the variety that exhibits chatoyancy, as cat's eye. The color is possibly due to Cr and Fe impurities that have been found. Iron is the usual impurity, substituting for Be and Al in the ferrous and ferric forms, respectively. The ferric form in amounts up to 6 percent by weight Fe_2O_3 has been reported [5]. Titanium has also been reported as an impurity, presumably due to mechanical inclusion of rutile.

2. Sample

The known naturally occurring chrysoberyl samples were considered too impure for the heat-capacity measurements. Semi-Elements, Inc., prepared on request a special sample by arc fusion of a stoichiometric mixture of high-purity BeO and Al_2O_3 powder. The procedure involved the formation of a melted mass within a relatively large charge of the mixture so that the powdered mixture would serve as the "container" for the melted sample to avoid chemical contamination. The fused sample was slowly cooled to room temperature and any material that was not fused adhering to the outer surface was removed mechanically. The fused material was crushed and sieved to collect particles between 10 and 50 mesh sizes (between 0.3 and 2 mm). Microscopic examination showed that these particles were not single crystals.

The material as received contained some particles that appeared gray, presumably from traces of graphite from the electrodes used in the arc fusion process. Qualitative spectrochemical examination

*This work was sponsored by the Advanced Research Projects Agency, Department of Defense, under ARPA Order No. 20.

[1] Figures in brackets indicate literature references at the end of this paper.

of the sample by the Spectrochemical Analysis Section of the National Bureau of Standards showed the limits of percentage impurities given in table 1.

TABLE 1. *Spectrochemical analysis of the beryllium aluminate (chrysoberyl)* $BeO \cdot Al_2O_3$, *sample* [a]

Element	Percentage limit	Element	Percentage limit
Si	<0.01	Ca	0.001–0.01
Cu	0.01–0.1	V	0.0001–0.001
Ni	0.01–0.1	Sn	<0.001
Fe	0.001–0.01	Pb	<0.001
Mg	0.001–0.01	Ag	<0.0001

[a] Analysis by Martha Darr, Spectrochemical Analysis Section of the National Bureau of Standards.

The $BeO \cdot Al_2O_3$ sample was examined by the petrographic (microscopic) method in the Crystallography Section of the National Bureau of Standards. The size of the crystals was found to be about 200μ. Since the material was subjected to a grinding process for the microscopic examination, the original $BeO \cdot Al_2O_3$ crystals in the 10 to 50 mesh polycrystalline particles were, therefore, considered larger than 200μ. The index of refraction was in agreement with that previously reported for the substance [5]. The crystals were clear but showed some growth defects presumably from rapid crystallization. A small volume of what appeared to be voids was observed. No impurity phases of BeO or Al_2O_3 crystals were found.

The $BeO \cdot Al_2O_3$ sample was also examined by x-ray diffraction techniques in the Crystal Chemistry Section of the National Bureau of Standards. The diffraction pattern showed several strong lines characteristic of the $BeO \cdot Al_2O_3$ crystal. No lines characteristic of separate crystalline phases of BeO, Al_2O_3 or $BeO \cdot 3Al_2O_3$ were found. A small amount of impurity phase was observed that could not be identified or its amount estimated from the x-ray results.

Two samples of the material were chemically analyzed for Al and Be by the National Bureau of Standards Analysis and Purification Section. One sample was hand picked to be clear and free from gray coloration; the other was a sample that represented the bulk lot and contained many particles with the gray coloration. The samples were first dissolved in concentrated hydrochloric acid in a sealed ampoule by heating for 24 hr at 250 to 300 °C within a pressurized bomb. A known mixture of BeO and Al_2O_3 was treated in the same manner as a control on the analysis. The aluminum was precipated as the 8-hydroxyquinolate, $Al(C_9H_6ON)_3$, after buffering with acetate to the *p*H of 4.2 to 4.5. The precipitate was ignited to Al_2O_3 and weighed. The beryllium was precipitated as $Be(OH)_2$ at the *p*H of 8 to 9 with ammonium hydroxide, ignited to BeO, and weighed. The results of the chemical analyses summarized in table 2 show the sample to be highly pure. The amount of graphite impurity was considered insignificant, and the sample was taken to be 100 percent pure in the processing of the heat-capacity data.

3. Apparatus and Method

The heat-capacity measurements were made in an adiabatic calorimeter similar in principle and design to that described previously [6]. The sample vessel was suspended within the adiabatic shield system by means of a Nylon cord instead of the filling tube shown in the above reference. The adiabatic shields were controlled automatically by means of electronic and electro-mechanical equipment. The details of the calorimeter design and the automatic adiabatic control equipment will be described in a subsequent publication.

TABLE 2. *Chemical analysis of the beryllium aluminate (chrysoberyl)*, $BeO \cdot Al_2O_3$, *samples* [a]

Sample	Percentage by weight		Molar ratio
	Al_2O_3	BeO	Al_2O_3/BeO
Hand Picked	80.25	19.73	0.998
Random	80.33	19.72	1.000
Theoretical	80.30	19.70	1.000

[a] Analysis by Thomas J. Murphy, Analysis and Purification Section of the National Bureau of Standards.

The electrical power input to the calorimeter heater was measured by means of a Wenner potentiometer with reference to saturated standard cells and standard resistors calibrated at the National Bureau of Standards. A volt box was employed for the measurement of the voltage drop across the calorimeter heater. Adjustments were made in the calculation of the power for the current in the volt box and for the resistance of the potential leads from the volt box to the calorimeter heater.

The time interval of heating was determined by means of a precision timer operated on a 60 Hz frequency, furnished at the National Bureau of Standards, that is derived from a 100 kHz quartz oscillator maintained stable within 0.5 ppm. The oscillator frequency is compared and adjusted periodically with the WWV frequency broadcasts.

Temperatures were determined by means of a platinum-resistance thermometer and a high precision Mueller bridge. The thermometer was calibrated by the Temperature Physics Section of the National Bureau of Standards. The calibration above 90 °K was on the 1948 International Practical Temperature Scale [7], and between 10 and 90 °K on the NBS–1955 provisional scale. The provisional scale as it is presently maintained at the National Bureau of Standards, and referred to as degrees K (NBS–1955), is numerically 0.01 deg lower than the NBS–1939 scale [8].

The 1961 atomic weights based on carbon 12 were used to convert the mass of sample investigated to molal basis [9]. Wherever the energy unit calorie is used, the conversion from the cgs unit of energy joule was made using the relation:

$$1 \text{ defined calorie} = 4.1840 \text{ J}.$$

4. Heat-Capacity Measurements and Results

The chrysoberyl sample, being considered quite stable, was poured directly into the calorimeter vessel; that is, the sample was handled exposed to the usual laboratory atmosphere. The vessel with its contents was pumped to a high vacuum and purged with dry helium gas several times and finally sealed with 58 torr pressure of helium gas. The mass of sample investigated was 210.4113 g.

The heat-capacity measurements were made on the calorimeter vessel plus sample from about 16 to 380 °K. This was followed by another series of measurements in the same temperature range on the empty vessel. The analyses and calculations on these measurements were performed on the IBM 7094 computer. Details of the computer codes used will be given in a future publication. Briefly, the analyses and calculations involved the following procedures. From the measurements of initial and final temperatures and the corresponding enthalpy increments, smooth values of heat capacity at regular temperature intervals were obtained for the calorimeter vessel plus sample and for the empty vessel. The heat capacity of the sample was obtained by differencing the smoothed values from the two series of measurements at the corresponding regular temperatures. A correction was made wherever significant for the heat capacity of helium gas. The values of heat capacity of the sample so obtained were smoothed further wherever necessary and finally converted to molal basis. The precision of each series of heat-capacity measurements is shown in figures 1 and 2 in which the deviations of the observed values from the smoothed values are plotted. The relatively large deviation at about 273 °K in both sets of measurements is considered to be due to the melting of a small amount of water sealed unintentionally somewhere in the calorimeter vessel system. Since this anomaly was repeatable in both sets of measurements, no errors were introduced in the final values of heat capacity of chrysoberyl. Also, the magnitude of the anomaly was less than 0.07 percent of the apparent heat capacity.

Figure 3 shows the plot of the "observed molal heat capacity." Table 3 gives the numerical values. These values were obtained by differencing the heat capacity of the empty vessel and that of the vessel plus sample at the observed temperatures (mid-temperature of the heating interval) of the latter series of measurements. The heat capacity of the empty vessel at the corresponding temperatures was obtained by interpolation in the table of smooth values at regular temperature intervals described earlier. These values were corrected for the heat capacity of the helium gas and for curvature wherever significant and converted to molal basis.

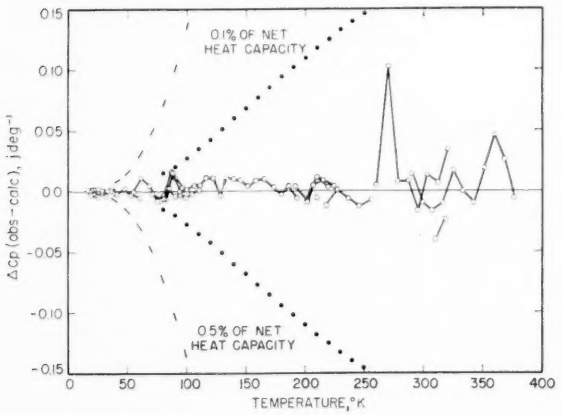

FIGURE 1. *Deviations of the heat-capacity measurements on calorimeter vessel plus beryllium aluminate (chrysoberyl),* $BeO \cdot Al_2O_3$.

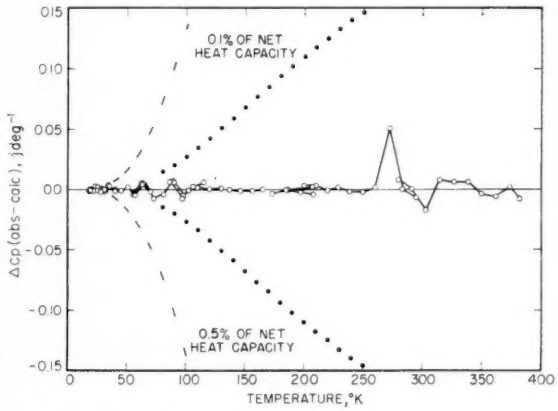

FIGURE 2. *Deviations of the heat-capacity measurements on the empty calorimeter vessel used with beryllium aluminate (chrysoberyl),* $BeO \cdot Al_2O_3$.

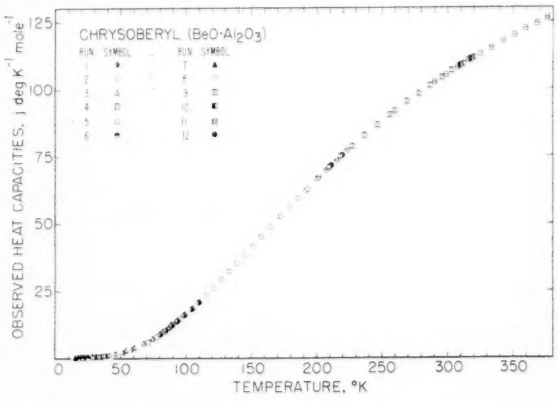

FIGURE 3. *Observed values of the molal heat capacity of beryllium aluminate (chrysoberyl),* $BeO \cdot Al_2O_3$ *as a function of the temperature.*

(The numerical values are given in table 3).

TABLE 3. *Observed heat capacity of beryllium aluminate (chrysoberyl), $BeO \cdot Al_2O_3$*

Gram molecular wt=126.9728 g, T °K=t °C+273.15°

T	C_P	T	C_P	T	C_P
RUN 1		RUN 5		RUN 9—Con.	
°K	J/deg-mole	°K	J/deg-mole	°K	J/deg-mole
80.5473	9.004	28.7003	0.323	269.0604	95.546
85.1541	10.601	33.3094	.515	277.9055	98.641
89.5817	12.213	37.3141	.742	286.5293	101.591
94.1573	13.972	41.4620	1.043	294.8939	104.322
99.0805	15.979	46.6291	1.550	303.1446	106.945
104.3141	18.235	52.9692	2.382	311.5147	109.488
109.8372	20.731	59.5633	3.521	320.0179	111.998
RUN 2		RUN 6		RUN 10	
81.6181	9.368	19.2684	0.092	309.7608	108.934
87.7681	11.557	20.8630	.120	317.7316	111.301
93.6407	13.773	22.8544	.158		
99.6463	16.223	25.2148	.216	RUN 11	
105.4574	18.746				
110.7585	21.160	RUN 7		290.0458	102.762
116.0659	23.675			298.7850	105.567
121.6485	26.400	16.4504	0.045	307.3395	108.215
127.4847	29.315	18.3613	.079	315.9789	110.797
133.3266	32.309	20.2893	.112	324.7663	113.340
139.1501	35.326	22.4282	.152	333.5567	115.764
145.0459	38.408	25.2495	.213	342.3312	118.096
151.3929	41.737	28.2888	.306	350.9917	120.335
158.0993	45.261	31.7145	.438	359.5197	122.458
165.1286	48.935	35.3961	.626	367.8734	124.451
172.4762	52.734	39.3311	.877	376.1640	126.394
179.4524	56.295				
186.1141	59.649	RUN 8		RUN 12	
193.0372	63.060				
RUN 3		201.7985	67.283	191.3362	62.230
		207.5974	70.018	201.1287	66.960
54.5979	2.637	215.3999	73.600	210.4197	71.327
61.0699	3.832	224.0728	77.459	219.2943	75.347
68.1901	5.443				
75.1174	7.308	RUN 9			
81.4060	9.297				
87.3603	11.408	209.6930	70.985		
RUN 4		218.4723	74.970		
		227.3537	78.883		
70.8972	6.134	236.6705	82.834		
77.5194	8.033	246.3094	86.771		
83.6752	10.081	255.8343	90.521		
89.7941	12.305	259.9653	92.108		
95.9958	14.715				

Considering the precision of the measurements (figs. 1 and 2), the purity of the sample, the accuracy of the various instruments used in the measurements, and the possible systematic errors, the uncertainty in the final values of heat capacity (table 4) was estimated to be ±0.1 percent between about 80 and 380 °K. Below 80 °K the uncertainty increased, because of the decrease in the contribution of the sample to the gross heat capacity. At 80 °K, the sample was 40 percent of the total; at 50 °K, 20 percent; at 30 °K, 13 percent; and at 16 °K, the lowest temperature of the measurements, only 6 percent. Below about 40 °K, the decrease in the dR/dT of the platinum resistance thermometer also lowered the accuracy. Considering in addition these factors, the estimated uncertainty is ±0.3 percent at 50 °K, ±1 percent at 30 °K, and ±3 percent at 16 °K.

5. Thermodynamic Functions and Discussion of the Results

The smoothed values of heat capacity at regular temperature intervals were used to derive the various thermodynamic functions. The values of heat capacity below 16 °K, the lower limit of the measurements, were obtained by extrapolation using the equation:

$$C=1.334\times10^{-5}T^3$$

fitted to the observed values at the lower temperatures (below 30 °K). Assuming $C_V=C_p$, the effective Debye characteristic temperature below 30 °K was calculated to be 1000 °K. The thermodynamic relations involving the heat capacity were evaluated by numerical integration using four-point Lagrangian integration coefficients on the IBM 7094 computer. The thermodynamic functions are given from 0 to 380 °K in table 4.

Often when the heat-capacity data are not available, an estimate is made by simple addition of the heat capacity of the components that comprise the compound or alloy. A comparison (fig. 4) of the heat

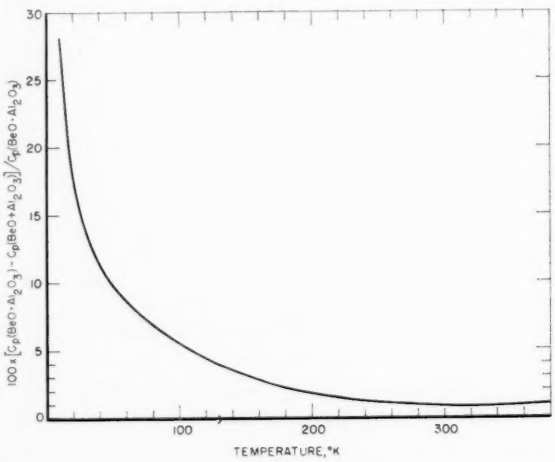

FIGURE 4. *Comparison of the heat capacity of beryllium aluminate (chrysoberyl), $BeO \cdot Al_2O_3$, with that of an equimolar mixture of BeO and Al_2O_3.*

capacity of chrysoberyl with that of an equimolar mixture of BeO and Al_2O_3 shows a positive deviation throughout the temperature range (10 to 380 °K). From 200 to 380 °K the agreement is within about 1 percent. At 100 °K the deviation is about 5 percent and below this temperature the deviation increases rapidly (28 percent at 10 °K).

This deviation from "additivity" of the heat capacity shown in figure 4 has been found to be typical of most mixed-metal oxides [10]. In the region from about 150 °K to room temperature and slightly above, the percentage deviation from additivity of most mixed-metal oxides is a few percent

TABLE 4. *Thermodynamic functions for beryllium aluminate (chrysoberyl) ($BeO \cdot Al_2O_3$) solid phase (at 1-atm pressure)*

Gram molecular wt = 126.9728 g, T °K = t °C + 273.15°

T	C_P°	$(H_T^\circ - H_0^\circ)$	$(H_T^\circ - H_0^\circ)/T$	S_T°	$-(G_T^\circ - H_0^\circ)$	$-(G_T^\circ - H_0^\circ)/T$
°K	J/deg-mole	J/deg-mole	J/deg-mole	J/deg-mole	J/deg-mole	J/deg-mole
0.00	.000	0.000	0.000	0.000	0.000	0.000
5.00	.002	.002	.001	.001	.001	.000
10.00	.013	.033	.003	.004	.011	.001
15.00	.045	.169	.011	.015	.056	.004
20.00	.107	.534	.027	.036	.178	.009
25.00	.209	1.303	.052	.069	.434	.017
30.00	.367	2.714	.090	.120	.901	.030
35.00	.600	5.099	.146	.194	1.676	.048
40.00	.924	8.865	.222	.294	2.881	.072
45.00	1.366	14.536	.323	.427	4.667	.104
50.00	1.950	22.763	.455	.600	7.215	.144
55.00	2.693	34.301	.624	.819	10.741	.195
60.00	3.599	49.964	.833	1.091	15.492	.258
65.00	4.664	70.555	1.085	1.420	21.745	.335
70.00	5.886	96.865	1.384	1.809	29.793	.426
75.00	7.266	129.68	1.729	2.262	39.944	.533
80.00	8.821	169.82	2.123	2.779	52.518	.656
85.00	10.540	218.17	2.567	3.365	67.850	.798
90.00	12.369	275.40	3.060	4.019	86.281	.959
95.00	14.305	342.03	3.600	4.739	108.15	1.138
100.00	16.365	418.66	4.187	5.524	133.78	1.338
105.00	18.535	505.86	4.818	6.375	163.50	1.557
110.00	20.802	604.17	5.492	7.289	197.63	1.797
115.00	23.152	714.02	6.209	8.265	236.49	2.056
120.00	25.574	835.80	6.965	9.302	280.38	2.337
125.00	28.057	969.86	7.759	10.396	329.60	2.637
130.00	30.589	1116.5	8.588	11.545	384.43	2.957
135.00	33.158	1275.8	9.450	12.748	445.15	3.297
140.00	35.756	1448.1	10.343	14.001	512.00	3.657
145.00	38.372	1633.4	11.265	15.301	585.23	4.036
150.00	40.997	1831.8	12.212	16.646	665.08	4.434
155.00	43.625	2043.4	13.183	18.033	751.76	4.850
160.00	46.247	2268.1	14.175	19.460	845.48	5.284
165.00	48.859	2505.8	15.187	20.923	946.42	5.736
170.00	51.453	2756.6	16.215	22.420	1054.8	6.204
175.00	54.026	3020.3	17.259	23.949	1170.7	6.690
180.00	56.572	3296.8	18.316	25.506	1294.3	7.191
185.00	59.089	3586.0	19.384	27.091	1425.8	7.707
190.00	61.572	3887.7	20.461	28.699	1565.2	8.238
195.00	64.020	4201.7	21.547	30.331	1712.8	8.784
200.00	66.430	4527.8	22.639	31.982	1868.6	9.343
205.00	68.800	4865.9	23.736	33.651	2032.7	9.915

TABLE 4. *Thermodynamic functions for beryllium aluminate (chrysoberyl) ($BeO \cdot Al_2O_3$) solid phase (at 1-atm pressure)*—Con.

Gram molecular wt = 126.9728 g, T °K = t° C273.15°

T	C_P°	$(H_T^\circ - H_0^\circ)$	$(H_T^\circ - H_0^\circ)/T$	S_T°	$-(G_T^\circ - H_0^\circ)$	$-(G_T^\circ - H_0^\circ)/T$
°K	J/deg-mole	J/deg-mole	J/deg-mole	J/deg-mole	J/deg-mole	J/deg-mole
210.00	71.129	5215.7	24.837	35.337	2205.1	10.501
215.00	73.417	5577.1	25.940	37.038	2386.1	11.098
220.00	75.662	5949.8	27.045	38.752	2575.5	11.707
225.00	77.865	6333.7	28.150	40.477	2773.6	12.327
230.00	80.026	6728.4	29.254	42.212	2980.3	12.958
235.00	82.145	7133.9	30.357	43.956	3195.7	13.599
240.00	84.223	7549.8	31.457	45.707	3419.9	14.249
245.00	86.260	7976.0	32.555	47.465	3652.8	14.909
250.00	88.256	8412.3	33.649	49.227	3894.5	15.578
255.00	90.210	8858.5	34.739	50.994	4145.1	16.255
260.00	92.124	9314.4	35.824	52.765	4404.5	16.940
265.00	93.997	9779.7	36.904	54.537	4672.7	17.633
270.00	95.828	10254.	37.979	56.312	4949.9	18.333
273.15	96.961	10558.	38.652	57.430	5129.0	18.777
275.00	97.618	10738.	39.047	58.086	5235.8	19.039
280.00	99.366	11230.	40.108	59.861	5530.7	19.753
285.00	101.07	11731.	41.163	61.635	5834.5	20.472
290.00	102.74	12241.	42.210	63.407	6147.1	21.197
295.00	104.37	12759.	43.250	65.177	6468.5	21.927
298.15	105.38	13089.	43.901	66.291	6675.6	22.390
300.00	105.96	13285.	44.282	66.945	6798.8	22.663
305.00	107.51	13818.	45.306	68.709	7138.0	23.403
310.00	109.04	14360.	46.322	70.470	7485.9	24.148
315.00	110.52	14909.	47.329	72.226	7842.7	24.897
320.00	111.98	15465.	48.328	73.978	8208.2	25.651
325.00	113.40	16028.	49.318	75.726	8582.4	26.407
330.00	114.79	16599.	50.300	77.468	8965.4	27.168
335.00	116.16	17176.	51.272	79.204	9357.1	27.932
340.00	117.49	17760.	52.237	80.935	9757.5	28.698
345.00	118.79	18351.	53.192	82.660	10166.	29.468
350.00	120.07	18948.	54.138	84.378	10584.	30.240
355.00	121.31	19552.	55.075	86.090	11010.	31.015
360.00	122.54	20161.	56.004	87.795	11445.	31.791
365.00	123.74	20777.	56.924	89.494	11888.	32.570
370.00	124.94	21399.	57.835	91.186	12340.	33.351
373.15	125.68	21794.	58.404	92.248	12629.	33.844
375.00	126.12	22026.	58.737	92.871	12800.	34.133
380.00	127.31	22660.	59.632	94.549	13269.	34.917

H_0^c is the enthalpy of the solid at 0 °K and 1 atm pressure.

(at most 5 to 10 percent) and fairly constant. Below about 150 or 100 °K, a rapid increase in positive deviation occurs. At 10 °K the deviation is as much as 100 percent. This behavior is interpreted to arise from the contribution to the heat capacity of the additional vibrational degrees of freedom present in the compound becoming predominant at the lower temperatures. Further study on the additivity of the heat capacity is in progress. Below 100 °K, the accuracy of some of the data used in the analysis [10] is somewhat uncertain.

The authors are indebted to several members of the staff at the National Bureau of Standards for the chemical and crystallographic analyses of the chrysoberyl sample investigated; to Martha Darr for the spectrochemical analysis, to A. Van Valkenburg for the petrographic analysis, to H. S. Peiser for the x-ray diffraction measurements, and to T. J. Murphy for the chemical analysis.

6. References

[1] K. K. Kelley and E. G. King, Contributions to the Data on Theoretical Metallurgy. XIV. Entropies of the Elements and Inorganic Compounds, U.S. Bureau of Mines Bull. No. 592 (1961).
[2] S. M. Lang, C. L. Fillmore, and L. H. Maxwell, J. Research NBS **48,** 298 (1952) RP2316.
[3] A. D. Fedoseev, Ogneupory **26,** 285 (1961).
[4] W. R. Foster and H. F. Royal, J. Am. Ceram. Soc. **32,** 26 (1949).
[5] C. Palache, H. Berman, and C. Frondel, The System of Mineralogy, **1,** 718 (J. Wiley & Sons, New York, 1944).
[6] R. B. Scott, C. H. Meyers, R. D. Rands, Jr., F. G. Brickwedde, and N. Bekkedahl, J. Research NBS **35,** 39 (1945) RP1661.
[7] H. F. Stimson, J. Research NBS **65A,** (Phys. and Chem.) No. 3, 139 (1961).
[8] H. J. Hoge and F. G. Brickwedde, J. Research NBS **22,** 351 (1939) RP1188.
[9] IUPAC Revises Atomic Weight Values, Chem. Eng. News **39,** 42 (1961).
[10] G. T. Furukawa and W. G. Saba, unpublished work.

(Paper 69A1–322)

JOURNAL OF RESEARCH of the National Bureau of Standards—A. Physics and Chemistry
Vol. 69A, No. 1, January–February 1965

Thermodynamics of the Ternary System: Water-Sodium Chloride-Barium Chloride at 25 °C

R. A. Robinson and V. E. Bower

(September 15, 1964)

Isopiestic vapor pressure measurements have been made on the ternary system water-sodium chloride-barium chloride at 25 °C. From these data the activity coefficient of each salt in the presence of the other has been calculated. The rule that the logarithm of the activity coefficient of one salt (which is equivalent to its chemical potential) varies linearly with the concentration of the other salt has been investigated. It is shown that this rule is at least approximately valid with the condition usually assumed, namely, that the total ionic strength is kept constant. It is shown, moreover, to be valid for another condition, namely, that the total concentration of ions is kept constant. This latter condition is more suited to isopiestic studies. Finally, the calculation of mutual solubilities from isopiestic data is described.

1. Introduction

Systems of the type H_2O-HCl-MCl, where M designates a univalent cation, have been studied extensively [1, 2],[1] using concentration cells with hydrogen and silver-silver chloride electrodes. Such cells are admirably suited to the determination of the chemical potential and activity coefficient of hydrochloric acid in the presence of added chloride and to a study of the variation of the activity coefficient of hydrochloric acid under selected conditions. Thus, one may ask how the activity coefficient of hydrochloric acid varies if the concentration of acid is kept constant and sodium chloride is added in increasing amounts. Or one may ask how the activity coefficient of the acid would vary if both the acid and the salt concentration were allowed to change subject to a restraining condition; such a condition might be that the total ionic strength remained constant.

Questions of this nature have been answered in considerable detail by Harned and his colleagues [1]. Moreover, studies have been extended to systems in which the added chloride is that of a polyvalent cation, for example, barium or strontium chloride [3, 4] or cadmium chloride [5]. Systems have also been studied in which there is no common ion, for example, the system water-hydrochloric acid-calcium perchlorate [6].

When, however, systems containing two salts with water as solvent are encountered, this emf method has only very limited application. In a few cases, suitable electrodes may be available; for example, the activity coefficient of zinc chloride in the presence of calcium chloride has been measured [7] using a cell with zinc amalgam and silver-silver chloride electrodes. Such well-behaved electrodes are not numerous and there are many interesting three-component systems where this emf method would be difficult, if not impossible, to apply. Thus it is difficult to see how suitable electrodes could be devised to study the very simple system water-sodium chloride-potassium chloride and even more difficult to suggest an emf method for the system water-sodium nitrate-potassium nitrate.

The isopiestic vapor pressure method has advantages in this respect and serves as a useful complement to the emf method. It has already been used to study the systems water-sodium chloride-potassium chloride [8] and water-potassium chloride-potassium bromide [9]. Results are now reported for the system water-sodium chloride-barium chloride; such results are of interest in themselves because they characterize a system of two simple inorganic solutes; in addition, this study reveals some difficulties which have to be overcome in extending the isopiestic method to solutions containing salts of different valence types.

2. Methods

2.1. Definitions

If an aqueous solution of sodium chloride is in isopiestic (vapor-phase) equilibrium with another aqueous solution containing both sodium chloride and barium chloride, then the two solutions have the same aqueous vapor pressure.

The following definitions are made.

M_B is the molality (moles per kilogram of solvent) of a solution containing only sodium chloride (sometimes termed the "reference" solution).

M_c is the molality of a solution containing barium chloride only, in isopiestic equilibrium with the sodium chloride solution of molality M_B.

m_B, m_c are the molalities of sodium chloride and barium chloride, respectively, in a solution containing both these salts and in isopiestic equilibrium with the sodium chloride solution of molality M_B and the barium chloride solution of molality M_c.

$R \equiv M_B/(m_B+1.5m_c)$ is the isopiestic ratio.

$x \equiv 1.5m_c/(m_B+1.5m_c)$ is the "ionic fraction" of barium chloride in the mixture of sodium chloride and barium chloride. m is any linear combination of the form

$$m = k_B m_B + k_c m_c.$$

[1] Figures in brackets indicate the literature references at the end of this paper.

For this study it is convenient to put

$$k_B=1,\ k_c=1.5,\ m=m_B+1.5m_c.$$

Γ_B is the (molal) activity coefficient of sodium chloride in the reference solution at molality M_B in equilibrium with the solution containing both sodium chloride and barium chloride.

Γ_c is the activity coefficient of barium chloride at molality M_c in equilibrium with the reference solution of sodium chloride at molality M_B.

γ_B, γ_c are the activity coefficients of sodium chloride and barium chloride, respectively, in the mixed solution at molalities m_B and m_c.

γ_B° is the activity coefficient of sodium chloride in a solution containing sodium chloride only at the same total ionic strength, $I=m_B+3m_c$, as the mixed solution. γ_c° is the activity coefficient of barium chloride in a solution of barium chloride only at the same total ionic strength, $I=m_B+3m_c$, as the mixed solution.

φ is the osmotic coefficient of the reference solution, defined by the equation

$$2M_B\varphi=-55.51\ \ln a_w,$$

a_w being the water activity of this solution.

The distinction between Γ_B and γ_B° and between Γ_c and γ_c° is important. This somewhat complicated, but unavoidable, terminology is illustrated schematically in figure 1. The primary result of an isopiestic experiment is the molality M_B of a sodium chloride solution (box 3) whose water activity a_w and activity coefficient Γ_B are known. This solution is in vapor-phase equilibrium with a barium chloride solution (box 5) at molality M_c, the activity coefficient of barium chloride in this solution, Γ_c, also being known. These two solutions are also in vapor-phase equilibrium with a mixed solution of sodium chloride and barium chloride (box 4) of molalities m_B and m_c, respectively. What are not known are the activity coefficients, γ_B and γ_c, of sodium chloride and barium chloride, respectively, in this mixed solution, but it will be shown in the next section that the information in these three boxes is sufficient to calculate γ_B and γ_c.

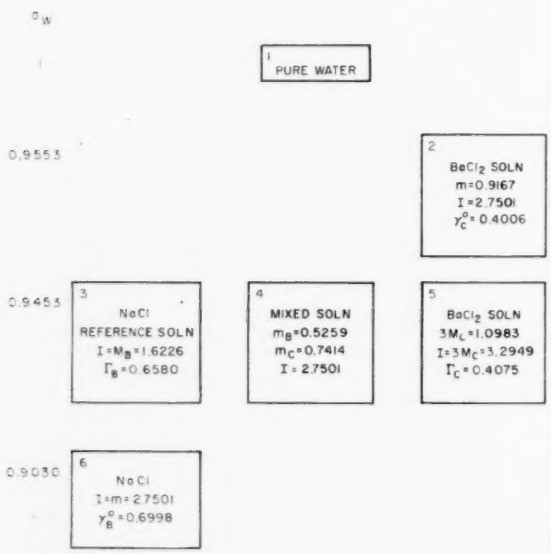

FIGURE 1.—*Schematic representation of the system water-sodium chloride-barium chloride.*

The solutions represented by boxes 3, 4, and 5 are in isopiestic equilibrium, having the same water activity. The solutions represented by boxes 2, 4, and 6 are not in isopiestic equilibrium but have the same total ionic strength. M_B, M_C, γ_B, Γ_c are known, as are m_B and m_c; γ_B and γ_c, the activity coefficients of sodium chloride and barium chloride, respectively, in the solution represented by box 4 are to be deduced.

One may now enquire how γ_B is related to γ_B°; in particular, is what is sometimes called Harned's rule [1, 2] obeyed? An equation can be written:

$$\log \gamma_B=\log \gamma_B^\circ-\alpha_B I_c-\beta_B I_c^2, \tag{1}$$

where $I_c=3\ m_c$ and α_B, β_B, are functions of the total ionic strength but not of the individual sodium chloride and barium chloride concentrations. Harned's Rule is equivalent to the statement that $\beta_B=0$. In order to investigate this, a knowledge of γ_B° is needed (box 6); that is to say we need to know the activity coefficient of a solution of sodium chloride only at the same total ionic strength as the mixed solution represented by box 4 in figure 1. Similarly, for the other component:

$$\log \gamma_c=\log \gamma_c^\circ-\alpha_c I_B-\beta_c I_B^2 \tag{2}$$

where $I_B=m_B$, and a knowledge of γ_c° (box 2) is needed to represent the variation of $\log \gamma_c$ with I_B.

2.2. McKay-Perring Method

McKay and Perring [10] have, using strict thermodynamic principles, derived an equation which can be put in the form:

$$\ln \gamma_B=\ln \Gamma_B+\ln R+\int_0^{M_B\varphi} f(m, M_B, x)\, d\,(M_B\varphi) \tag{3}$$

where

$$f(m, M_B, x)=\frac{1}{m^2}\left(\frac{\partial m}{\partial \ln x}\right)_{a_w}+\frac{1}{m}-\frac{1}{M_B}. \tag{4}$$

The isopiestic ratio, R, is the immediate result of the experiment; it is in the evaluation of the integral in eq (3) that difficulty is encountered. Let the reference solution be equilibrated, not with one mixed solution as illustrated in figure 1, but with a series of mixed solutions of sodium chloride and barium chloride in different proportions, i.e., with different values of x, all the solutions having the same value of a_w. The quantity in the integral,

$$\frac{1}{m^2}\left(\frac{\partial m}{\partial \ln x}\right)_{a_w}=-\frac{x}{M_B}\left(\frac{\partial R}{\partial x}\right)_{a_w} \tag{5}$$

is determined by the tangent to the curve of R versus x for this particular water activity; this tangent will, in general, be a function of x and the tangent is to be taken at that value of x corresponding to which it is desired to evaluate the activity coefficients γ_B and γ_c. The experiment must then be repeated to that $(\partial R/\partial x)$, at this particular value of x, can be determined as a function of $(M_B\varphi)$ and the integration over the interval 0 to $(M_B\varphi)$ performed. There is no theoretical way of predicting the variation of $(\partial R/\partial x)$ with $(M_B\varphi)$ but a considerable simplification ensues if, for the system in question, the isopiestic ratio can be expressed as

$$R=a-bx-cx^2 \tag{6}$$

where a, b, and c are functions of M_B but not of x; for, in this case, the integral reduces to [8]

$$x^2\int_0^{M_B\varphi}(c/M_B)d(M_B\varphi)$$

and the integral vanishes if $c=0$,

$$R=a-bx. \tag{7}$$

In this case, eq (3) takes the very simple form

$$\log\gamma_B=\log\Gamma_B+\log R \tag{8}$$

and for the other component

$$\log\gamma_c=\log\Gamma_c+\log R' \tag{9}$$

where

$$R'=\frac{1.5M_c}{m_B+1.5m_c}.$$

2.3. Experimental Procedure

The apparatus was that used in an earlier investigation of the system water-sodium chloride-urea [11]. Eleven gold-plated silver dishes were used; three of them contained the reference sodium chloride solution and the remaining eight dishes were divided into four groups with four different mixtures each in duplicate (or three different mixtures and one pair containing a solution of barium chloride only). The sodium chloride was part of the sample used previously [11]; barium chloride was recrystallized twice from water. Analysis showed the presence of 25 ppm of calcium and 350 ppm of strontium.[2] In each run, stock solutions of sodium chloride and barium chloride were prepared and mixed in different proportions. The stock solution of barium chloride was analyzed by the method of Newton and Tippetts [12].

The results of one experiment are quoted in detail to illustrate the agreement between the molalities of solutions in duplicate (or triplicate) dishes:

[2] Analyses by R. W. Burke of the Analysis and Purification Section.

m_B	2.6189	1.7265	1.0075	0.2911	0
	2.6183	1.7261	1.0071	.2911	0
	2.6182				
m_c	0	0.5781	1.0450	1.5105	1.6998
	0	.5780	1.0445	1.5107	1.6998

3. Results

The experimental results are given in table 1. The second column gives the molality (M_B) of the reference sodium chloride solution, the third and

TABLE 1. *Isopiestic data for the system: water—sodium chloride (B)—barium chloride (C) at 25 °C*

Set	M_B	m_B	m_c	x	R(obs.)	R(calc.)	Δ_1	Δ_2
1	0.5044	0.3591	0.1045	0.3038	0.9780	0.9787	+0.07	+0.06
		.2213	.2037	.5800	.9576	.9574	−.02	+.04
		.0794	.3060	.8526	.9368	.9364	−.04	−.04
			.3638	1.0	.9244	.9250	+.06	0
	.5063	.4033	.0736	0.2149	.9855	.9855	0	−.04
		.2797	.1628	.4661	.9666	.9662	−0.04	+.01
		.1453	.2597	.7283	.9465	.9460	−.05	−.01
			.3645	1.0	.9248	.9250	+.02	−.04
2	.9728	0.7382	0.1644	0.2504	0.9878	0.9880	+0.02	0
		.4910	.3378	.5079	.9750	.9747	−.03	−0.02
		.2610	.4999	.7418	.9623	.9626	+.03	+.04
			.6832	1.0	.9493	.9493	0	−.03
3	1.2328	0.9479	0.1963	0.2370	0.9923	0.9924	+0.01	0
		.6389	.4092	.4900	.9841	.9836	−.05	−0.02
		.3356	.6193	.7346	.9749	.9752	+.03	+.05
			.8507	1.0	.9661	.9660	−.01	−.02
4	1.5683	1.1653	0.2730	0.2600	0.9959	0.9959	0	−.01
		0.7442	.5586	.5297	.9913	.9913	0	+.01
		.2721	.8790	.8290	.9860	.9861	+0.01	+.01
			1.0634	1.0	.9832	.9832	0	−.02
5	1.6226	1.4141	0.1421	0.1311	0.9972	0.9978	+0.06	+0.08
		0.9784	.4356	.4005	.9944	.9939	−.05	−.04
		.5259	.7414	.6790	.9906	.9899	−.07	−.07
			1.0983	1.0	.9849	.9853	+.04	+.03
6	1.8749	1.3930	0.3219	0.2574	0.9995	0.9991	−0.04	−0.01
		1.0035	.5821	.4653	.9990	.9992	+.02	+.02
		0.4308	.9647	.7706	.9985	.9994	+.09	+.07
			1.2498	1.0	1.0001	.9995	−.06	−.06
7	1.9873	1.2466	0.4905	0.3712	1.0025	1.0027	+0.02	+0.04
		0.7037	.8501	.6444	1.0042	1.0048	+.06	+.06
		.3073	1.1124	.8445	1.0058	1.0063	+.05	+.04
			1.3149	1.0	1.0076	1.0074	−.02	−.04
	2.0021	1.5471	0.3006	0.2257	1.0021	1.0017	−.04	−.03
		1.0496	.6303	.4739	1.0035	1.0035	0	+.01
		0.5733	.9452	.7121	1.0055	1.0053	−0.02	−.02
			1.3245	1.0	1.0077	1.0074	−.03	−.05
8	2.1724	1.8885	0.1878	0.1298	1.0010	1.0011	+.01	+.02
		1.3509	.5407	.3752	1.0048	1.0044	−.04	−.10
		0.7850	.9136	.6358	1.0079	1.0078	−.01	−.02
		.3184	1.2206	.8519	1.0107	1.0106	−.01	+.06
	2.1839	1.0177	0.7670	.5306	1.0072	1.0064	−.08	−.11
		0.7602	.9375	.6491	1.0081	1.0080	−.01	−.02
		.4557	1.1377	.7892	1.0100	1.0098	−.02	+.02
		.3008	1.2396	.8607	1.0110	1.0108	−.02	+.05
	2.1980	1.9192	0.1845	.1260	1.0010	1.0011	+.01	+.02
		1.3574	.5542	.3798	1.0042	1.0044	+.02	−.02
		0.8234	.9060	.6227	1.0071	1.0076	+0.5	+.04
		.3348	1.2274	.8461	1.0102	1.0106	+.04	+.10
9	2.3615	1.7350	0.4108	0.2621	1.0044	1.0043	−0.01	0
		1.1799	.7744	.4961	1.0085	1.0086	+.01	0
		0.5922	1.1591	.7459	1.0131	1.0131	0	0
			1.5466	1.0	1.0179	1.0178	−0.01	0
10	2.6185	1.7263	0.5781	0.5343	1.0097	1.0098	+0.01	0
		1.0073	1.0448	.6087	1.0171	1.0170	−.01	0
		0.2911	1.5106	.8862	1.0241	1.0241	0	+0.01
			1.6998	1.0	1.0270	1.0271	+0.01	−.01
11	2.7147	2.0250	0.4451	0.2480	1.0082	1.0087	+.05	0
		1.3969	.8514	.4776	1.0152	1.0147	−.05	−0.01
		0.6356	1.3458	.7605	1.0228	1.0221	−.07	−.03
			1.7610	1.0	1.0277	1.0283	+.06	+.03

$\Delta_1=[R(\text{calc by eq}(6))-R(\text{obs})]\times10^2$.
$\Delta_2=[R(\text{calc by eq}(5))-R(\text{obs})]\times10^2$

fourth columns give values of the molalities of sodium chloride (m_B) and barium chloride (m_c) in the mixed solutions which were found to be in isopiestic equilibrium with the reference sodium chloride solution. The next column gives values of the "ionic fraction" (x) and the sixth values of the isopiestic ratio. Figure 2 is a plot of isopiestic ratio versus ionic fraction for 3 of the 11 sets of results obtained; from this plot it would appear that R is a linear function of x. The data in each set were therefore fitted to eq (7) and the a and b parameters evaluated by the method of least squares. These values of a and b are given in the second and third columns of table 2 and the values of R calculated by eq (7) are given in the seventh column of table 1. The next column gives the difference (multiplied by 100) between the observed values of R and those calculated by eq (7). The average of these differences for each set is given in the sixth column of table 2. It will be seen from figure 2 and from table 2 that the a parameter does not have exactly the theoretical value of unity, suggesting that the plot of R versus x does have slight curvature, more pronounced at low values of x. The data were therefore fitted to eq (6) with $a=1$ and the b and c parameters, calculated by the method of least squares, are given in table 2. Values of R have been calculated with the aid of these parameters; they are not recorded in table 1 but the last column of this table gives the difference (multiplied by 100) between the observed values of R and those calculated by eq (6); the average difference for each set is given in the last column of table 2. It will be seen that any superiority eq (6) may have over eq (7) in representing the experimental data is within the experimental error; the simpler equation, (7), will therefore be used in subsequent calculations.

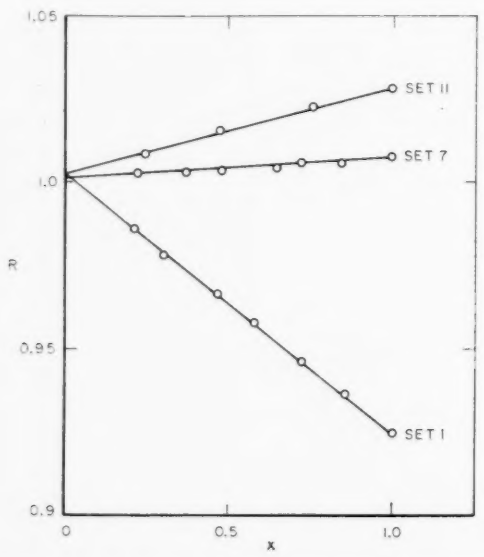

FIGURE 2. *Isopiestic ratio (R) versus ionic fraction (x).*

TABLE 2. *Values of the parameters of eq (7) and eq (6)*

Set	Eq (7)		Eq (6), a=1		Avg Δ_1	Avg Δ_2
	a	b	b	c		
1	1.002!	0.0771	0.0681	0.0075	0.04	0.03
2	1.0079	.0516	.0481	.0029	.02	.02
3	1.0006	.0345	.0318	.0023	.03	.03
4	1.0004	.0172	.0156	.0014	0	.01
5	0.9997	.0144	.0152	−.0004	0.06	.05
6	.9990	.0006	−.0030	.0025	.05	.04
7	1.0000	−.0074	−.0080	.0008	.03	.04
8	0.9994	−.0132	−.0085	−.0056	.04	.05
9	.9995	−.0183	−.0164	−.0015	.01	0
10	1.0012	−.0259	−.0300	.0031	.01	0.01
11	1.0023	−.0260	−.0349	.0069	.06	.02

4. Calculation of Activity Coefficients

This study of a mixture of a 1:1 electrolyte and a 2:1 electrolyte reveals a difficulty not encountered with mixtures of two electrolytes of the same valence type. This can be illustrated as follows. It was found [8] in a study of the system water-sodium chloride-potassium chloride that the following solutions were in isopiestic equilibrium:

m_{NaCl}	2.3248	1.8865	1.4490	1.0324	0.5630
m_{KCl}	0	0.4894	0.9701	1.4238	1.9269
$m_{NaCl}+m_{KCl}$	2.3248	2.3759	2.4191	2.4562	2.4899

Thus only a small interpolation was needed to study the system at a total ionic strength of 2.4. It is very different with the system water-sodium chloride-barium chloride as the following example, taken from set 9 of table 1, shows:

m_B	2.3615	1.7350	1.1799	0.5922	0
m_c	0	0.4108	0.7744	1.1591	1.5466
$m_B+3\ m_c$	2.3615	2.9674	3.5031	4.0695	4.6398
$m_B+1.5\ m_c$	2.3615	2.3512	2.3415	2.3309	2.3199

Thus what remains approximately constant is not the total ionic strength (m_B+3m_c) but the "total ionic concentration" as measured by ($m_B+1.5\ m_c$); for, as the above table shows, the total ionic concentrations of the five isopiestic solutions are very nearly the same—the average value is 2.3410 and the largest deviation from this value is only 0.8 percent. We therefore considered whether Harned's Rule can hold in this form: the logarithm of the activity coefficient of sodium chloride is a linear function of the molality of barium chloride in mixtures of constant total ionic concentration, with a corresponding proposition for the activity coefficient of barium chloride. We therefore rewrite eq (1) and eq (2) as:

$$\log \gamma_B = \log \gamma_B^\circ - \alpha_B m_c \qquad (10)$$

$$\log \gamma_c = \log \gamma_c^\circ - \alpha_c m_B \qquad (11)$$

γ_B° and γ_c° do not have the meanings assigned to

them in section 2.1; in the present context, γ_B° is now the activity coefficient of sodium chloride in a solution of sodium chloride only at a molality equal to the ionic concentration ($m_B+1.5\ m_c$) of the mixed solution; γ_c° that of barium chloride in a solution of barium chloride only at a molality equal to ($m_B+1.5\ m_c$)/1.5. It would be possible to devise new symbols but there is no need to complicate the symbolism still further.

We now use eq (8) and eq (9) to calculate the activity coefficients of each salt in the mixture at constant total ionic concentration and then calculate α_B and α_c by eq (10) and eq (11). Values of γ_B° have already been tabulated [13]; data are available for barium chloride but the osmotic and activity coefficients have been computed again[3] from earlier isopiestic data (14,15] together with those results in table 1 which pertain to solutions of barium chloride without added sodium chloride. The data are given in table 3.

TABLE 3. *Osmotic and activity coefficients of barium chloride in aqueous solution at 25 °C*

m	φ_c	γ_c	m	φ_c	γ_c
0.10	0.8422	0.5078	1.10	0.9520	0.4076
.20	.8382	.4523	1.20	.9681	.4128
.30	.8440	.4265	1.30	.9845	.4188
.40	.8534	.4121	1.40	1.0010	.4255
.50	.8648	.4039	1.50	1.0175	.4329
.60	.8775	.3996	1.60	1.0340	.4408
.70	.8912	.3979	1.70	1.0503	.4492
.80	.9056	.3982	1.80	1.0665	.4580
.90	.9206	.4001	1.90	1.0823	.4672
1.00	.9361	.4033	2.00	1.0978	.4767

Table 4 gives the values of α_B and α_c. Substituted in eq (10) and eq (11), they will represent the data with a maximum difference of 0.0005 in log γ_B or log γ_c, the average difference being much less than this. Within experimental error, therefore, it can be concluded that the proposed modification of Harned's Rule is valid for this system. Figure 3 is a plot of α_B and α_c versus M_B. This emphasizes the fact that α_B and α_c have large values in dilute solutions and small values in concentrated solutions. Thus there are large excess free energy terms in mixing dilute solutions of sodium chloride and barium chloride at constant total ionic concentration but these terms are much smaller (and of opposite sign) if the solutions are concentrated. This is a somewhat surprising result but confirms what has been observed before, particularly for the system water-hydrochloric acid-cesium chloride.

Table 4 also contains values of ($\alpha_B+1.5\ \alpha_c$) and these are plotted versus M_B in figure 3. Now it has been shown [16, see also appendix] as a direct result of the cross-differentiation relation,

$$2\left(\frac{\partial \log \gamma_B}{\partial m_c}\right)_{m_B} = 3\left(\frac{\partial \log \gamma_c}{\partial m_B}\right)_{m_c} \qquad (12)$$

that the α_B and α_c parameters of eq (10) and eq (11) must obey the relation

$$(\alpha_B+1.5\ \alpha_c) = \text{constant independent of } (m_B+1.5\ m_c) \qquad (13)$$

provided that

(1) α_B and α_c are functions of ($m_B+1.5$ m$_c$) only, and

(2) there are no terms in m_B and m_c other than $\alpha_B\, m_c$ and $\alpha_c m_B$, i.e., terms such as $\beta_B m_c^2$ are excluded. It will be seen that ($\alpha_B+1.5\ \alpha_c$) is very nearly constant, the largest deviation is at the lowest concentration where ($\alpha_B+1.5\ \alpha_c$) is the summation of two large terms of opposite sign. No significance is attached to the very slight variation of ($\alpha_B+1.5\,\alpha_c$) which is well within the experimental error and it is concluded that eq (10) and eq (11) suffice without the need for additional terms in higher powers of m_B and m_c.

TABLE 4. *Values of the parameters α_B and α_c of eq (10) and eq (11)*

Set	α_B	α_c	$(\alpha_B+1.5\alpha_c)$
1	0.0859	−0.0602	−0.0044
2	.0320	−.0225	−.0018
3	.0175	−.0128	−.0017
4	.0069	−.0047	−.0002
5	.0060	−.0046	−.0009
6	.0005	0	.0005
7	−.0025	.0019	.0004
8	−.0040	.0033	.0010
9	−.0055	.0044	.0011
10	−.0081	.0058	.0006
11	−.0085	.0055	−.0002

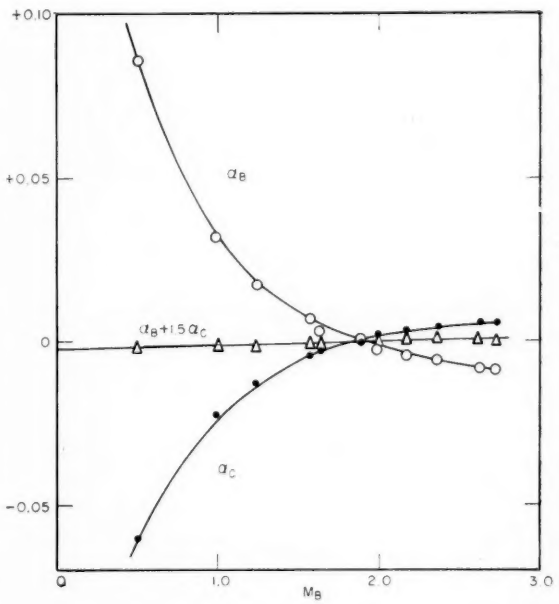

FIGURE 3. *α_B, α_c, and ($\alpha_B+1.5\alpha_c$) versus M_B for systems at constant total ionic concentration.*

[3] We thank Dr. Wallace Davis, Jr., of the Oak Ridge National Laboratory for these computations.

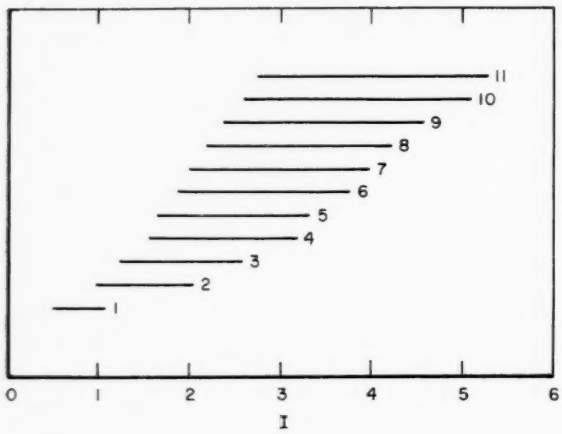

FIGURE 4. *Span of total ionic strength in each set of measurements.*

We could stop at this point because we have obtained a complete description of the system over the concentration range $0.5 < (m_B + 1.5\ m_c) < 2.7$; eq (10) and eq (11) with the α_B, α_c parameters of table 4 give this information. It is of interest, however, to pursue the calculation and consider variations at constant total ionic strength instead of constant total ionic concentration. The difficulty of applying the isopiestic method to systems of different valence types at constant total ionic strength has already been referred to; figure 4 illustrates this in another way by showing the span of values of total ionic strength covered in each of the eleven sets of measurements. It shows that, whereas the set of five results quoted above for the system water-sodium chloride-potassium chloride contribute five points to the data at a total ionic strength, 2.4, any one set in the water-sodium chloride-barium chloride system contributes effectively only one point at any selected total ionic strength. Thus, results from different sets have to be harnessed in order to obtain data at different values of x at any given total ionic strength. Moreover, the number of contributions depends on the total ionic strength. Thus, at $I=3$, sets 4 to 11 make eight contributions; at $I=5$, sets 10 and 11 only contribute.

We proceed as follows. At a total ionic strength of $I=3$, for example, we could have five solutions of the following compositions:

No.	$m_B = I_B$	I_c	1.5 m_c	m
1	0.5	2.5	1.25	1.75
2	1.0	2.0	1.00	2.00
3	1.5	1.5	0.75	2.25
4	2.0	1.0	.50	2.50
5	2.5	0.5	.25	2.75

A value of $\log \gamma_B$ for each solution can be calculated by eq (10) using the value of $\log \gamma_B^\circ$ appropriate to each value of m and a value of α_B for each value of m is read from a large scale plot of figure 3. Then a new value of α_B is calculated by eq (1), ignoring the $\beta_B I_c^2$ terms. The calculation is as follows:

No.	$-\log \gamma_B^\circ$	α_B eq (10)	$-\log \gamma_B$	α_B eq (1)	$-\log \gamma_B$ (calc.)
1	0.1799	0.0025	0.1820	0.0142	0.1818
2	.1755	−.0018	.1743	.0139	.1747
3	.1702	−.0050	.1677	.0141	.1677
4	.1627	−.0070	.1604	.0139	.1606
5	.1550	−.0085	.1531	.0132	.1536

The best value of α_B for use in eq (1) is 0.0141 and, substituting for $-\log \gamma_B^\circ = 0.1465$ at $I=3$, we get

$$\log \gamma_B = -0.1465 - 0.0141\ I_c$$

Values of $-\log \gamma_B$ calculated by this equation are given in the last column of the above table; it is evident that, at least at $I=3$, eq (1) is adequate with only a term linear in I_c, so that $\beta_B = 0$. Table 5

TABLE 5. *Values of the parameters of eq (1) and eq (2)* $\beta_B = \beta_c = 0$

I	α_B	α_c	$(2\alpha_B + \alpha_c)$
0.75	0.0082	−0.0077	0.0087
1.5	.0095	−.0085	.0105
2.0	.0111	−.0118	.0104
2.5	.0127	−.0155	.0099
3.0	.0141	−.0173	.0109
3.5	.0159	−.0191	.0127
4.0	.0167	−.0206	.0128
4.5	.0178	−.0218	.0138
5.0	.0188	−.0225	.0151

gives values of α_B and α_c calculated in this way at different values of the total ionic strength. The last column gives values of $(2\alpha_B + \alpha_C)$, a quantity which is important because it can be shown [16, see also appendix] that in a system represented by eq (1) and eq (2) with $\beta_B = \beta_c = 0$, the quantity $(2\alpha_B + \alpha_c)$ should be independent of the total ionic strength. Not all the values of α_B and α_c in table 5 are of equal reliability, partly because at some values of I we can use more sets of data from tables 1 and 4 than at others, and partly because there is some difficulty in interpolating in figure 5 at low values of I; the data at $I=2.5$, 3.0, and 3.5 are probably more reliable, those at higher and lower total ionic strengths less so.

Figure 5 compares these values of α with those given by Harned and Gary [1, 4] for the system water-hydrochloric acid-barium chloride. We note that the α value for barium chloride is negative in both systems, so that the replacement of barium chloride by either hydrochloric acid or sodium chloride in a system at constant total ionic strength raises the activity coefficient of barium chloride; the effect is, however, much larger with hydrochloric acid. The α values for hydrochloric acid and sodium chloride are positive so that the activity coefficient of each is

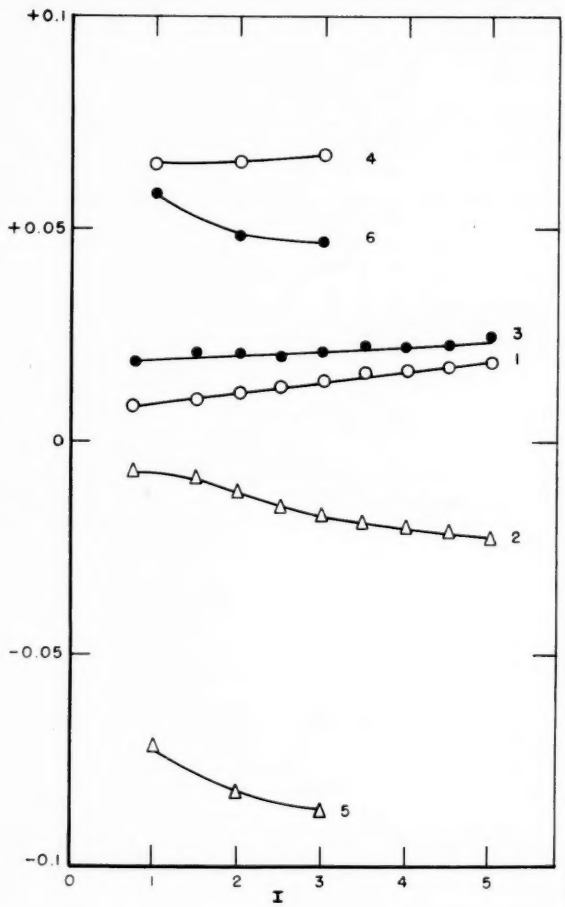

FIGURE 5. *Parameters of eq (1) and eq (2).*

System water; sodium chloride (B)-barium chloride (C) curve 1 α_B; curve 2 α_c; curve 3 $(2\alpha_B+\alpha_c)$, the curve has been raised by 0.01 for the sake of clarity. System water-hydrochloric acid (B)-barium chloride (C) curve 4 α_B; curve 5 α_c; curve 6 $(2\alpha_B+\alpha_c)$.

decreased by barium chloride; again the effect is very much larger with hydrochloric acid. For the sodium chloride-barium chloride system, $(2\alpha_B+\alpha_c)$ increases slightly with increasing total ionic strength. The effect may be spurious, due to the difficulty we have in evaluating data in systems of constant total ionic strength. If the effect is real, it suggests that the β terms in eq (1) and eq (2) are not both zero; $\beta_B=-0.0003$, $\beta_c=0$ would satisfy the condition demanded by the cross-differentiation relation, eq (12).

5. Solubility Relations

Let m_s be the solubility of sodium chloride in water and γ_s its activity coefficient at this molality. Let m_B be the solubility of sodium chloride in a solution of barium chloride of molality m_c and γ_B its activity coefficient. Then

$$m_s^2\gamma_s^2=m_B(m_B+2m_c)\gamma_B^2$$

or

$$m_s\gamma_s=m_B(1+2m_c/m_B)^{1/2}\gamma_B$$

or

$$\log m_B/m_s=-\log \gamma_B/\gamma_s-1/2\log(1+2m_c/m_B).$$

Furthermore,

$$\log \gamma_B=\log \gamma_B^\circ-3\alpha_B m_c.$$

At 25 °C, $m_s=6.147$ mole kg^{-1} [17] and $\log \gamma_s=0.0020$. Moreover, in the vicinity of $m_B=6$ mole kg^{-1}, $\log \gamma_B^\circ$ is almost linear in the total ionic strength,

$$\log \gamma_B^\circ=\log \gamma_s+0.0545\,(m_B+3m_c-m_s).$$

Hence

$$\log m_B/m_s=-0.0545\,(m_B+3m_c-m_s)+3\alpha_B m_c-1/2\log(1+2m_c/m_B).$$

Now α_B is a function of (m_B+3m_c) and m_B is not known in advance. However, an inspection of table 5 and figure 5 shows that in concentrated solutions the value of α_B is not very sensitive to the value of the total ionic strength and for our present purpose we can put $\alpha_B=0.02$ as a good approximation. The solution of this equation predicts a solubility of 5.465 mole kg^{-1} in 0.5 m barium chloride solution and of 4.813 mole kg^{-1} in 1.0 m barium chloride solution (such solution would be supersaturated with respect to barium chloride).

The solubility of barium chloride in sodium chloride solutions is governed by somewhat different considerations because it is the dihydrate which is the stable solid phase. Representing the molality and activity coefficient of barium chloride in the saturated aqueous solution by m_s and γ_s, respectively, we have:

$$4m_s^3\gamma_s^3a_{w(s)}^2=m_c(m_B+2m_c)^2\gamma^3a_w^2$$

where $a_{w(s)}$ is the water activity of the saturated aqueous solution and a_w that of the saturated solution containing sodium chloride at molality m_B. Thus,

$$\log m_c/m_s=-\log \gamma_c/\gamma_s-2/3\log(1+m_B/2m_c)-2/3\log(a_w/a_{w(s)}).$$

At 25 °C, $m_s=1.790$ mole kg^{1-}[18], $\log \gamma_s=-0.3400$. Again, $\log \gamma_c^\circ$ is almost linear in the total ionic strength:

$$\log \gamma_c^\circ=\log \gamma_s+0.0283\,(m_B+3m_c-3m_s)$$

so that

$$\log m_c/m_s = -0.0283\ (m_B+3m_c-3m_s)+\alpha_c m_B$$
$$-\tfrac{2}{3}\log\ (1+m_B/2\ m_c)-\tfrac{2}{3}\log\ (a_w/a_{w(s)}).$$

From table 5 and figure 5 it would appear that $\alpha_c \approx -0.023$ for the saturated solution. In this way we have calculated solubilities of barium chloride of 1.401, 1.045, 0.736, 0.484, 0.299, 0.175, and 0.100 moles/kg in solutions of 1.0, 2.0, 3.0, 4.0, 5.0, 6.0, and 7.0 *m*-NaCl, respectively. These data have been used to construct the two curves in figure 6. There seem to be no direct measurements of mutual solubility at 25° but Findlay and Cruickshank [19] determined the compositions of eight saturated solutions at 20 °C; these are represented by closed circles in figure 6. Schreinemakers and de Baat [20] made eight measurements at 30 °C and these are represented by open circles in figure 6. In spite of the approximations we made in calculating solubilities from isopiestic data, the agreement is good and confirms the validity of the data given in table 5 to describe the activity coefficients of the salts in the system water-sodium chloride-barium chloride.

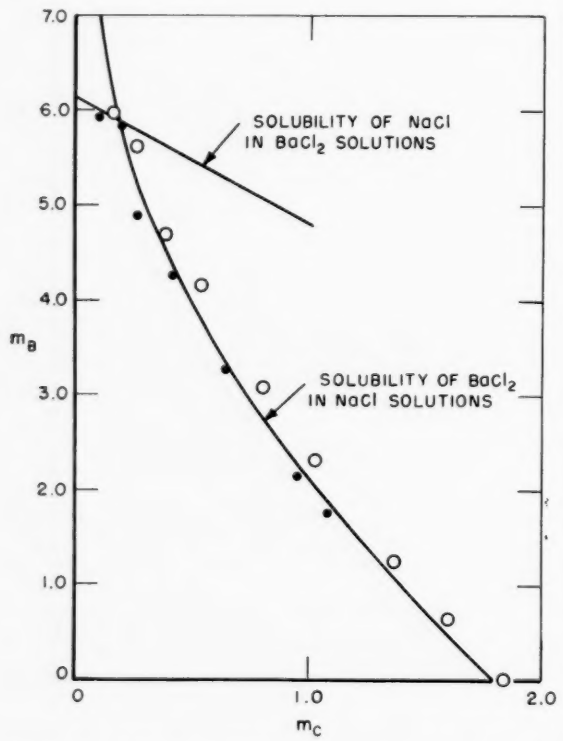

FIGURE 6. *Solubility relations in the system water-sodium chloride-barium chloride.*

———, Solubility curves calculated from isopiestic data at 25 °C.
●, Direct measurements at 20 °C.
○, Direct measurements at 30 °C.

7. Appendix

Although the derivation of eq (13) has already been described [1, 16], it is worthwhile considering the more general case of a mixture of electrolytes of different valence types for which the β terms of eq (1) and eq (2) are not zero. Consider a solution of electrolyte B (giving ν_B ions) at molality m_B, and electrolyte C (giving ν_c ions) at molality m_c. Let ζ be a linear combination of the form

$$\zeta = k_B m_B + k_c m_c$$

and let the activity coefficients at constant ζ be given by

$$\log \gamma_B = \log \gamma_B^\circ - A_B m_c - B_B m_c^2$$

$$\log \gamma_c = \log \gamma_c^\circ - A_c m_B - B_c m_B^2$$

where A_B and A_c are functions of ζ but not of m_B and m_c individually and B_B, B_c are parameters independent of ζ, m_B, and m_c. The cross-differentiation relation:

$$\nu_B\left(\frac{\partial \log \gamma_B}{\partial m_c}\right)_{m_B} = \nu_c\left(\frac{\partial \log \gamma_c}{\partial m_B}\right)_{m_c}$$

can be written:

$$\nu_B k_c\left(\frac{\partial \log \gamma_B}{\partial \zeta}\right)_{m_B} = \nu_c k_B\left(\frac{\partial \log \gamma_c}{\partial \zeta}\right)_{m_c}.$$

Moreover,

$$\log \gamma_B = \log \gamma_B^\circ - A_B(\zeta - k_B m_B)/k_c - B_B(\zeta - k_B m_B)^2/k_c^2$$

and

$$\log \gamma_c = \log \gamma_c^\circ - A_c(\zeta - k_c m_c)/k_B - B_c(\zeta - k_c m_c)^2/k_B^2.$$

As $\log \gamma_B^\circ$, $\log \gamma_c^\circ$, A_B, and A_c are functions of ζ only,

$$\nu_B k_c\left\{\frac{d \log \gamma_B^\circ}{d\zeta} - \frac{A_B}{k_c} - \frac{\zeta - k_B m_B}{k_c}\frac{dA_B}{d\zeta} - 2B_B\frac{\zeta - k_B m_B}{k_c^2}\right\}$$
$$= \nu_c k_B\left\{\frac{d \log \gamma_c^\circ}{d\zeta} - \frac{A_c}{k_B} - m_B\frac{dA_c}{d\zeta} - 2B_c m_B/k_B\right\}.$$

If this equality is to hold for all values of ζ and m_B, the coefficient of m_B must vanish, and

$$\nu_B k_B k_c\frac{dA_B}{d\zeta} + \nu_c k_B k_c\frac{dA_c}{d\zeta}$$
$$= -2(\nu_B k_B B_B + \nu_c k_c B_c)$$

or

$$k_B k_c(\nu_B A_B + \nu_c A_c) = \text{constant} - 2(\nu_B k_B B_B + \nu_c k_c B_c)\zeta$$

If $\nu_B=2$, $\nu_c=3$, $k_B=1$, $k_c=3$, as with sodium chloride and barium chloride at constant total ionic strength,

$(6A_B+9A_c)$=constant $-2(2B_B+9B_c)I$ or, putting $A_B=3\alpha_B$, $A_c=\alpha_c$, $B_B=9\beta_B$, $B_c=\beta_c$,

$\log \gamma_B=\log \gamma_B^\circ-\alpha_B I_c-\beta_B I_c^2$
$\log \gamma_c=\log \gamma_c^\circ-\alpha_c I_B-\beta_c I_B^2$

which are eq (1) and eq (2), then

$$(2\alpha_B+\alpha_c)=\text{constant}\ -2(2\beta_B+\beta_c)I.$$

If $v_B=2$, $v_c=3$, $k_B=1$, $k_c=1.5$, as with sodium chloride and barium chloride at constant total ionic concentration,

$1.5\ (2A_B+3A_c)$=constant $-2(2B_B+4.5B_c)\ (m_B+1.5m_c)$

or, putting $A_B=\alpha_B$, $A_c=\alpha_c$, $\beta_B=\beta_c=0$,

$$\log \gamma_B=\log \gamma_B^\circ-\alpha_B m_c,$$
$$\log \gamma_c=\log \gamma_c^\circ-\alpha_c m_B$$

which are eq (10) and eq (11), then

$$(\alpha_B+1.5\alpha_c)=\text{constant}.$$

Alternatively, we could put $A_B=1.5\,\alpha_B$,

$A_c=\alpha_c$, $B_B=1.5^2\beta_B$, $B_c=\beta_c$, so that:

$\log \gamma_B=\log \gamma_B^\circ-\alpha_B(1.5m_c)-\beta_B(1.5m_c)^2$,

$\log \gamma_c=\log \gamma_c^\circ-\alpha_c m_B-\beta_c m_B^2$

and obtain the more compact equation:

$(\alpha_B+\alpha_c)=\text{constant}-2(\beta_B+\beta_c)(m_B+1.5m_c)$.

8. References

[1] H. S. Harned and B. B. Owen, The physical chemistry of electrolytic solutions, ch. 14, 3d. Ed., (Reinhold Publ. Corp., New York, N.Y., 1958).
[2] R. A. Robinson and R. H. Stokes, Electrolyte solutions, ch. 15, 2d. Ed., (Butterworths Scientific Publications, London, 1959).
[3] H. S. Harned and T. R. Paxton, J. Phys. Chem. **57,** 531 (1961).
[4] H. S. Harned and R. Gary, J. Am. Chem. Soc. **76,** 5924 (1954).
[5] W. J. Argersinger, L. Leifer, and A. W. Davidson, J. Phys. Chem. **57,** 531 (1961).
[6] J. M. Stokes and R. H. Stokes, J. Phys. Chem **67,** 2442 (1963).
[7] R. A. Robinson and R. O. Farrelly, J. Phys. Chem. **51,** 704 (1947).
[8] R. A. Robinson, J. Phys. Chem. **65,** 662 (1961).
[9] W. H. McCoy and W. E. Wallace, J. Am. Chem. Soc. **78,** 1830 (1956).
[10] H. A. C. McKay and J. K. Perring, Trans. Faraday Soc. **49,** 163 (1953).
[11] V. E. Bower and R. A. Robinson, J. Phys. Chem. **67,** 1524 (1963).
[12] E. A. Tippetts and R. F. Newton, J. Am. Chem. Soc. **56,** 1675 (1934).
[13] Reference 2, p. 476.
[14] R. A. Robinson, Trans. Faraday Soc. **36,** 735 (1940).
[15] R. A. Robinson, Proc. Roy. Soc. New Zealand **75,** 203 (1955).
[16] E. Glueckauf, H. A. C. McKay, and A. R. Mathieson, J. Chem. Soc. (London) S299 (1949).
[17] F. J. Kelly, R. A. Robinson, and R. H. Stokes, J. Phys. Chem. **65,** 1958 (1961).
[18] H. W. Foote and F. C. Hickey, J. Am. Chem. Soc. **59,** 648 (1937).
[19] A. Findlay and J. Cruickshank, J. Chem. Soc. (London) **129,** 316 (1926).
[20] F. A. H. Schreinemakers and W. C. de Baat, Z. Phys. Chem. **65,** 586 (1908–1909).

(Paper 69A1–323)

JOURNAL OF RESEARCH of the National Bureau of Standards—A. Physics and Chemistry
Vol. 69A, No. 1, January–February 1965

Compressibility of Eleven Inorganic Materials

C. E. Weir

(September 2, 1964)

Volume compression measurements were made on eleven inorganic materials to a maximum pressure of 10,000 atm. Coefficients of the empirical equation $-\Delta V/V_o = a(P-2000) + b(P-2000)^2$ were determined for the substances studied. Values of a in units of 10^{-6} atm^{-1} and b in units 10^{-10} atm^{-2} are as follows: Monel—$a=0.62$ $b=0$; Waspalloy—$a=0.65$, $b=0$; sapphire—$a=0.34$, $b=0$; rutile—$a=0.46$, $b=0$; spinel—$a=0.39$, $b=0$; BaS—$a=3.99$, $b=-1.6$; CaS—$a=2.48$, $b=-1.1$; B_2O_3 (crystalline)—$a=3.24$, $b=-0.29$; H_3BO_3—$a=11.65$, $b=-3.2$; As_2O_3 (glass)—$a=8.34$, $b=-1.7$; and As_2S_3 (glass)—$a=8.12$, $b=-2.8$.

1. Introduction

During several years of systematic studies of P–V behavior of solids, data were occasionally obtained on a few miscellaneous materials. These materials were studied because of requests for the data or as part of a proposed systematic study which never materialized. Inasmuch as the P–V data (and the derived compressibilities) were of sufficient interest to warrant investigation, they appear to deserve publication. This report contains volume compression data on 11 inorganic materials studied at room temperature to a maximum pressure of 10,000 atm.

2. Experimental Method and Materials

The method used has been described previously in considerable detail [1] [1] and will be outlined here briefly. The specimen was immersed in Varsol in the bore of a heavy-walled steel vessel. A leakproof piston forced into the bore generated pressure in the Varsol, thereby compressing both the Varsol and the specimen. A similar experiment was performed in which a steel bar of similar volume replaced the specimen. Comparison of the piston position at equal pressures in the two experiments permitted calculation of the compression ($-\Delta V/V_o$) of the unknown in terms of the compression of steel which is known [2].[2] Pressure was measured by means of a manganin coil immersed in the Varsol inside the pressure vessel. The pressure gage was calibrated at the water-ice VI transition point at room temperature [3]. In such experiments a fiducial point at 2,000 atm was used because of friction in the packing washers of the movable piston. All volume changes were calculated from this pressure.

The materials studied and their method of preparation were as follows:

1. Monel metal[3]—this Nickel-copper alloy was obtained commercially.

2. Waspalloy—a complex alloy of nickel was also obtained commercially. Both of these alloys were studied in the annealed state in the form of bars approx. ½ in. diam.×4 in. long.

3. Sapphire—several rods of Al_2O_3, each a single crystal, prepared by the flame-fusion process comprised the specimen studied. The specimens were obtained commercially.

4. Rutile—a single crystal rod of TiO_2 approx. ½ in. diam.×4 in. long was prepared by flame fusion. The specimen was heated in an oxygen atmosphere subsequent to formation but was still oxygen deficient as indicated by its purplish color.

5. Spinel—hand-picked natural spinel crystals obtained from Ceylon gravel. The specimen studied was composed of a quantity of small crystals contained in an open steel cylinder.

6. B_2O_3—crystalline B_2O_3 was obtained from dehydrated H_3BO_3 by the method described by Kracek et al. [4]. The specimen consisted of

[1] Figures in brackets indicate the literature references at the end of this paper.

[2] The question of the variability of compressibility of steel with composition was investigated by L. H. Adams. He did not publish the results but found that Bridgman's compressibility value for steel was valid for straight carbon steels within the experimental error of the measurement of the compressibility. The reference steel bars used here were fabricated from drill rod, which contains approximately 0.9 percent carbon.

[3] Both Monel and Waspalloy are nickel alloys with the following nominal compositions (values reported are percentages, given only for those components present in excess of 1%).
Monel; Ni–67, Cu–30, Fe–1.5, Mn–1.0, Si, C.
Waspalloy; Ni–59, Cr–19.5, Co–13.5, Mo–4.3, Ti–3.0, Al–1.4, Fe, B, Zr.

several large fragments contained in an open steel cylinder. Although the specimen was crystalline it was not certain that it did not also contain a small quantity of uncrystallized B_2O_3 glass.

7. H_3BO_3—orthoboric acid was a reagent grade material. The specimen consisted of polycrystalline powder contained in an open steel cylinder.

8. As_2O_3—glass, prepared by melting reagent grade material in a sealed, evacuated tube. The specimen consisted of a cylindrical bar.

9. As_2S_3—glass, preparation and specimen similar to As_2O_3.

10. CaS—powdered material of commercial origin. The specimen was contained in a steel cylinder.

11. BaS—also commercially prepared powder. Handled as in the case of CaS.

3. Results and Discussion

The experimental compression data are divided into two groups based on the magnitude of the compression. The data are given in tables 1 and 2. In table 1 data are given for the compression of the less compressible materials while those for the more compressible materials are given in table 2.

For each material of low compressibility at least two independent measurements were made on each specimen and the averages are given in table 1. In general, the duplicate measurements showed that variations occurred in the fourth significant figure. Measurements made to five significant figures have been rounded off in the data of table 1 to four figures. For substances of medium compressibility duplicate measurements were made on only BaS and CaS, all other data represent the results of one determination. Several measurements were made on fresh specimens of both BaS and CaS from the same samples with some evidence that decomposition of the samples occurred with time. This result was inferred from a small but significant increase in compression with age of sample. The data reported for these two sulfides represent the averages of data obtained in the first two measurements on each compound.

TABLE 1. *Compression data for inorganic solids of low compressibility*

Pressure, atm	Compression, $-\Delta V/V_0$				
	Monel	Waspalloy	Sapphire	Rutile	Spinel
10000	0.0048	0.0050	0.0026	0.0035	0.0032
9000	44	45	24	32	29
8000	38	40	21	25	23
7000	31	33	19	23	18
6000	25	28	16	19	13
5000	19	21	10	15	10
4000	12	14	5	10	8
3000	6	6	4	4	5
2000	0.0000	0.0000	0.0000	0.0000	0.0000

For each set of data of tables 1 and 2 an empirical equation of the form

$$-\Delta V/V_0 = a(P-2000) + b(P-2000)^2 \qquad (1)$$

was fitted and the coefficients determined by the method of least squares. For the data of table 1 it is unlikely that values of the coefficient b would be meaningful because of the low compressibility.

TABLE 2. *Compression data for inorganic solids of medium compressibility*

Pressure atm	Compression, $-\Delta V/V_0$					
	BaS	CaS	B_2O_3 (cryst)	H_3BO_3	As_2O_3 (glass)	As_2S_3 (glass)
10000	0.0218	0.0132	0.0241	0.0728	0.0556	0.0467
9000	200	120	210	659	496	432
8000	178	104	187	584	437	382
7000	157	96	156	503	372	330
6000	133	79	128	419	308	275
5000	105	64	93	324	238	218
4000	78	49	59	214	151	158
3000	42	35	33	110	87	84
2000	0.0000	0.0000	0.0000	0.0000	0.0000	0.0000
1000	−0.00042	−0.0026	.....	−0.0097	−0.0093	−0.0096

For these materials the linear form was assumed and only a single coefficient was derived. For the substances of table 2, the pressure-compression relation is distinctly nonlinear and a nonzero value of b is required. The appropriate values of a and b are given in table 3.

TABLE 3. *Value of coefficients* a *and* b *of the equation* $-\Delta V/V_0 = a(P-2000) + b(P-2000)^2$

Material	a, 10^{-6}atm^{-1}	$-b$, 10^{-10}atm^{-2}
Monel	0.62	.....
Waspalloy	.65	.....
Sapphire (Al_2O_3)	.34	.....
Rutile (TiO_2)	.46	.....
Spinel ($MgAl_2O_4$)	.39	.....
BaS	3.99	1.6
CaS	2.48	1.1
B_2O_3 (cryst)	3.24	0.29
H_3BO_3	11.65	3.2
As_2O_3	8.34	1.7
As_2S_3	8.12	2.8

The data given in tables 1, 2, and 3 require little discussion. The data for Monel and Waspalloy appear to be in reasonable agreement with the values expected from simple mixtures of their respective components. Volume compression data on sapphire and rutile were obtained to provide a check on the data of Bridgman who measured only linear compression [5, 6, 7]. The agreement between volume compressions calculated from Bridgman's linear compression data and the experimental values reported here is very good. In fact, the agreement is much better than might be expected considering the experimental difficulties in measuring volume compressions of such incompressible materials. So far as can be ascertained there are no previous compression data on spinel. Data on BaS and CaS were obtained because it was suspected that Bridgman's results might be too large [8, 9]. However, the compressions obtained here are fully as large and in addition do not agree with Bridgman's results particularly well. From observations made here, it would appear that the question of purity may be of importance in producing the somewhat discordant

data obtained on these two sulfides. The compressibility of crystalline B_2O_3 is considerably less than that obtained previously on the glass [10], as is to be expected. It is to be noted that the value of b for B_2O_3 is much lower than the corresponding values found for BaS and CaS, even though the values of a are comparable in these three compounds. Inasmuch as b represents the pressure coefficient of compressibility which is large for B_2O_3 glass [10] it may be concluded that the quantity of glass in the specimen of crystalline B_2O_3 is small and that the numerical data are representative of the crystals. The compression data on H_3BO_3 was measured routinely as were the two arsenic glasses. These results require no comment.

The author is indebted to A. Friedman for the specimens of Monel and Waspalloy, to J. Wachtman for the sapphire and rutile, and to H. Yoder for the spinel. R. Waxler assisted in a few of the measurements.

4. References

[1] C. E. Weir, J. Res. NBS **45,** 468 (1950) RP2160.
[2] P. W. Bridgman, The physics of high pressure, p. 417 (G. Bell & Sons Ltd., London, 1949).
[3] P. W. Bridgman, Proc. Am. Acad. Arts & Sci. **47,** 441 (1911).
[4] F. C. Kracek, G. W. Morey, and H. E. Merwin, Am. J. Sci., **35A,** 143 (1938).
[5] P. W. Bridgman, Proc. Am. Acad. Arts & Sci. **68,** 27 (1933).
[6] P. W. Bridgman, Am. J. Sci. **10,** 483 (1925).
[7] P. W. Bridgman, Am. J. Sci. **15,** 1 (1928).
[8] P. W. Bridgman, Proc. Am. Acad. Arts & Sci. **74,** 21 (1940).
[9] M. L. Huggins and Y. Sakamoto, J. Phys. Soc. Japan **12,** 241 (1957).
[10] C. E. Weir and L. Shartsis, J. Am. Ceram. Soc. **38,** 299 (1955).

(Paper 69A1–324

JOURNAL OF RESEARCH of the National Bureau of Standards—A. Physics and Chemistry
Vol. 69A, No. 1, January-February 1965

Determination of the Intermolecular Entanglement Coupling Spacings in Polyisoprene by Viscosity Measurements

Lewis J. Fetters*

(August 14, 1964)

The entanglement molecular weight (M_e) for polyisoprene has been estimated from the dependence of solution viscosity on molecular weight. Polymer concentrations of 1.82, 3.64, and 14.56 g/100 cm³ were used. Certain theoretical relationships between viscosity and molecular weight have been confirmed, and the prediction concerning the dependence of the entanglement molecular weight on polymer concentration has been substantiated. Furthermore, no variation in M_e was detected in the range of 25 to 75 °C.

1. Introduction

In the prevailing conceptual scheme [1] [1] of entanglement coupling, the parameter, M_e, is defined as the average molecular weight of a chain segment between intermolecular junction points [1, 2]. The presence of these chain entanglements markedly influences the viscoelastic properties of undiluted polymers and their concentrated solutions. Hence, these entanglements behave as mobile transient cross-links [3, 4].

Some commonly employed methods [1, 2, 5] for characterizing entanglement spacings involve the analysis of the value of the storage modulus $G'(\omega)$, the relaxation modulus $G(t)$, the storage compliance $J'(\omega)$, or the creep compliance $J(t)$ in the vicinity of the time or frequency scale where the slope of the complex modulus or compliance versus time or frequency curve is very small and possesses an inflection point. Hence, by utilizing this value as a pseudo-equilibrium modulus, G_e, or compliance, J_e, it is possible to estimate the average molecular weight between the entanglement loci from rubber elasticity theory [6, 7]. In addition, the position and value of the maximum in the loss compliance, $J''(\omega)$, have also been used [2, 8, 9] to determine the magnitude of M_e. However, as it has been pointed out elsewhere [1, 10], since the adequacy of the theories upon which these dynamic methods are based is not high, the quantitative results concerning entanglements obtained by their use may be suspect. In addition, further difficulty is sometimes encountered in selecting a suitable value of G_e or J_e.

The measurement of viscosity should provide an accurate and precise tool for investigating chain entanglements, since the effect of these intermolecular couplings on viscosity is very large. Empirically [11], it is recognized that in the region in which the molecular weights of an undiluted polymer system are above some critical value, M_e, characteristic of the polymer's chemical structure, the following relation is found to hold:

$$\log \eta = \log K + 3.4 \log M$$

where M is the molecular weight of the polymer and the constant K depends upon temperature and the nature of the polymer. The above relation is also valid for concentrated solutions provided the following relation is obeyed [1, 11, 12].

$$v_2 M \geq M_e$$

where v_2 denotes the volume fraction of polymer. For polymers possessing molecular weights below the minimum chain length required for incipient entanglement network formation, the observed viscosity is approximately proportional to the molecular weight.

These empirical facts can be interpreted in terms of the theoretical derivations of Eyring [13] and Bueche [14]. In the region where the polymer molecular weight is above its critical value, the long chain interactions are usually thought of as being communicated through the valence bonds and entanglement points. Hence, the polymer system is considered to consist of a loosely bound infinite network of intermeshed chains which tend to drag each other along as they slide over one another in flow. A precise picture of these entanglements does not currently exist.

The purpose of this paper is to present a reasonably accurate estimate of the magnitude of the entanglement spacings in polyisoprene. In addition, the effects of moderate variations in temperature and concentration on the spacing of the coupling points are reported. Conflicting conclusions concerning these two variables have appeared in the literature in conjunction with various polymeric systems.

*National Academy of Sciences-National Research Council Postdoctoral Resident Research Associate.

[1] Figures in brackets indicate the literature references at the end of this paper.

2. Experimental Procedures

For the determination of M_e from the dependence of viscosity on molecular weight, a number of polymer samples of known molecular weight must be used. Recent advances [15–25] in homogeneous anionic polymerization now permit the synthesis of linear, nearly monodisperse polyisoprene, which is structurally a close counterpart of Hevea rubber. The samples used in this work were prepared by the *n*-butyllithium-initiated polymerization of isoprene in *n*-hexane. Care was taken to maintain the reaction conditions [20, 24–26] which facilitate the formation of linear, relatively monodisperse polymer with a cis-1,4 content of 90–95 percent. Polyisoprene formed by the heterogeneous Ziegler-Natta catalysts, e.g., triisobutyl aluminum and $TiCl_4$, is unsuitable [27–29], since the resultant polymer has a broad molecular weight distribution and contains some branched polymer as well as microgel, which is difficult to separate by fractionation alone.

Characterization of four of the samples indicated, as expected, that linear polymer, with a narrow distribution ($\overline{M}_w/\overline{M}_n = 1.11$–$1.03$) of molecular weights, was indeed formed. The samples were stored in the terminated state, under vacuum, at −20 °C until just prior to use. This kind of storage does not impair the structural integrity of the polymer [30]. The molecular weights reported here are from intrinsic viscosity measurements in toluene by use of the following relations:

$$[\eta]_{30\,^\circ C} = 2.00\times10^{-4}\overline{M}_w^{0.728} \text{ [29]} \quad (1)$$

$$[\eta]_{25\,^\circ C} = 1.08\times10^{-4}\overline{M}_n^{0.82} \text{ [31]} \quad (2)$$

Equation (1) was used for samples with molecular weights greater than 1.5×10^5 while eq (2) was applied to the samples with molecular weights in the range of 2.5×10^4 to 1.5×10^5. The samples prepared had molecular weights which ranged from 2.5×10^4 to 1.3×10^6.

All of the concentrated solution viscosity measurements were taken at very low shear rates. Corrections for rate of shear proved to be very small under the experimental conditions employed. Henceforth the results given here are those one would obtain at zero rate of shear.

Solution of the polymers was carried out in decane. The viscosities were measured in capillary viscometers, which had been calibrated by the use of standard viscosity oils supplied by the National Bureau of Standards. Viscosities of the polyisoprene-decane solutions were measured at temperatures of 25 °C and 75 °C and at concentrations of 1.82 g, 3.64 g, and 14.56 g/100 cm^3 of solution. The density of the synthetic polyisoprene was taken as 0.91 g/cm^3. The reported viscosities are expressed in poises. Molecular disintegration under the employed experimental conditions was undetectable.

3. Results and Discussion

The viscosity-molecular weight relationships of the various solutions are presented in figures 1, 2, and 3. For a particular polymer the point of intersection of the straight lines, the "break" point, defines a characteristic polymer molecular weight M_b, i.e., the molecular weight at the "break" point. From this value, M_e can be calculated from the following relation: [1,11,12]

$$v_2 M_b \simeq M_e.$$

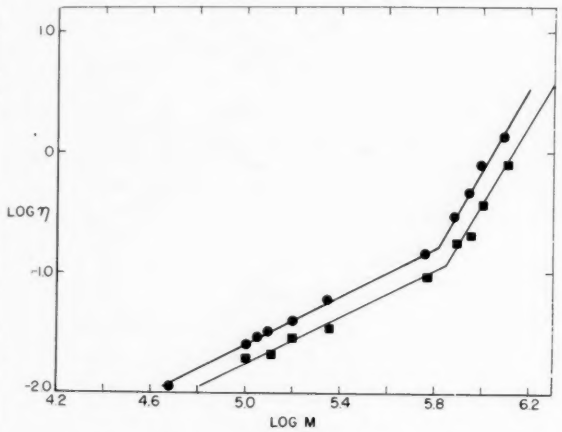

FIGURE 1. *Zero shear viscosities of polyisoprene in decane at a concentration of 2.5 weight percent.*

●, 25 °C
■, 75 °C

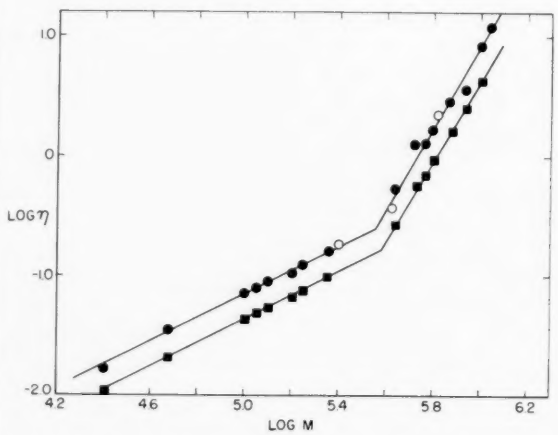

FIGURE 2. *Zero shear viscosities of polyisoprene in decane at a concentration of 4.9 weight percent.*

●, 25 °C
■, 75 °C
0, cis-1,4 content 70 to 85 percent

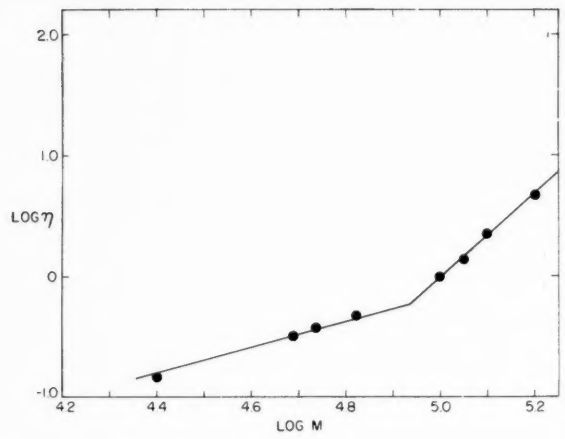

FIGURE 3. *Zero shear viscosities for polyisoprene in decane at a concentration of 19.2 weight percent.*

●, 25 °C

Table 1 lists the pertinent data collected from figures 1 to 3. The polymer concentrations reported correspond to volume percent values of 2, 4, and 16 at 25 °C. Since each sample served for measurements at the two temperatures, it was necessary to correct for the density change at the higher temperature in order to accurately calculate M_e at 75 °C.

TABLE 1

Polymer concentration (wt percent)	T	M_b 10^{-4}	M_e 10^{-3}	a*	b*
	°C				
2.5	25	66.0	13.2	3.40	1.00
	75	71.5	14.0	3.38	0.98
4.9	25	35.5	14.2	3.38	.99
	75	37.6	14.2	3.40	.98
19.2	25	8.6	13.8	3.41	1.05

*a and b denote the slopes of the intersecting straight lines above and below the transition point, respectively.

These results clearly indicate the existence of the transition point to at least two volume percent concentration and the inverse first power dependence of the molecular weight for transition (M_b) on concentration. This latter point is at variance with the interpretation given to data obtained from studies [32–34] of the dynamic behavior of a series of methacrylates. It was ascertained that $M_e \sim c^{-2.3}$ for this polymer series. A somewhat similar result has been reached from studies [35] carried out on solutions of polystyrene. From low-shear viscosity polymer-concentration plots, it was ascertained that $M_e \sim c^{-2}$.

The constancy of the molecular weight-concentration product found for the polyisoprene solutions is in complete accord with the results obtained from investigations [36–42] of the rheological behavior of polystyrene and polyisobutylene in bulk and concentrated solutions. A similar conclusion is reached from the combined results of Bueche [10, 12] and Bletso [43] for solutions of poly(methyl methacrylate).

Data acquired by the use of dynamic methods for a series of methacrylate polymers indicate that M_e is temperature dependent [2, 32–34, 44], i.e., the entanglements tend to dissociate with increasing temperature. In conjunction with his point, it should also be mentioned that a slight dependence of M_e on temperature was apparently found [45, 46] for polyethylene when the relationship between viscosity and molecular weight was determined at 110 and 160 °C.

However, the insensitivity of M_e to temperature variations has been demonstrated by bulk and solution viscosity measurements of polystyrene and polyisobutylene [11, 37–39]. Similar results were obtained from studies on the concentrated solutions of poly(methyl methacrylate) [10] and the undiluted polybutadiene [47] system.

These findings tend to corroborate the results reported in table 1. Clearly the increase in temperature from 25 °C to 75 °C has not seriously altered M_e. One can say that if temperature variations in M_e do occur, they are not very large.

In conclusion, it can be seen that the values of a and b are in close accord with the values of 3.5 and 1.0 predicted by Bueche [14] and Hayashi [48] as well as those of 3.33 and 1.33 as predicted by Eyring [13]. It might be added that these results are in semiquantitative agreement with the theoretical derivations of Chikahisa [49]. Tentative conclusions pertaining to the close agreement of the theoretical and empirical values of a are reported elsewhere [50].

The value of M_e has been regarded as being equivalent to $M_e/2$, based on considering [8] the entanglement points to be located near the center of the polymer chains. This factor of two has also been justified on the basis of the hypothesis [12] that both accelerating and retarding elements simultaneously exist within the flowing system.

It has recently been proposed [5] that the introduction of this factor of two is perhaps unwarranted. In analogy with gelation theory [51], Markovitz, Fox, and Ferry [5] contend that, at the point of network formation, since there is one cross-linked unit on each of the joined chains in the cross-linkage, there exists, on the average, one cross-linked unit per primary polymer chain. From this point of view the molecular weight at the transition point (M_e) is equal to the average molecular weight (M_e) between the intermolecular junction points. Eyring [13] has also identified M_e as equivalent to M_e. However, pending future developments, final conclusions as to the exact relationship between M_e and M_e must currently be left in abeyance.

In lieu of M_e, the symbol Z has been applied to denote the magnitude of the spacings between nearest coupling points. The term Z however has multiple significance—a frequent occurrence in polymer science. It may denote either the degree of polymerization or the number of chain atoms between the coupling loci. In an attempt to obviate this multiplicity of meaning, it has been suggested [5 that the degree of entanglement spacing be expressed

in terms of the average number of chain bonds between nearest entanglement points. For this purpose, it has been proposed that the symbol Λ be adopted to denote this value. This nomenclature is used for the presentation of the data in table 2 where the various values of Λ, as determined from elastic measurements, are presented. For comparison, two recently reported values of Λ for polybutadiene are also included.

TABLE 2. *Estimates of* Λ *for Hevea rubber and synthetic polydienes**

Polymer	Max. in J''		Inflection in $G'(\omega)$	Inflection in $J(t)$	Dependence of η on M	Reference
	J''_m	ω_m				
Hevea rubber	272	400	120; 400 296	504		52 53 54
Synthetic polyisoprene					824	This work
polybutadiene**				222	414	47

*Portions of the data presented herein have come from a recent compilation presented elsewhere [5].
**Microstructure: 10 percent vinyl; 40 percent cis-1, 4; and 50 percent trans-1, 4.

In presenting the value of Λ determined from the dependence of η on M, the value of M_e has been taken as equal to M_c. Thus, Λ is equal to $4M_c/M_0$; where M_0 denotes the monomer molecular weight. If, however, the introduction of the factor of two should prove to be valid, the values of Λ, as presented herein, determined from the viscosity technique and from the position and value of the maximum of the loss compliance, $J'(\omega)$, should be divided by two. The factor of two can be introduced into the data obtained from the loss compliance since these values involve assumptions similar to those used in the treatment of the viscosity-molecular weight relation. Since there exists no uncertainty involving a factor of two in the calculations of Λ involving the pseudo-equilibrium modulus or compliance, these estimates of the entanglement spacings would remain unchanged.

It would appear that the value of Λ reported herein should be applicable to Hevea rubber. However, there may exist some subtle structural differences between the two polyisoprenes which might render the foregoing conclusion invalid. Qualitatively, this aspect was briefly investigated. Several samples of polyisoprene were prepared under conditions which yield polymer with a cis-1,4 content of 70 to 85 percent. Their flow behavior, figure 2, was similar to polyisoprenes with the higher cis-1,4 content. This apparent insensititivy of the flow properties to small structural changes may indicate that the minute differences in microstructure between Hevea rubber and synthetic polyisoprene may not cause any great differences in Λ for the two polydienes.

The author wishes to express his thanks to Lee A. Dunlap for his experimental assistance in the intrinsic viscosity determinations. Several conversations with F. Bueche are gratefully recalled.

4. References

[1] F. Bueche, Physical Properties of Polymers (John Wiley and Sons, Inc., New York, N.Y., 1962).
[2] J. D. Ferry, Viscoelastic Properties of Polymers, (John Wiley and Sons, Inc., New York, N.Y., 1961).
[3] R. Buchdahl, J. Colloid Sci. **3,** 87 (1948).
[4] L. E. Nielson and R. Buchdahl, J. Chem. Phys. **17,** 839 (1949); J. Colloid Sci. **5,** 282 (1950).
[5] H. Markovitz, T. G Fox, and J. D. Ferry, J. Phys. Chem. **66,** 1567 (1962); Polymer Preprints **3,** No. 1, 12 (1962).
[6] H. Mark and A. V. Tobolsky, Physical Chemistry of High Polymeric Systems, (Interscience Publishers, New York, N.Y., 1950).
[7] J. D. Ferry, R. F. Landel, and M. L. Williams, J. Appl. Phys. **26,** 359 (1955)
[8] R. S. Marvin, Chapter in J. T. Bergen, Ed., Viscoelasticity: Phenomenological Aspects, (Academic Press, Inc., New York, N.Y., 1960).
[9] H. Oser and R. S. Marvin, J. Res. NBS **67B** (Math. and Math. Phys.) No. 2, 87 (1963).
[10] F. Bueche, C. J. Coven, and B. J. Kinzig, J. Chem. Phys. **39,** 128 (1963).
[11] T. G Fox, S. Gratch, and S. Loshaek, Chapter in F. Eirich, Ed., Rheology, Theory and Applications, Vol. I, (Academic Press, Inc., New York, N.Y., 1956).
[12] F. Bueche, J. Appl. Phys. **26,** 738 (1955).
[13] H. Eyring, T. Ree, and N. Hirai, Proc. Natl. Acad. Sci. **44,** 1213 (1958).
[14] F. Bueche, J. Chem. Phys. **20,** 1959 (1952); **25,** 599 (1956).
[15] H. Morita and A. V. Tobolsky, J. Am. Chem. Soc. **79,** 5853 (1957).
[16] H. Hsieh, D. J. Kelly, and A. V. Tobolsky, J. Polymer Sci. **26,** 240 (1957).
[17] F. W. Stavely et al., Ind. Eng. Chem. **48,** 778 (1956).
[18] A. V. Tobolsky and C. E. Rogers, J. Polymer Sci. **40,** 73 (1959).
[19] S. E. Bresler, A. A. Korotkov, M. I. Mosevitsky, and I. Ya. Poddubnyi, Zhur. Tekh. Fiz. **28,** 114 (1958).
[20] M. Morton, E. E. Bostick, and R. G. Clarke, J. Polymer Sci. **1A,** 475 (1963).
[21] M. Morton, E. E. Bostick, R. A. Livigni, and L. J. Fetters, J. Polymer Sci. **1A,** 1735 (1963).
[22] M. Morton, E. E. Bostick, and L. J. Fetters, J. Polymer Sci., Part C, No. 1, 311 (1963).
[23] N. Calderon and K. W. Scott, Polymer Preprints **4,** No. 2, 154 (1963).
[24] M. Morton, N. Calderon, L. J. Fetters, and J. F. Meier, Polymer Preprints **2,** No. 2, 310 (1961).
[25] R. E. Stearns and L. A. Forman, J. Polymer Sci. **41,** 381 (1959).
[26] E. Bauer and M. Magat, J. Chim. Phys. **47,** 841 (1950).
[27] L. I. Zakharkin, Doklady Akad. Nauk, SSSR **131,** 1069 (1960).
[28] W. M. Saltman, W. E. Gibbs, and J. Lal, J. Am. Chem. Soc. **80,** 5615 (1958).
[29] W. H. Beattie and C. Booth, J. Appl. Polymer Sci. **7,** 507 (1963).
[30] J. F. Meier, Ph.D. Thesis, University of Akron, Akron, Ohio (1963).
[31] M. Morton and H. Brantley, unpublished results.
[32] D. M. Stern, J. W. Berge, S. F. Kurath, C. Sakoonkim, and J. D. Ferry, J. Colloid Sci. **17,** 409 (1962).
[33] T. P. Yin and J. D. Ferry, J. Colloid Sci. **16,** 166 (1961).
[34] T. E. Newlin, S. E. Lovell, P. R. Saunders, and J. D. Ferry, J. Colloid Sci. **17,** 10 (1962).
[35] S. Onogi, T. Kobayashi, Y. Kojima, and T. Taniguchi, Trans. Soc. Rheology **6,** 390 (1962); J. Appl. Polymer Sci. **7,** 847 (1963).
[36] T. Kotaka, M. Kurata, and M. Tamura, Rheology Acta. **2,** 179 (1962).
[37] F. Bueche and F. Kelly, J. Polymer Sci. **45,** 267 (1960); ibid. **50,** 549 (1961).
[38] T. G Fox and V. Allen, Conference on High Temperature Polymer and Fluid Research, Technical Documentary Report No. ASD–TDR–62–372, p. 323 (1962).
[39] T. G Fox and P. J. Flory, J. Am. Chem. Soc. **70,** 2384 (1948); J. Appl. Phys. **21,** 581 (1950); J. Phys. and

Colloid Chem. **55,** 221 (1951); J. Polymer Sci. **14,** 315 (1954); T. G. Fox and H. Nakayasu, Rheol. Bull. **29,** 3 (1960).
[40] T. G Fox and S. Loshaek, J. Appl. Phys. **26,** 1080 (1955).
[41] J. F. Rudd, J. Polymer Sci. **44,** 459 (1960).
[42] R. S. Porter and J. F. Johnson, J. Polymer Sci. **50,** 379 (1961); Polymer **3,** 11 (1962); Trans. Soc. Rheology **7,** 241 (1963).
[43] N. C. Bletso, Ph.D. Thesis, University of Akron, Akron, Ohio (1962).
[44] J. W. Berge, P. R. Saunders and J. D. Ferry, J. Colloid Colloid Sci. **14,** 135 (1959).
[45] K. Ueberreiter and H. J. Orthmann, Kolloid-Z. **126,** 140 (1952).
[46] R. S. Porter and J. F. Johnson, J. Appl. Phys. **32,** 2326 (1961).
[47] J. T. Gruver and G. Kraus, J. Polymer Sci. **2A,** 797 (1964).
[48] S. Hayashi, J. Physical Soc. (Japan) **19,** 101 (1964).
[49] Y. Chikahisa, J. Physical Soc. (Japan) **19,** 92 (1964).
[50] M. Morton and L. J. Fetters, J. Polymer Sci. **2A,** 3311 (1964).
[51] P. J. Flory, Principles of Polymer Chemistry (Cornell University Press, Ithaca, N. Y., 1953).
[52] A. R. Payne, Chapter in P. Mason and N. Wookey, Ed. Rheology of Elastomers (Pergamon Press, London, 1958).
[53] L. J. Zapas, S. L. Shufler and T. W. DeWitt, J. Polymer Sci. **18,** 245 (1955).
[54] F. Bueche, J. Polymer Sci. **25,** 305 (1957).

(Paper 69A1–325)

JOURNAL OF RESEARCH of the National Bureau of Standards—A. Physics and Chemistry
Vol. 69A, No. 1, January–February 1965

Electrical Conductivity of Dilute Solutions of "Sea Water" From 5 to 120 °C

Cyrus G. Malmberg

(August 13, 1964)

Data are reported for solutions of sea salt at concentrations up to 161 ppm (2.5 equivalent ppm chlorine) over the temperature range 5 to 120 °C. Analysis is made in terms of equivalent conductance and the limiting law, $\Lambda = \Lambda_0 - \alpha\sqrt{C}$, with evaluation of Λ_0 and α in terms of the temperature. As a result, the conductivity due to sea salt in water is calculable over these ranges of temperature and concentration with an estimated error of ± 0.3 percent or less.

1. Introduction

The conductivity-temperature relationship of dilute solutions of "sea-salt" in water is used as a base for rapid instrumental analysis of the salinity of such solutions. Furthermore, the degree of contamination of distilled water and steam condensate by sea water due to condenser leakage or entrainment of boiler water can be determined with suitable conducitvity equipment. The relationship between conductivity and temperature can also be used conveniently as a rough measure of ionic contamination of nearly neutral salt solutions and as a partial correction in the analysis of acidic or basic salt solutions. Pertinent information both with regard to salinity indicator systems and the specific problems involved in utilization of conductivity methods and data for analysis is available in the literature [1 to 23].[1]

Empirically the present investigation paralleled that of previous determinations of this relationship [1, 2], with the exception that conductivities were determined on solutions above their normal boiling points and considerable emphasis was placed upon determination of the solvent conductivity, so that the contribution due to the salt was more precisely determinable. It was therefore necessary to employ suitable pressurized equipment to avoid ebullition during the course of the measurements and to refine further the techniques of measurement in order to avoid significant residual contamination of the solutions and concomitant vitiation of the results.

[1] Figures in brackets indicate the literature references at the end of this paper

2. Experimental Procedure

Solutions: The synthetic ocean water used as a reference solution was prepared by dissolving the salts listed in table 1 in an air-equilibrated grade of conductivity water. Its composition was practically identical with that of the proposed "Synthetic Ocean Water" composition for Class II work listed in table XII of NRL report P–2909 [3]. Commercially available reagent-grade materials were used in the preparation of this solution, except where the formula called for $MgCl_2 \cdot 6H_2O$. In this case, since the degree of hydration of magnesium chloride is difficult to determine, the required amount of the salt was prepared in solution by neutralization of constant boiling hydrochloric acid with magnesium oxide.

TABLE 1. *Composition of synthetic ocean water at 20 °C*

NRL Report P–2909

Salt	Class II designation [a] g. l^{-1}	Anhydrous state g. l^{-1}	Equivalents l^{-1} [b]
NaCl	24.540	24.540	0.41989
$MgCl_2 \cdot 6H_2O$	11.110	5.320	.10926
Na_2SO_4	4.094	4.094	.05764
$CaCl_2$	1.159	1.159	.02088
KCl	0.695	0.695	.00932
$NaHCO_3$	.201	.201	.00239
KBr	.101	.101	.00084
H_3BO_3	.027	.027	.00043
$SrCl_2 \cdot 6H_2O$	.042	.025	.00032
NaF	.003	.003	.00007
Total salt	41.972	36.048	0.62014

[a] Class II designation (test purposes) differs from Class I designation (fundamental research purposes) by 1.3 mg/liter of total solutes.
[b] 1961 atomic weights.

TABLE 2. *Dilutions of synthetic sea water*

Concentration chlorine	Content chlorine			Content anhydrous salt		
			Chlorine and salt content			
eq. ppm	*ppm*	*g/liter 20 °C*	C_{Cl} *eq.* Cl/*kg*	*ppm*	*g/liter 20 °C*	C_s *eq. "Sea Salt"/kg*
2.505	88.81	0.08867	2.505×10^{-3}	161.35	0.16109	$2.779_7 \times 10^{-3}$
1.503	53.29	.05320	1.5031×10^{-3}	96.81	.09665	$1.667_8 \times 10^{-3}$
1.002	35.52	.03546	1.0019×10^{-3}	64.54	.06442	$1.111_7 \times 10^{-3}$
.5009	17.76	.01773	$.5009 \times 10^{-3}$	32.27	.03221	$.555_8 \times 10^{-3}$
.3007	10.66	.01064	$.3007 \times 10^{-3}$	19.36	.01933	$.333_7 \times 10^{-3}$
.1503	5.329	.005319	$.1503 \times 10^{-3}$	9.680	.009663	$.1668 \times 10^{-3}$
.1002	3.552	.003546	$.1002 \times 10^{-3}$	6.454	.006442	$.1112 \times 10^{-3}$
.06014	2.132	.002128	$.06014 \times 10^{-3}$	3.873	.003866	$.06673 \times 10^{-3}$
.02004	.7105	.0007092	$.02004 \times 10^{-3}$	1.290	.001288	$.02224 \times 10^{-3}$

From this primary reference solution a secondary reference solution containing 2.505_0 equivalent ppm of chlorine was prepared on a weight basis. Volumetric glassware was then employed in diluting this solution to obtain the other solutions with the concentrations listed in table 2. A common source of ammonia-free distilled water at equilibrium with the carbon dioxide of the atmosphere (*p*H about 5.7 at 25 °C) was used throughout the course of the work.

Apparatus: Suitable equal ratio capacitance conductance bridges supplied with a Wagner earth were used to determine the resistance of the cells in the frequency range 1 to 12 kc/s.

Oil-filled thermostats were employed to control temperature which was determined by resistance thermometers in some of the measurements and by calibrated mercury thermometers in others.

Five conductivity cells were employed during the course of the measurements. They were constructed of Pyrex glass and had electrodes of platinum or platinum-iridium alloy. Of these only one, which was specially constructed for the purpose, was suitable both from the standpoint of its dimensions and its cell constant (ca. 0.2 cm^{-1}) for use over the entire range of temperature and concentration. The other four cells, pipet and dilution types with constants in the range 4.4 to 0.06 cm^{-1}, were used as needed over a temperature range from 5 to 60 °C.

A manostat suitable for use up to 2½ atmospheres absolute was fashioned from a one-gallon can and, with supporting framework, was used to contain the special cell for the measurements in the temperature range between 75 and 120 °C. Pressure within the manostat was maintained at the desired level by application of gas from a nitrogen tank through a reducing valve. In use, the manostat was partially filled with oil to the extent that the cell was nearly immersed and the manostat itself was completely immersed in the oil bath at the temperature of measurement. Equilibrium of the resistance of the cell was usually achieved in one hour or less.

Procedure: Conductivities of the solutions were determined in two series of measurements. One series was made at 35, 5, 20, 50, 60, and again 35 °C and the other at 35, 75, 90, 105, 120, and again 35 °C. By bracketing the measurements at other temperatures between those at 35 °C, it was possible to determine the magnitude of any changes which had taken place in the resistance of a cell during the course of a series, and this served as a partial check upon the precision of the measurements. Ordinarily the resistance of the cell was read directly in terms of the adjacent arm of the bridge, but in some cases, at low concentrations in the special cell and for the companion measurements on equilibrium water, a shunt method with a 10,000 or 100,000 ohm standard resistor was used.

The variation of resistance of the cells with frequency was determined at 1, 3, and 12 kc/s so that the magnitude of electrode polarization and other frequency-dependent phenomena present could be evaluated and corrections applied where necessary.

3. Results

Discussion: The data obtained were converted to values of specific conductance by means of the relation $\gamma = S \times 10^6 / R$ where γ is the specific conductance in micromhos/cm, S the cell constant in cm, $^{-1}$ and R the observed resistance of the cell. The values so calculated for the sea water data are listed in table 3.

The conductivity of these solutions may be considered to be the sum of the specific conductance of the salt present and of the water used. Since the conductivity of otherwise pure distilled water is rather widely variable, due to the presence of volatile impurities such as carbon dioxide and ammonia, it is desirable that the specific conductance due to the salt alone be known. For nearly neutral solutions this may be obtained from the relation $\gamma' = \gamma - \gamma_w$ where γ' is the specific conductance due to the salt and γ_w is that due to the water. Values of γ' so calculated are listed in table 4.

The procedure adopted for determining the values of γ_w used in computing γ' was based upon the fact that the observed values of γ when plotted with respect to the concentration C gave nearly straight lines at any one temperature and the data for such a temperature could be expressed by an equation of the type $\gamma = \gamma_w + MC - NC^2$. For low concentrations (0.02–0.15 eq. ppm Cl) the NC^2 term is of negligible proportions and $\gamma = \gamma_w + MC$.

TABLE 3. *Observed values of γ in micromhos/cm*

Chlorine eq. ppm / temperature		0.02004	0.06014	0.1002	0.1503	0.3007	0.5009	1.0019	1.5031	2.5050
°F	°C									
41.0	5.0	2.31	5.78	9.14	13.33	26.02	42.60	84.11	124.8	205.4
68.0	20.0	3.43	8.56	13.40	19.46	38.09	62.20	122.8	182.1	299.8
95.0	35.0	4.65	11.35	18.04	26.46	51.49	84.04	165.6	245.8	404.2
122.0	50.0	5.91	14.43	23.15	33.52	65.44	107.2	212.1	314.4	516.8
140.0	60.0	6.76	16.42	26.59	38.43	75.15	123.4	244.1	362.0	594.6
167.5	75.3	7.98	19.95	31.88	47.09	91.42	149.5	293.4	435.7	712.7
194.9	90.5	9.20	23.34	37.35	55.22	107.3	175.4	344.4	511.0	838.3
221.7	105.4	10.40	26.58	42.62	63.07	122.9	200.5	393.8	584.8	959.6
249.1	120.6	11.82	29.79	47.94	70.75	138.7	226.3	443.3	656.8	1,075.0

TABLE 4. *Values of γ' in micromhos/cm $\gamma' = \gamma - \gamma_w$*

Chlorine eq. ppm / temperature		0.02004	0.06014	0.1002	0.1503	0.3007	0.5009	1.0019	1.5031	2.5050
°F	°C									
41.0	5.0	1.71	5.12	8.48	12.67	25.36	41.94	83.45	124.19	204.73
68.0	20.0	2.51	7.47	12.31	18.37	37.00	61.11	121.75	181.03	298.67
95.0	35.0	3.36	10.06	16.75	25.17	50.20	82.75	164.31	244.51	402.91
122.0	50.0	4.29	12.81	21.53	31.90	63.82	105.60	210.48	312.77	515.22
140.0	60.0	5.02	14.68	24.85	36.69	73.41	121.66	242.38	360.23	592.81
167.5	75.3	6.03	18.00	29.93	45.14	89.47	147.56	291.43	433.77	710.71
194.9	90.5	7.05	21.19	35.2	53.07	105.16	173.27	342.30	508.88	836.15
221.7	105.4	8.08	24.26	40.3	60.75	120.59	198.21	391.47	582.48	957.23
249.1	120.6	9.15	27.12	45.27	68.08	135.99	223.59	440.66	654.13	1,072.33

The constants M and γ_w were evaluated for each temperature by the use of simultaneous equations, and the values of γ_w were used to calculate the values of γ' in all except two cases. In these, experimental considerations made it preferable to use directly determined values of γ_x. The values of γ_w so calculated are given in table 5. Included are values of γ_x obtained by graphical extrapolation of γ to zero concentration. The conductivity, γ_e, of the distilled water used for preparation of the solutions was determined over the temperature range. Corrections of these values for the observed drift, assumed to be entirely due to loss of carbon dioxide, gives the listed values of γ_c which compare favorably with those of γ_w and γ_x.

TABLE 5. *Solvent water conductivity as derived and measured*

(Micromho/cm)

Temp.	γ_w	γ_x	γ_e	γ_c
°C				
20			0.92	
5	0.66	0.63	.61	0.61
20	1.09	.93	.92	.92
35	1.29	1.25	1.19[3]	1.19[3]
50	1.62	1.52	1.46[8]	1.51
60	1.74	1.71	1.62[2]	1.69
75.2[8]	1.95	1.86	1.77[9]	1.88
90.5[1]	2.15	2.12	1.92[7]	2.04
105.4[1]	2.32	2.31	2.04[8]	2.17
120.5[6]	2.67	2.72	2.53[6]	2.68
35			1.12[9]	1.19[3]

γ_w, values calculated from sea water data.
γ_x, values obtained by graphical extrapolation of data.
γ_e, values obtained by direct measurement.
γ_c, values obtained by correction of γ_e for drift observed between measured values at 35 °C. Drift assumed to be due to a partial loss of carbon dioxide assumed to be complete at 75 °C. No such significant drift could be established in the solution measurements.

Evaluation: The magnitudes of the errors known to be associated with these results are estimated to be as follows.

Measurement of the resistance of the cells; less than ± 0.04 percent.

Preparation of the solutions by adding the known weights of salts to the water; not greater than ± 0.1 percent.

The temperatures of measurement were controlled to better than 0.01 °C in the range between 5 and 60 °C and to ± 0.02 °C in the range 75 to 120 °C. In all cases they were probably accurate within 0.1 °C, which would lead to an error not greater than ± 0.1 percent in measured values of conductance.

The cell constants were known to 0.05 percent or better at 35 °C. Although no corrections were applied for their change with temperature, it is probable that any error due to such change is no greater than 0.1 percent at the most extreme temperature of measurement with respect to that at 35 °C.

Of the recognized errors, that due to variation of the conductivity of the water used is of greater magnitude at the lower concentrations than all the others. This error is difficult to evaluate precisely, since it can vary both with the carbon dioxide content of the atmosphere and the variation of its solubility and ionization in the solution with partial pressure and temperature.

In the present work, this latter effect became significant when cells of the dilution type were used to obtain some of the data for 50 and 60 °C at lower concentrations, with the result that these data at 60° are the least dependable (uncertain to ± 1 percent) of all the sea water data.

From an analysis of the data obtained and the derived values of γ', it is estimated that the limits of the accuracy of the individual values of γ' listed in table 4 vary with increasing concentration from ± 1 percent to ± 0.2 percent, which may be considered to be an overall measure of the empirical validity of the results.

4. Discussion

The values of γ listed in table 3 are representative of actual dilutions of "sea water" using a better than average grade of distilled water as solvent. The solvent conductivity is almost entirely due to its air equilibrium content of carbon dioxide combined with the ionization of the water. The values as such can be used directly as a base for scaling and calibration of salinity indicators or for the determination of salinity where equilibrium conditions exist or can be assumed to exist. When such assumptions cannot be made, the values of γ' from table 4 can be used with a "water correction" applied as appropriate.

Comparison of the values listed in table 5 will indicate the order of uncertainty involved in assigning a water correction even when considerable effort is made to use a reasonably stable reference condition and to minimize contamination.

In this regard it may be pertinent to state briefly certain characteristics of distilled water. According

to Kohlrausch and others [24, 25, 26, 31] the specific conductance of pure water is about 0.05_8 micromho/cm at 25 °C and has a temperature coefficient of about 5 percent per deg C. On the other hand, ordinary distilled water, in which the content of total solids (i.e., both salt and nonconducting material) is extremely low, has a conductivity of 1 to 3 micromhos/cm or more at 25 °C and a temperature coefficient of about 2 percent per deg C. In the main this conductivity is due to variable quantities of dissolved carbon dioxide and ammonia. These quantities are subject to variation with the temperature of condensation and the constitution of the boiler water as well as exposure to the atmosphere as a source of contamination.

It is usual to represent conductivity data in terms of an equivalent conductance

$$\Lambda=\frac{10^{-3}\gamma'}{C} \tag{1}$$

where C is the electrolyte concentration in equivalents per liter, and in very dilute solution to represent the variation of Λ with concentration by

$$\Lambda=\Lambda_0-\alpha\sqrt{C} \tag{2}$$

where Λ_0 and α are constants for a given electrolyte and temperature.

Theory [27, 28, 29, 30] permits computation of the values of α for single electrolytes but is not generally applicable to mixtures. Given the variation of Λ_0 and α with temperature then either γ' or C can be derived in terms of the other over the appropriate range of temperature and concentration. When the concentration is in equivalents of sea salt per liter up to 3×10^{-3} and the temperature is between 5 and 120 °C

$$\Lambda_0=66.1+2.1616t+0.01004t^2-1.740\times10^{-5}t^3 \tag{3a}$$

and

$$\alpha=57.0+2.035t+5.75\times10^{-3}t^2+1.267\times10^{-4}t^3 \tag{3b}$$

where t is the temperature in degrees Celsius.

Since on this scale the concentration of a particular solution is temperature dependent, it is convenient, for purposes of analysis, to express concentration in equivalents per kilogram. For these concentrations in terms of chlorine, C_{Cl}, (a scale commonly used for sea water)

$$\Lambda_0^{Cl}=73.4+2.391t+0.0110t^2-3.40\times10^{-5}t^3 \tag{4a}$$

and

$$\alpha^{Cl}=67.3+2.148t+0.01506t^2+5.9\times10^{-5}t^3 \tag{4b}$$

Correspondingly for sea salt in equivalents per kilogram C_s,

$$\Lambda_0^s=66.1+2.154_3t+0.00991_3t^2-3.064\times10^{-5}t^3 \tag{5a}$$

and

$$\alpha^s=57.0+1.820t+0.012765t^2+5.00\times10^{-5}t^3. \tag{5b}$$

A comparison of the locus of $\Lambda_0-\alpha\sqrt{C}$ calculated from these relationships with the best apparent graphical locus obtained from plots of Λ versus $\sqrt{C}$ shows a deviation as great as 0.41 percent only at one end of the 60 °C plot and an average maximum deviation of 0.29 percent over the range. As a result, it is likely that appropriate values of Λ so calculated within the applicable range of temperature and concentration are accurate to ±0.3 percent or better.

Additional evaluation of the data was accomplished using large plots of the Walden product, $\Lambda\eta$, versus the temperature, where η is the solvent or solution viscosity. This gives a family of curves for solutions of different concentrations, as shown in figure 1. From these it is easy to detect any appreciable inconsistency of the data. Interpolation in terms of viscosity allows a reasonable evaluation of Λ at other concentrations and temperatures. To a degree this procedure is an extension of that used with limiting ion conductances [29, 30] and deserves more extensive use as an aid in evaluation of conductance data. The results obtained support the estimation of accuracy made regarding the individual values of γ' in table 4 and that ascribed to the use of eq (2) combined with eq (3, 4, or 5).

It is interesting to compare the values of Λ_0 for sea salt with those for sodium chloride calculated from acceptable values of limiting ion conductances [29] and also the observed values of α with those calculated, α', assuming sea salt to be a 1:1 electrolyte.

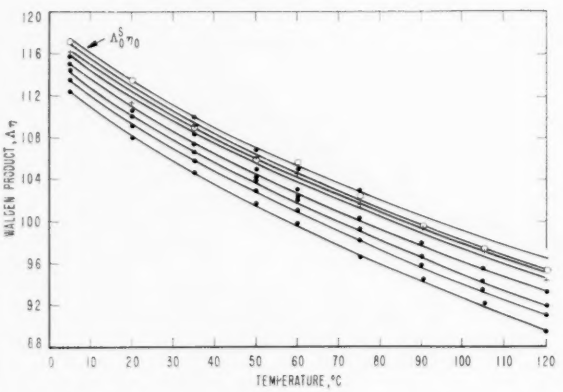

FIGURE 1. *The variation of the Walden product for sea salt with temperature and concentration.*

Curves in descending order represent concentrations of 0.0, 2.2×10^{-4}, 1.1×10^{-4}, $3.3\times^{-4}$, 5.6×10^{-4}, 1.1×10^{-3}, 1.7×10^{-3}, and 2.8×10^{-3} in equivalents/kg.

TABLE 6. *Comparison of the derived and measured constants of eq (2) for* NaCl *and sea salt*

Temp. °C	NaCl Λ_0	Sea salt Λ_0	α	1:1 electrolyte α'	$\Lambda_0{}^x$	$\Lambda_0{}^x/\Lambda_0$ salt
0	67.5[a]	66.1[b]	57[b]	44[c]	68.4[d]	1.035
5	77.81	77.2	67	53	.....	.....
15	101.18	100.8	89	70	.....	.....
18	108.8	108.2	96	76	110.1	1.016
20	.....	113.2	101	80	.....	.....
25	126.45	126.2	114	90	128.09	1.015
35	153.75	153.4	141	111	.....	.....
45	182.65	182.2	172	135	.....	.....
50	.....	197.1	190	148	.....	.....
55	213.28	212.5	207	161	.....	.....
60	.....	228.1	227	175	.....	.....
75.28	.....	279.6	299	219	.....	.....
90.51	.....	331.0	381	268	.....	.....
100	357	365.3	444	302	367	1.004
105.41	.....	385.1	484	322	.....	.....
120.56	.....	442.1	608	388	.....	.....

[a] NaCl values Λ_0 calculated. Appendix 6.1 (Robinson and Stokes) [29].
[b] Λ_0 and α for sea salt calculation, eqs (3a and 3b).
[c] α' values calculated for sea salt as a 1:1 electrolyte. Appendix 7.1 Electrolyte solutions (Robinson and Stokes) [29].
[d] $\Lambda_0{}^x$ = value of Λ_0 for sea salt calculated through proportional use of equivalent ion conductances. Appendix 6.2 (Robinson and Stokes) [29].

Comparative values are given in table 6. Included are values of limiting equivalent conductances of sea salt, $\Lambda_0{}^x$, calculated using appropriate limiting ion conductances weighted in proportion to the ionic composition of the sea salt (see table 1).

The values of Λ_0 for sodium chloride and the sea salt show a good and parallel agreement (not particularly to be expected) between 5 and 55 °C where the sodium chloride data are exceptionally good. On the other hand, the agreement between Λ_0 and $\Lambda_0{}^x$ for the sea salt is not as good as might be expected from a simple application of Kohlrausch's law of independent migration of ions, a relationship which is well established for one solute solutions of electrolytes. Assuming that the absolute error in calculating Λ_0 is not greater than that estimated, it would appear that a simple application of Kohlrausch's law is only roughly valid for mixtures of this type [30A].

The observed differences in α and α' are such that their misuse within the effective range of temperature and concentration would lead to a maximum error of 2.5 percent in γ' or C. In terms of 2:1 and 2:2 electrolytes the error would be considerably larger.

The use of the conductance method in analysis of dilute solutions of unknown composition is admittedly subject to considerable uncertainty. Mixture effects as they influence both Λ_0 and α are not well understood, and in addition limiting ionic conductances show wide variation with ionic species. At the same time the method is particularly useful for rapid determinations and for comparative purposes. Since the present data are representative of dilute solutions of a common mixture of electrolytes they can be useful as reference data. From this base it is likely that conductometric analysis of nearly neutral natural waters can be made within 10 percent if an adequate water correction is made. On the other hand, conductometric analysis of dilute sea water solutions should be possible to 100.0 ± 0.3 percent through appropriate use of equation 2 and correct values of Λ_0 and α.

5. References

[1] C. Huev, J. Am. Soc. Naval Engineers 39, 658 (1927).
[2] E. G. Lunn and W. Whybrew, Navy Dept., Office of Naval Research, Resistance—Temperature Curves of Salinity Solutions, NRL Report No. P–1381 (July 1937).
[3] T. P. May and C. E. Black, Synthetic Ocean Water, Navy Dept., Office of Naval Research, NRL Report No. P–2909 (August 1946).
[4] Sverdrup, Johnson, and Fleming, The Oceans (Prentice Hall, New York, N.Y., 1942).
[5] Data of Geochemistry, F. W. Clarke, Bull No. 770 U.S. Geological Survey.
[6] A. Barnes, Analyst **80,** 573 (1955).
[7] Symposium on Problems and Practice in Determining Steam Purity by Conductivity Methods, Proc. ASTM **41,** 1261–1340 (1941).
[8] Symposium on Continuous Analysis of Industrial Water and Waste Water 1952, ASTM Special Tech. Pub. No. 130, (1953).
[9] Symposium on Steam Quality, ASTM Special Tech. Publ. No. 192 (1956).
[10] Symposium on Impurities in Steam, Proc. ASTM **61,** 1369–1423 (1961).
[11] Standard Methods for Examination of Water, Sewage and Industrial Wastes. 10th ed., pages 19 and 89. (Am. Public Health Assoc. Inc., New York, N.Y. 1955).
[12] R. W. Lane, C. H. Neff and T. E. Larsen, Am. Power Conference XXIII, 550 (1961).
[13] John D. Betz, Power Generation No. 12, 60–62 (1948).
[14] L. V. Wilcox, J. Am. Water Works Assoc. **42,** 775 (1950).
[15] J. W. Polsky, Analytical Chemistry **19.** 657 (1947).
[16] H. Gustafson and A. S. Behrman, Ind. and Eng. Chem., Anal. ed. **11,** 355 (1939).
[17] C. S. Howard, Ind. and Eng. Chem. **5,** 5 (1933).
[18] F. Oehme, Gles-Instrument Tech. **4,** 119 (1960).
[19] Madeleine Martin, Rev. inst. franc. petrole et ann. Combustible Liquides **13,** 985 (1958).
[20] G. Whitehead, J. Applied Chem. London **11,** 136 (1961).
[21] Alex Deubner and Ruth Heise, Ann. Physik. **9,** 213–24 (1951).
[22] Franco de Francisco, Bull. Lab. chim provencialle, Bologna **4,** 79 (1953).
[23] J. R. Rossum, Analytical Chem. **21,** 631 (1949).
[24] F. Kohlrausch and A. Heydweiller, Weid. ann. **53,** 209 (1894); Zeit physik. chem. **14,** 317 (1894).
[25] N. E. Dorsey, Properties of Ordinary Water Substance, A.C.S. monograph No. 81 (Reinhold Publishing Corp., New York, N.Y., 1940).
[26] W. Haller and H. C. Duecker, J. Research NBS **64A,** 527 (1960).
[27] L. Onsager, Physik, Z. **28,** 277 (1927); **27,** 388 (1926).
[28] D. A. MacInnes, The Principles of Electrochemistry (Reinhold Publishing Corp., New York, N.Y., 1939).
[29] R. A. Robinson and R. H. Stokes, Electrolyte Solutions 2d ed. (Butterworths Sci. Pub., London, 1959).
[30] H. S. Harned and B. B. Owen, The Physical Chemistry of Electrolyte Solutions, 2d ed. (Reinhold Publishing Corp., New York, N.Y., 1950).
[30A] Ibid., pp. 142–146.
[31] A. Iverson, J. Phys. Chem. **68,** 515 (1964).

(Paper 69A1–326)

JOURNAL OF RESEARCH of the National Bureau of Standards—A. Physics and Chemistry
Vol. 69A, No. 1, January–February 1965

Preparation of a Carbonate-Free Complex Calcium Aluminate

H. A. Berman

(September 29, 1964)

Compounds found in portland cement are difficult to prepare completely free of carbon dioxide. The difficulty is further intensified in the case of calcium aluminate monosulfate by the instability of the compound in the course of its precipitation from solution and the consequent need for preparing it within a limited time. The compound has been prepared in a large quantity, free of carbon dioxide, by using a closed-system precipitation and filtration assembly, in which rapid movement of the reagent solutions and mother liquor is achieved by the manipulation of trapped pockets of previously prepared CO_2-free air. The precipitate is conditioned and packaged in a glove box in which a CO_2-free atmosphere is maintained. Techniques are described in detail.

1. Introduction

The study of the compounds present in dry and hydrated portland cement is complicated by the ease with which all these materials absorb, adsorb, and react with carbon dioxide. Failure to account for this sensitivity has led many workers to erroneous identification of some of these compounds or to inaccurate determinations of their properties. Notable among these errors has been the postulation of the existence of hexagonal tricalcium aluminate hexahydrate, shown recently to be a mixture of dicalcium aluminate and tetracalcium aluminate carbonate hydrates [1].[1]

Among the CO_2-sensitive compounds either found in or related to hydrated portland cement are the calcium aluminate complex salts of the general formula $3CaO \cdot Al_2O_3 \cdot qCaX \cdot nH_2O$, where $q=1$ or 3 and $n=10$ to 12 or 30 to 33, respectively, and X is a divalent ion or two units of a monovalent ion. The two sulfates in this group, $3CaO \cdot Al_2O_3 \cdot CaSO_4 \cdot 12H_2O$ and $3CaO \cdot Al_2O_3 \cdot 3CaSO_4 \cdot 32H_2O$, are readily transformed in the presence of CO_2 to hydrated alumina and $CaCO_3$, and often to the corresponding calcium aluminate monocarbonate, $3CaO \cdot Al_2O_3 \cdot CaCO_3 \cdot 11H_2O$ [2]. (In the process, the monosulfate is changed to the trisulfate or free $CaSO_4$ may appear.) The monocarbonate and its corresponding tricarbonate, $3CaO \cdot Al_2O_3 \cdot 3CaCO_3 \cdot 30H_2O$, are similarly converted by additional CO_2 to $CaCO_3$ and hydrated alumina [3].

In the course of a thermochemical program designed to determine the heat of formation of the complex calcium aluminate salts, attempts have been made to prepare these salts as free of carbonate impurity as possible. Samples of calcium aluminate monosulfate have been prepared with analyzed CO_2 contents from 0.09 to 0.45 percent by weight [2]; samples of calcium aluminate trisulfate, from 0.24 to 2.1 percent [4]. In general, the monosulfate and those trisulfates lowest in CO_2 were made in closed systems with precautions taken to exclude carbon dioxide.

However, the ubiquity of CO_2 has defeated attempts to prepare these materials entirely CO_2-free. Up to the present work, no successful preparation entirely CO_2-free has reached the attention of the author. It is difficult to handle these materials in the complete absence of room air when grinding and mixing the dried powder or during such operations as transfer from filters to conditioning desiccators and thence to storage bottles. It is almost impossible to maintain completely tight vacuum desiccators in an ordinary laboratory. The experiences of many investigators have been similar [5, 6].

An additional problem in the precipitation of calcium aluminate monosulfate is the necessity for bringing together large quantities of $Ca(OH)_2$ and $Al_2(SO_4)_3$ in a short time. The monosulfate is transformed to the trisulfate if the precipitate stands too long in contact with the mother liquor. The larger the molar ratio of $Ca(OH)_2$ to $Al_2(SO_4)_3$ added (up to about 20:1), the longer the time available before this conversion begins to take place, but, at the same time, the lower the yield of precipitate. A 50-liter batch produces only about 30 g of the dried monosulfate. This problem has been met [2] by filling the reaction bottle several times, mixing, and drawing off the supernatant liquor between fillings. A large quantity of precipitate builds up and is all digested with the same mother liquor after the last mixing operation.

[1] Figures in brackets indicate the literature references at the end of this paper.

The National Bureau of Standards has been participating in a group effort to study the properties of portland cement constituents and improve methods of identification. As part of the effort, this laboratory was asked to prepare reference samples of the two calcium aluminate sulfates in large quantity (about 100 g) for distribution to the participating laboratories.

A sample of the highest purity, as free of CO_2 as possible, was desired. The results obtained for two lots of calcium aluminate monosulfate are given first, followed by a description of the apparatus and techniques employed. The procedure used is then given in sufficient detail to illustrate the techniques.

2. Results

Two samples of calcium aluminate monosulfate, $3CaO \cdot Al_2O_3 \cdot CaSO_4 \cdot 12H_2O$, were prepared. Lot 1, produced with a yield of 40 g, had a CO_2 content (by conventional methods of calculation from sample and blank determinations) of 0.015 percent, with a negligible standard error in precision. The estimated uncertainty in accuracy is 0.03,[2] inasmuch as the CO_2 determinations were made at the limit of detectability of this compound. Lot 2, containing 79 g, had 0.005 percent CO_2, with a standard error estimate of ± 0.005 percent in precision, by the same conventional calculation, with the same uncertainty in accuracy.

The values obtained in the sample and blank CO_2 determinations are shown in table 1.

The figure for accuracy is based on the fact that the largest value for a blank determination for each sample is equal to or greater than the largest value for a sample determination. The upper limit of uncertainty in accuracy is taken as the largest weight increase found for a sample determination without making a subtraction for the blank.

It is probable that the materials contained no CO_2 at all.

The analyses of the samples and calculated compound compositions are shown in table 2.

TABLE 1. *Carbon dioxide determinations*

Lot	1		2	
Determination	A	B	A	B
Weight increase in absorption tube:				
Blank, prior to sample determination, g	0.0003	0.0002	0.0005	0.0002
Sample determination, g	.0003	.0003	−.0001	.0003
Blank, after sample determination, g	.0000	.0000	.0002	.0001
Sample minus blank average, g	.00015	.0002	[b] .0000	.00015
Weight of sample, g	1.0147	1.4164	.8734	1.5204
Calculated percent "CO_2" in sample [a]	0.015	0.014	.00	0.01

[a] See discussion in text. The uncertainty of the determination is 0.03 percent, or twice the calculated value for Lot 1.
[b] Negative values ignored.

[2] The uncertainty in accuracy is given as a range rather than a standard deviation.

TABLE 2. *Analysis of the samples*

Lot	1	2
Weight percent:		
CaO	36.26	36.13
Al_2O_3	16.29	16.27
SO_3	12.86	12.72
H_2O	34.66	34.77
CO_2 [a]	0.0_{15}	0.0_{05}
Molar ratios:		
$CaO:Al_2O_3$	4.04_7	4.03_8
$SO_3:Al_2O_3$	1.00_5	0.99_6
$H_2O:Al_2O_3$	12.04	12.10
Compound composition, moles/mole Al_2O_3: [b]		
$3CaO \cdot Al_2O_3 \cdot CaSO_4 \cdot nH_2O$	1.00	1.00
where n=	11.99	12.06
$CaSO_4 \cdot 2H_2O$	0.00_5	
$Ca(OH)_2$	0.04	0.04

[a] See table 1 for actual determinations of CO_2, and see text for discussion. The uncertainty of the determination is 0.03 percent, or twice the calculated value for Lot 1.
[b] Calculations of compound composition are based on the procedure described in the appendix to reference [4].

3. Apparatus and Techniques, Materials, and Procedures

The general steps in the procedure were as follows. The samples were prepared by precipitation from essentially CO_2-free solutions of $Ca(OH)_2$ and $Al_2(SO_4)_3$ in the closed-system assembly shown schematically in figure 1, and in simplified form in figure 2. The precipitate was filtered in a closed system shown in figure 1. The filter funnel containing the precipitate was transferred (with exit and entrance tubes closed off) to the glove box shown schematically in figure 3. There the precipitate was placed in a desiccator, for conditioning at 33 percent relative humidity, until its loss on ignition was constant. It was then ground inside the glove box, mixed in a sealed jar, and packaged inside the box.

The equipment and techniques used in each of these steps are first described generally. In succeeding sections, enough of the detailed procedure is described to illustrate these techniques.

3.1. Apparatus and Techniques

a. Precipitation

The precipitation system shown in figure 1 was designed to move large quantities of liquid into and out of the reaction bottle in a short time. It consists of four storage bottles for $0.02M$ $Ca(OH)_2$, labeled A_1, A_2, A_3, and A_4; a bottle containing approximately $4N$ NaOH, labeled A_0; a bottle for the reaction, B; and an overflow bottle, C. These are nominal 13-gal polyethylene containers capable of holding 58 liters. Bottle D is a 2.5-liter commercial reagent acid bottle, containing $0.1M$ $Al_2(SO_4)_3$ solution; and bottle E is a long, narrow container graduated to measure the quantity of $Al_2(SO_4)_3$ solution fed to bottle B.

Bottle B is closed with a rubber stopper furnished with the seven tubes shown in figure 1, and also with a ground-glass bearing which serves as a guide for a ground-glass stirring shaft 86 cm long. When lubricated with a grease furnished by the manufac-

turer, the shaft closure is air-tight, but the shaft is free to turn. This type of stirrer was used instead of a magnetic stirrer, which could not effectively stir 50 liters of solution when activated through the thick bottom of the polyethylene bottle.

To obtain rapid flow, glass tubing 9 mm o.d. was used for the liquid lines, whereas 7-mm tubing was adequate for the air lines. For steps in which the speed of transferring a liquid was most important, three or four lines were used in parallel. Since stopcock bores are small in cross section, pinchcocks with screw-thread closure on tygon tubing were used instead for all the one-way valves.

Figure 2 is a simplified drawing of the essential parts of the precipitation system, from which the principles involved are more readily evident than they are from figure 1. Rapid transfer of liquid must be accomplished with rapid movement of CO_2-free air. Since it is impossible to remove all the CO_2 by absorption from an air stream moving at high velocity, a slow stream of air is passed through a CO_2-absorption train, and the air is stored in bottles B and C prior to the mixing operation. $Ca(OH)_2$ is then siphoned from one of the A bottles into bottle B, while the air in B rapidly moves into A to displace the $Ca(OH)_2$. Similarly, in drawing off the supernatant liquor from B to C, air in C rapidly moves into B, providing at the same time a source of displacement air for the next transfer of $Ca(OH)_2$ from an A bottle to B.

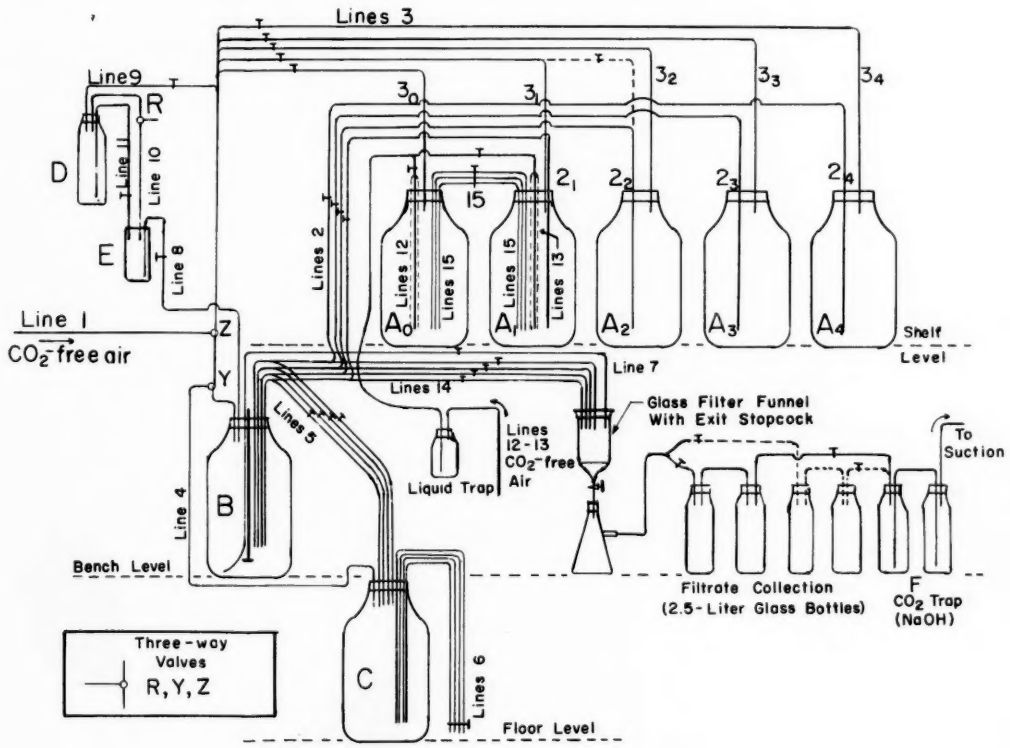

FIGURE 1. *Closed system for precipitation and filtration.*

Polyethylene bottles, 58 liter:
- A_0—4N NaOH
- A_1, A_2, A_3, A_4—0.02M $Ca(OH)_2$
- B—reaction bottle
- C—overflow bottle

Glass bottles:
- D—$Al_2(SO_4)_3$ storage, 2.5 liters
- E—$Al_2(SO_4)_3$ metering, graduated 0–900 ml.

R, Y, Z—Three-way valves
T—marks indicate pinchcoks

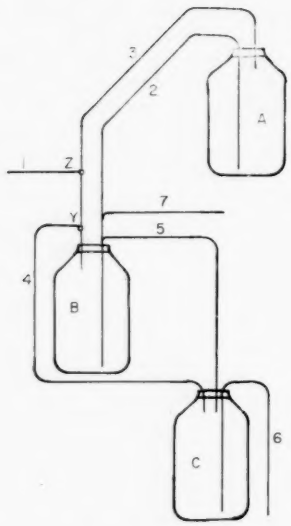

FIGURE 2. *Simplified representation of a portion of figure 1.*

A. Calcium hydroxide storage bottle.
B. Reaction bottle.
C. Overflow bottle.
Y, Z. Three-way valves.

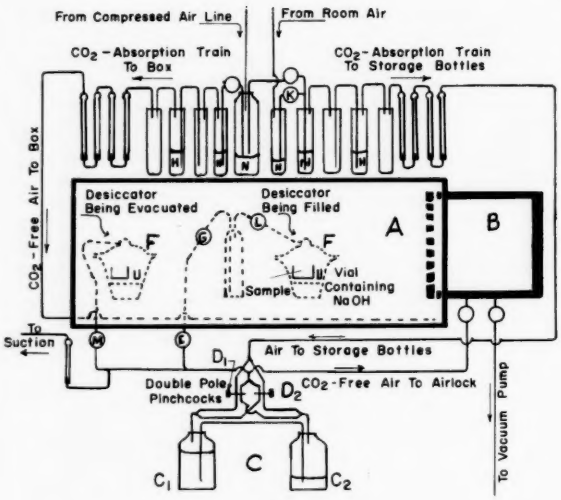

FIGURE 3. *Glove box and air storage system.*

A. Main chamber.
B. Airlock.
C. CO_2-free air storage bottles.
D. "Double-pole, double-throw" pinchcock system for reversing flow in air storage bottle C. When one pinchcock is open, the other is closed; each cock controls two lines simultaneously.
E, G, K, L, M. Pinchcocks.
F. Conditioning desiccators.
H. Sulfuric acid.
N. Sodium hydroxide solution.

b. Conditioning

The glove box shown in figure 3 consists of a main chamber A, and a 30-liter airlock B which can be evacuated to 1 cm Hg or better. Two CO_2-absorption trains, similar to those described in the section immediately following, provide air for the main chamber, airlock, and conditioning chambers F inside the box. The train on the left serves the main chamber directly and provides continuous positive pressure in the chamber. The box had been provided with an air outlet with NaOH traps, but the positive pressure was found to be accommodated by movement of the rubber gloves and by some residual leakage. The train on the right feeds air to two sets of air-storage bottles C (shown in fig. 3 only as two bottles) with a total capacity of 120 liters (45 liters of air and 75 of saturated $Ca(OH)_2$ solution with excess solid $Ca(OH)_2$). The bottles are so arranged that when air is fed to one set, the $Ca(OH)_2$ solution is displaced to the other set, in turn displacing the air in the second set to the particular chamber which is being purged. The object of this procedure is to fill the chamber rapidly from a stored supply of CO_2-free air (from set C_2, for example, with pinchcock D_1 open, D_2 closed). In the process, air passing rapidly through the train enters set C_1 in an amount equal to the air leaving C_2. Only partially purified by the train, the air in C_1 is allowed to stand in contact with the $Ca(OH)_2$ solution overnight to complete the removal of CO_2. It is then available for another rapid purge the next day, when the flow through the bottles, but not through the system, is reversed by closing pinchcock D_1 and opening D_2, the pinchcock system acting in a manner analogous to that of a double-pole, double-throw reversing switch.

The conditioning chambers F are vacuum desiccators containing both $MgCl_2 \cdot 6H_2O$ for maintaining 33 percent relative humidity and small vials with a few pellets of NaOH to remove any traces of CO_2 from the desiccator air.[3] The desiccator and contents are purged several times outside the glove box by evacuating to about 2 cm Hg pressure with an aspirator and refilling with CO_2-free air passed through saturated $MgCl_2$ solution. The desiccator is then evacuated and placed in the airlock. The airlock is evacuated, refilled with CO_2-free air from the storage bottles (air entering the right-hand train from the room through valve K). The airlock is then opened to the main chamber and the desiccator transferred thereto. Desiccators are prepared in this manner for later use. When it is time to place the precipitated and filtered material into a desiccator, the latter is refilled with CO_2-free air by opening valves D, E, G, and L, the air passing through a bottle of saturated $MgCl_2$ solution before entering the desiccator. After the material is placed in the desiccator, it is evacuated by an aspirator through valve M.

[3] A solution of 11.4 *N* NaOH was first used because its water-vapor pressure corresponds to 33 percent relative humidity, but the NaOH solution picked up water from the precipitates faster than it surrendered it to the $MgCl_2$ solution and overflowed into the latter solution. The small quantity of solid NaOH is not enough to disturb the water-vapor equilibrium in the desiccator.

3.2. Materials

a. CO_2-Free Air

The CO_2-free air used during the precipitation (figs. 1 and 2) and during the conditioning (fig. 3) was furnished by several trains, only one of which is illustrated (fig. 3). Compressed air from a 40-psi line is passed successively through: (1) a pressure-reducing valve (0–25 psi outlet); (2) a needle valve; (3) five test tubes or gas-washing bottles, of which the first, third, and fifth are traps, the second contains 4 *N* NaOH, and the fourth contains concentrated H_2SO_4; (4) and finally through a series of four straight absorption bulbs, each of which contains ascarite, magnesium perchlorate, and indicating anhydrite. For independent, trouble-free operation, each CO_2-free air train is provided with its own reducing and needle valve. The bulbs with solid absorbents last almost indefinitely if the NaOH and H_2SO_4 solutions are replenished often. The NaOH solution lasts longer if it is made from CO_2-free water and 20 *N* NaOH which has been filtered or decanted from its Na_2CO_3 impurity.

b. Aluminum Sulfate (Approximately 0.1 *M*)

The apparatus is shown in figure 4. All containers are filled with CO_2-free air either by evacuation and refilling, or by filling them with CO_2-free water and displacing the water with the air. A 1-lb bottle of reagent $Al_2(SO_4)_3 \cdot 18H_2O$ (not purged before being placed in the assembly) is fitted with a 3-hole stopper and tubes as shown in B, figure 4. It is placed in a water bath C over a hot plate F. The bottle is evacuated, then boiling distilled H_2O is admitted to it from flask A. After a few minutes of digestion, the hot solution is transferred by pressure to fritted glass filter funnel E and the filtrate eventually collected in the 2.5-liter storage bottle D, later to be connected to the assembly in figure 1. The reagent bottle B is again evacuated, more hot H_2O is admitted, and the process is continued until all the solid has been dissolved. The filtrate is thoroughly mixed and divided roughly equally among three bottles (D, figs. 1 and 4). The transfer is made with CO_2-free air. The divided filtrates are cooled in CO_2-free air, and CO_2-free H_2O is added to fill the D bottles. The contents are mixed, and, under CO_2-free air pressure, a sample is removed from each bottle for analysis to determine the Al_2O_3 and SO_3 concentrations, to be used later in proportioning the precipitation mixture and in calculating material balances.

c. Calcium Hydroxide

Eleven liters of distilled H_2O is boiled in a 12-liter flask about 15 min. and allowed to cool to room temperature with the flask stoppered but connected to the outlet of a CO_2-free air line. About 18 g of CaO, prepared by igniting low-alkali reagent $CaCO_3$ at 1000 °C to constant weight, is added to the cooled H_2O while the flask is momentarily unstoppered.

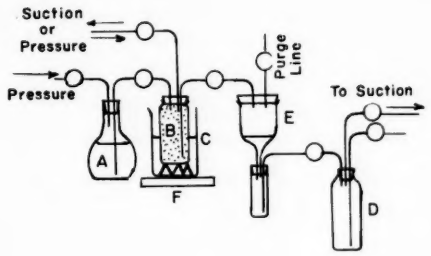

FIGURE 4. *Closed system for preparing aluminum sulfate solution.*

A. Boiling CO_2-free H_2O.
B. Aluminum sulfate in original reagent bottle.
C. Hot water bath.
D. Aluminum sulfate storage bottle.
E. Filter funnel.
F. Hot plate.

The mixture is stirred with a magnetic stirrer several hours. Before the system shown in figure 1 is completely assembled,[4] the four A bottles are filled with $Ca(OH)_2$ solution in the following manner. An exit delivery tube from the 12-liter flask (not shown in the figures) is connected to one of the A bottles through the appropriate line 2. With the stirrer still on, the $Ca(OH)_2$ solution is transferred to the A bottle under pressure of CO_2-free air. The air in the A bottle is displaced through lines 3 and 1 (line 1 disconnected from the CO_2-free air line). Successive batches are made in this manner until bottles A_1 to A_4 are filled. The undissolved $Ca(OH)_2$ in these bottles serves to keep the solution CO_2-free; any $CaCO_3$ that forms settles to the bottom and is not carried over into the reaction bottle.

With the system of figure 1 still only partially assembled, any $Ca(OH)_2$ remaining in lines 14 is flushed out with CO_2-free water, added from a flask in the same manner as the $Ca(OH)_2$ was added, and ejected from the open end of the flexible tubing which normally connects line 2 to bottle B when the apparatus is fully assembled.

3.3. Procedures

a. Precipitation

The procedure is described here only in sufficient detail to illustrate the principles involved, and, for this purpose, reference is first made to the simplified drawing in figure 2.

Bottles B and C are filled with hot CO_2-free water. The water is slowly displaced with CO_2-free air, a process which takes about two days per bottle. The bottles are again filled with hot CO_2-free water and once more with CO_2-free air. The water is added to bottle B through line 7 from a 12-liter flask under CO_2-free air pressure, the room air in the bottles being displaced through lines 3 and 1 with valves Y and Z in the appropriate positions, and line 1

[4] At this time, bottles B and C, the filtration system, and the A bottles, are three separate closed systems.

disconnected from the CO_2-free air line but connected to the NaOH trap of the filtration system F at a convenient point (fig. 1). Water is added to bottle C through line 6, displacing the air through lines 4, 3, and 1. Air is added to the bottles in the reverse directions with line 1 connected to the CO_2-free air line.

After bottles B and C have been purged in this manner, the entire precipitation and filtration assembly of figure 1 may be connected together, so that the precipitation may be started.

At the start of the working day, bottle B is filled with $Ca(OH)_2$ from bottle A_1 (fig. 1) or A (fig. 2) by the following two-step procedure. Line 2 is filled with $Ca(OH)_2$ solution by allowing CO_2-free air to pass through lines 1 and 3 into bottle A, thereby forcing $Ca(OH)_2$ solution to fill line 2. Valve Y is set to allow the air from B to pass through line 4 into bottle C. This step takes only a moment and therefore requires no venting of bottle C. As soon as line 2 is full of liquid, the hydrostatic head in line 2 permits the flow to continue without air pressure from line 1. Valves Y and Z are then turned to close off lines 1 and 4 and open line 3 to bottle B. Air in bottle B is now displaced to bottle A as the $Ca(OH)_2$ in bottle A fills bottle B.

Bottle E (fig. 1) is then filled with $Al_2(SO_4)_3$ solution from bottle D by a similar two-step procedure, in which line 11 is first filled with the solution under air pressure through lines 1, 3, and 9. When line 11 is full, the air pressure is no longer needed, and the $Al_2(SO_4)_3$ solution continues to flow into E, the air being displaced from E to D through line 10. When E is full of solution, the flow continues up line 10 until the level in line 10 is the same as the level in D. Since line 10 is only 1.8 mm i.d., only a negligible quantity of $Al_2(SO_4)_3$ solution enters line 10.

The stirrer in bottle B is turned on, line 11 is closed off, and air pressure to E via lines 1, 3, 9, and 10 forces $Al_2(SO_4)_3$ solution to flow from E to B through line 8. Flow continues until the desired quantity of $Al_2(SO_4)_3$ solution, measured in bottle E, has been added; line 8 is then shut off.

Stirring is continued as long as necessary (6 min for the calcium aluminate monosulfate), and the precipitate is then allowed to settle (about 10 min).

As described in the introduction, it is now necessary to remove the supernatant liquor and replace it with a second batch of reagent solutions. The liquor is transferred to bottle C by a two-step technique identical to that used to fill B with solution from A, the air in C replacing the liquor from B. Thus, the CO_2-free air originally trapped in B and C is used to help transfer these liquids rapidly without depending on slow movement of air through a CO_2-removal train. To insure rapid flow of the liquid, line 5 actually consists of four parallel lines, as shown in figure 1.

The second, third, and fourth batches of reagent solutions are added in a similar manner, except that rapid transfer of $Ca(OH)_2$ in each addition is more critical because the first precipitate is already in contact with the mother liquor. Rapid flow is achieved by drawing from three $Ca(OH)_2$ bottles simultaneously (A_2, A_3, and A_4 in fig. 1). The technique, in principle, is to cause air to flow rapidly into bottle A_0, bubbling in the process through the NaOH solution in that bottle, displacing the NaOH into bottle A_1. The CO_2-free air already in bottle A_1 is allowed to flow into A_2, A_3, and A_4, pushing the $Ca(OH)_2$ solution in these bottles into B. The air in B is displaced into C, where it in turn forces the spent liquor in C into the room through line 6. When bottle B contains the desired quantity of $Ca(OH)_2$, the flow is stopped, and $Al_2(SO_4)_3$ solution is added as for the first batch.

The arrangement makes it possible to complete a four-batch precipitation of calcium aluminate monosulfate in 5 hr. This time period allows for 6 min of stirring and 10 min of settling after each of the first three additions, and 10 min of stirring and 20 min of settling before the filtration. The filtration requires two more hours. At a $Ca(OH)_2/Al_2(SO_4)_3$ molar ratio of 20, this total period of 7 hr is within the limit for preparation of monosulfate without any conversion to trisulfate. The first addition of $Ca(OH)_2$ has not been included in this time because reaction does not start until the $Al_2(SO_4)_3$ has been first added.

b. Filtration

On the day prior to the precipitation, the filter funnel is filled with CO_2-free water through line 7 and vented through line 14, with the exit stopcock of the funnel closed and both lines temporarily disconnected from bottle B. CO_2-free air is introduced through line 7 and the water removed from the funnel by suction with the stopcock open. The funnel is purged several times in this manner; then, with air in the funnel, the stopcock is closed and the filtrate flask disconnected and emptied of its water. The apparatus is then reassembled as in figure 1.

After the final addition of $Ca(OH)_2$ and $Al_2(SO_4)_3$, and a final stirring period of 10 min and a settling period of 20 min (in the particular case of preparing calcium aluminate monosulfate), the filtration is started. Suction is turned on in the suction line shown in figure 1, the exit stopcock of the filter funnel is opened, and clear liquid is first drawn rapidly from bottle B through lines 14 into the filter funnel. The liquid in bottle B is displaced by stored CO_2-free air from bottle A_2, which is in turn replenished by fast-flowing air that has bubbled rapidly through the NaOH solution in bottle A_0. When the liquid level in bottle B approaches the bottom, the stirrer is turned on, and the necessary pinchcocks are adjusted to allow the slurry to flow through line 7, which reaches to the bottom of bottle B. The precipitate then collects in the filter funnel. The filtrate collection bottles are so arranged that when two are full they may be disconnected from the system, their contents discarded, and the empty bottles returned to the system; meanwhile, the filtrate has been collecting in the other two filtrate collection bottles.

c. Conditioning

When the filtration is completed, the stopcock of the filter funnel is closed and the suction end of the trap F (fig. 1) in the filtrate collection system is disconnected from the suction line, restoring atmospheric pressure to the system. The entrance tubes to the filter funnel are closed off by pinchcocks and disconnected from lines 7 and 14. An absorption bulb containing ascarite is attached to one of these entrance tubes, the pinchcock opened and the funnel-tube assembly is placed in the airlock of the glove box. The airlock is evacuated and refilled with CO_2-free air from the storage bottles as described above. The inner door is then opened and the assembly transferred to the main chamber. A conditioning desiccator in the main chamber is filled with CO_2-free air (via $MgCl_2$ solution) and the precipitate is transferred from the filter funnel to a suitable container and placed inside the desiccator. It is kept there until its loss on ignition is constant, being moved to other desiccators as the solid $MgCl_2 \cdot 6H_2O$ is exhausted. The time required for conditioning is usually about two months. To obtain a sample for loss-on-ignition determination, a platinum crucible is ignited and weighed, then transferred inside a desiccator through the airlock into the box. A sample of the precipitate is placed in the crucible, which is then returned inside the desiccator to the room.

d. Further Handling

When the loss on ignition is constant, the sample is removed from the conditioning desiccator and ground inside the glove box with an agate mortar and pestle. It is then transferred to a jar which has been purged, evacuated, transferred to the glove box, and refilled with conditioned air in the same manner as the desiccators. The jar is closed, sealed with plastic tape, placed inside a polyethylene bag containing ascarite, and removed through the airlock to the room. The contents of the jar are mixed several days on a rotating wheel. The jar is returned to the glove box, removed from the polyethylene bag, and stored inside a conditioning desiccator. A sample for chemical analysis is placed in a weighing bottle and removed from the glove box by the same technique used to obtain a loss-on-ignition sample, as described in the preceding section.

After chemical analysis has been completed, the preparation is packaged in glass vials inside the glove box. The cap of the vial is taped to provide a seal and the vials are protected from the atmosphere in the following manner (shown in fig. 5): A length of glass tubing is sealed at one end. Freshly ignited CaO is placed in the sealed end and covered with glass wool. The glass tube is transferred to the glove box and a taped glass vial is inserted with the cap toward the sealed end. A plug of glass wool, a layer of CaO, and another plug of glass wool are then inserted. The assembly is removed from the glove box and the open end of the tube is sealed as rapidly as possible, leaving enough empty space to effect the seal without heating the sample.

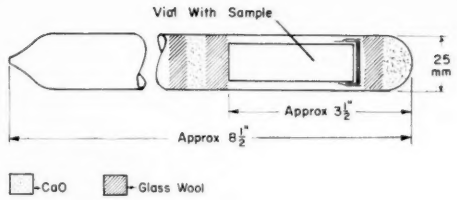

FIGURE 5. *Packaging container.*

4. Summary and Conclusions

Apparatus, techniques, and procedures have been described for the preparation of a complex calcium aluminate essentially free of carbonate impurity. The system has been used to prepare two lots of calcium aluminate monosulfate, $3CaO \cdot Al_2O_3 \cdot CaSO_4 \cdot 12H_2O$, and can be used in the form described, or with modifications, to prepare by precipitation other compounds that are sensitive to carbon dioxide. The system has also been used to make a large lot of calcium aluminate trisulfate, although in this case rapid liquid flow during the precipitation is not critical. As in the case of the monosulfate, it is particularly useful in those instances where the compound desired is stable only for a limited time in the presence of its mother liquor.

5. References

[1] R. Rabot and M. T. Mounier, On the existence of hexagonal tricalcium aluminate hydrate (in French) Revue des Matériaux de Construction et Travaux Publics **554,** 449 (1961).

[2] H. A. Berman and E. S. Newman, Heat of formation of calcium aluminate monosulfate at 25° C. J. Res. NBS **67A** (Phys. and Chem.), No. 1, 1 (1963).

[3] E. T. Carlson and H. A. Berman, Some observations on the calcium aluminate carbonate hydrates, J. Res. NBS **64A,** (Phys. and Chem.), No. 4, 333 (1960).

[4] H. A. Berman and E. S. Newman, Heat of formation of calcium trisulfoaluminate at 25° C, Proceedings of the Fourth International Symposium on the Chemistry of Cement (Washington, 1960); NBS Mono 43, pp. 247–257.

[5] D. L. Kantro, L. E. Copeland, and E. R. Anderson, An X-ray diffraction investigation of hydrated portland cement pastes, ASTM Proceedings **60,** 1020 (1960); Portland Cement Association Bulletin 128.

[6] P. Seligmann and N. R. Greening, Studies of early hydration reactions of portland cement by X-ray diffraction, in press.

(Paper 69A1–327)

JOURNAL OF RESEARCH of the National Bureau of Standards—A. Physics and Chemistry
Vol. 69A, No. 1, January–February 1965

Synthesis and Thermal Stability of Bis(8–hydroxyquinoline)–Schiff Base Coordination Polymers

Emanuel Horowitz and Theodore P. Perros*

(June 16, 1964)

This report describes the synthesis of a new bis-bifunctional derivative of 8-hydroxyquinoline, its reaction with a number of divalent, first-row transition metals to form coordination polymers, and a thermogravimetric study of the thermal stability of the polymers. The ligand, 5,5′-[methylenebis(*p*-phenylenenitrilomethylidyne)]di-8-quinolinol was prepared in a condensation reaction between 5-formyl-8-hydroxyquinoline and 4,4′-methylenedianiline and subsequently treated with the acetate salts of Mn(II), Co(II), Ni(II), Cu(II), and Zn(II). The metal coordinated in the backbone of the polymer is shown to be an important factor in governing the thermal stability when the samples are heated in vacuum.

1. Introduction

In an earlier paper [1] [1] the authors reported the synthesis and thermal properties of coordination polymers of bis(8-hydroxy-5-quinolyl)methane. The thermal stability of Schiff base and related coordination systems has been studied by other workers [2–7], although not under the conditions used in our experiments. For example, Friihof [2] prepared a variety of interesting 8-hydroxyquinoline-Schiff bases which he reacted with metal ions to obtain insoluble coordination polymers in the form of colored powders. He examined the thermal stability of a number of the polymers by heating 200 mg samples at fixed temperatures and measuring the weight loss after a 12-hr interval.

Marvel and coworkers [3] investigated the thermal stability of Zn(II), Ni(II), and Cu(II) chelates containing ligands I and II.

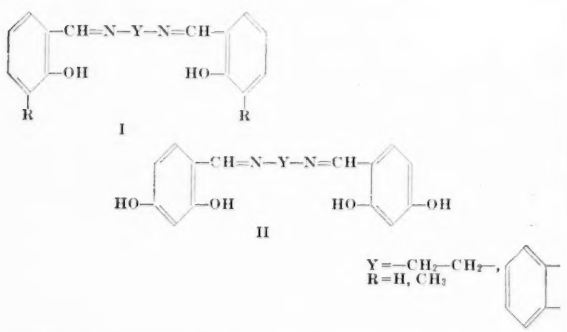

I

II

They found that the copper complexes were always less stable than those of either zinc or nickel, and the relative stability of the two latter complexes depended, to a large extent, upon the nature of the bridging group. Charles [7] studied the heat stabilities of some Schiff base chelates of *N*-alkylsalicylaldimine,

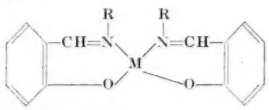

and found that in all cases the copper complexes were less stable than those of zinc. The relative stability of the nickel and the zinc chelates appeared to be a function of the alkyl substituent on nitrogen. The zinc complexes containing heptyl, decyl, and dodecyl groups were more stable than the nickel complexes. However, with propyl and amyl groups on nitrogen, the nickel chelates were more stable than the zinc compounds.

The work to be described here is an extension of the original investigation [1] and deals with the synthesis and thermal stability of coordination polymers of 5,5′-[methylenebis(*p*-phenylenenitrilomethylidyne)] di-8-quinolinol. These polymers differ from those in the first group chiefly because the $-CH_2-$ bridge in bis(8-hydroxy-5-quinolyl)methane has been replaced by a

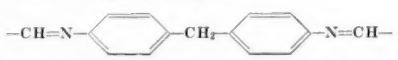

bridging group. The coordination polymers of bis(8-hydroxy-5-quinolyl)methane were found to be very insoluble, even in boiling organic solvents. As is well known, the insoluble nature of coordination polymers has severely limited their use as engineering materials and has impeded more fundamental

*Chemistry Department, The George Washington University, Washington, D.C.

[1] Figures in brackets indicate the literature references at the end of this paper.

research dealing with such problems as molecular weights and polymer morphology. On the basis of chemical considerations, the bis-bifunctional nature of the ligand leads one to expect that polymers were formed during the reactions with metal ions. This view is supported by infrared and elemental analysis, the insolubility of the products from the reactions and, moreover, by their enhanced thermal stability. The properties of the products differed markedly from the known behavior of the nonpolymeric complexes of 8-hydroxyquinoline. In part, the insertion of the large organic bridge in the present group of polymers was an attempt to improve their solubility characteristics in organic solvents. In addition, it was of interest to study the effect of this large bridging group on the thermal stability and other properties of the coordination polymers.

2. Experimental Procedure

Synthesis of 5,5′-[methylenebis(p-phenylenenitrilomethylidyne)] di-8-quinolinol. The 5-formyl derivative of oxine was prepared by means of a Reimer Tiemann reaction of 8-hydroxyquinoline with chloroform in alkaline solution [8]. The product ultimately obtained from this reaction was extracted with petroleum ether, and on cooling, a brown-orange solid crystallized in the extract. This was recrystallized from acetone, yielding an orange-tan product in the form of fine needles that melted at 178.5–179.5 °C.

Anal. Calc.	$C_{10}H_7O_2N$:	C 69.4	H 4.02	N 8.09
Found		C 69.3, 69.2	H 4.07, 4.01	N 7.81, 8.23

The 5-formyl oxine (0.8658 g) and purified 4,4′-methylenedianiline (0.4957 g, m.p. 92 °C) were refluxed in 35 ml of methanol, using magnetic stirring. After about 15 min a yellow-brown solid formed in accordance with the reaction shown in eq (1). The reaction mixture was heated for an additional 30 min and then allowed to cool to room temperature, the product was collected, washed with methanol, and dried in vacuum. The yellow powder melted at 229 to 230 °C.

Anal. Calc.	$C_{33}H_{24}O_2N_4$:	C 78.0	H 4.75	N 11.0
Found		C 78.1	H 4.96	N 11.0

3. Synthesis of Schiff Base Coordination Polymers

The coordination polymers were prepared, as shown in the general equation (eq 2, below), by dissolving the ligand in boiling dimethylformamide[2] and adding, drop-wise, a stoichiometric amount of the metal acetate contained in a dimethylformamide solution, while the reaction mixture was under reflux conditions. When the cation was added to the solution containing the ligand there was a sudden change in the color of the solution accompanied by the precipitation of the polymer. The polymers, in the form of colored powders, were found to be insoluble in a wide variety of solvents and could not be purified by recrystallization. Therefore, each polymer was collected, wrapped in filter paper prior to insertion in a paper thimble, and extracted with dimethylformamide for 16 hr in a Soxhlet apparatus. This was designed to purify the polymer by extracting unreacted starting materials and soluble nonpolymeric substances. After 16 hr the solution in the extraction flask was highly colored while the solvent in contact with polymer in the extractor was colorless. The polymers were then extracted with absolute alcohol to remove adsorbed dimethylformamide

[2] The dimethylformamide was first treated with KOH pellets and then distilled at atmospheric pressure in the presence of CaO. The fraction which distilled between 152 to 154 °C was collected and used in this work.

Equation 1:

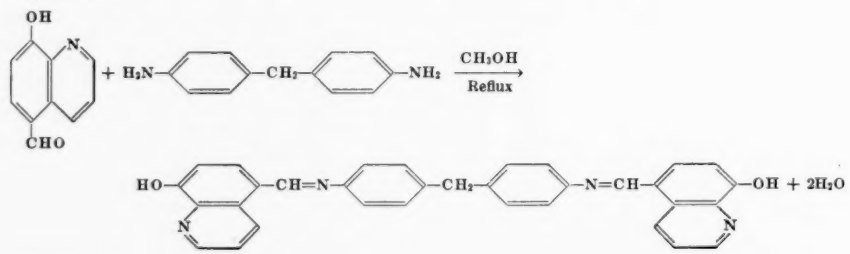

Equation 2:

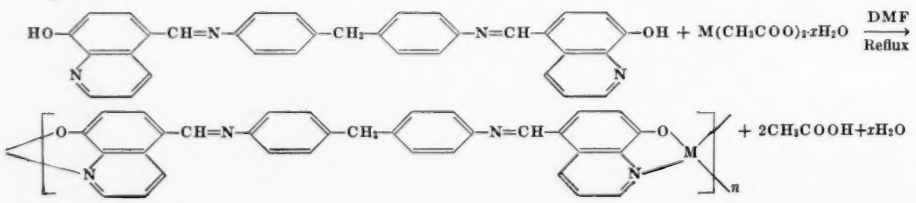

and any alcohol-soluble constituents. The product was dried over P_2O_5 in vacuum at 140 °C for 24 hr. The results of the elemental analyses of the polymers are given in table 1.

TABLE 1. *Elemental analyses of coordination polymers*

Polymer	Calculated, %				Found, %			
	C	H	N	M	C	H	N	M
$[MnL \cdot H_2O]_n$	68.4	4.17	9.67	9.48	68.2	4.10	.....	.....
$[MnL \cdot 2H_2O]_n$	66.3	4.39	9.37	9.19				
$[CoL \cdot H_2O]_n$	67.9	4.14	9.60	10.1	67.3	4.58	9.00	9.20
$[CoL \cdot 2H_2O]_n$	65.9	4.36	9.31	9.80				
$[NiL \cdot H_2O]_n$	68.0	4.15	9.61	10.1	66.2	4.34	9.54	10.4
$[NiL \cdot 2H_2O]_n$	65.9	4.36	9.32	9.76				
$[CuL \cdot H_2O]_n$	67.4	4.11	9.53	10.8	69.3	4.11	9.46	11.2
$[CuL \cdot 2H_2O]_n$	65.4	4.32	9.24	10.5				
$[ZnL \cdot H_2O]_n$	67.2	4.10	9.50	11.1	66.9	4.19	9.12	10.7
$[ZnL \cdot 2H_2O]_n$	65.2	4.31	9.22	10.8				

$L = C_{23}H_{22}O_2N_4$

4. Thermogravimetric Analysis

The thermal stability of the Mn(II), Co(II), Ni (II), and Zn(II) 5,5′-[methylenebis(*p*-phenylenenitrilomethylidyne)]di-8-quinolinol coordination polymers was studied under vacuum conditions using an Eyraud Electronic Thermobalance.[3] A 50-mg sample contained in a platinum crucible was heated from room temperature to 1000 °C at a heating rate of 2.5 °C/min. The weight loss was determined as previously described [1]. The thermal stability of the Cu(II) coordination polymer was evaluated with a modified Cahn Electronic Balance to be described in a subsequent publication, after it was demonstrated on reference materials that the data were in agreement with results obtained with the Eyraud Balance. For each polymer, at least two samples were taken, and thermogravimetric analysis curves were obtained on each sample.

5. Results and Discussion

The weight loss of each polymer, on a percentage basis, over the temperature intervals studied are listed in table 2. These data are plotted in figure 1 where each curve represents the average of two separate runs conducted on different days.

The initial slopes in the thermograms probably represent the volatilization of water, organic solvent such as dimethylformamide, and low molecular weight moieties. For example, the Mn(II) coordination polymer lost approximately 6 percent of its weight prior to the sharp break in the thermogram while the weight loss for the Co(II) and Ni(II) coordination polymers was about 5 to 8 percent.

[3] Eyraud Recording Balance Manual, Anthony M. Kohler, 535 West 110th Street, New York, N.Y.

TABLE 2. *Percentage weight loss of polymers between 25 to 1000 °C (Heating Rate in Vacuum; 2.5 °C/min)*

Temperature	Percentage weight loss (avg of two runs)				
	Zn	Cu	Ni	Co	Mn
°C					
25	0.2	0	0	0	0
50	1.2	0.2	0.1	0.1	0
75	3.0	1.1	.5	.4	0
100	4.3	2.2	.6	.8	0
125	4.7	2.8	.9	1.4	0
150	5.1	3.1	1.3	1.9	0
175	5.5	3.1	2.1	2.6	0
200	6.2	3.2	2.2	2.9	0.4
225	7.5	3.8	2.6	3.2	.6
250	8.6	4.5	2.9	4.0	1.2
275	9.8	5.4	3.5	4.4	1.3
300	10.6	6.3	3.9	4.5	1.6
325	12.1	7.4	4.7	4.8	2.1
350	13.1	9.8	6.3	6.2	2.4
375	14.3	16.5	9.0	7.0	2.8
400	15.1	33.5	13.4	7.9	3.2
425	16.0	45.7	19.6	11.0	4.0
450	19.0	47.6	23.0	14.6	4.7
475	26.0	48.5	26.0	20.0	6.4
500	33.5	49.3	28.1	25.0	17.8
525	35.5	50.0	30.2	26.9	24.7
550	37.7	50.7	32.8	29.5	28.8
575	39.9	51.3	34.7	32.4	30.3
600	42.3	51.9	37.1	35.4	31.7
650	48.1	52.7	42.7	41.9	35.2
700	53.0	54.1	48.0	49.8	39.3
750	57.9	54.9	50.4	57.7	43.3
800	60.4	55.4	54.9	63.9	49.0
850	62.4	.....	55.5	67.2	54.8
900	64.3	.....	59.3	70.5	56.5
950	65.9	.....	60.0	73.9	63.8
1000	68.3	.....	64.5	76.6	68.3

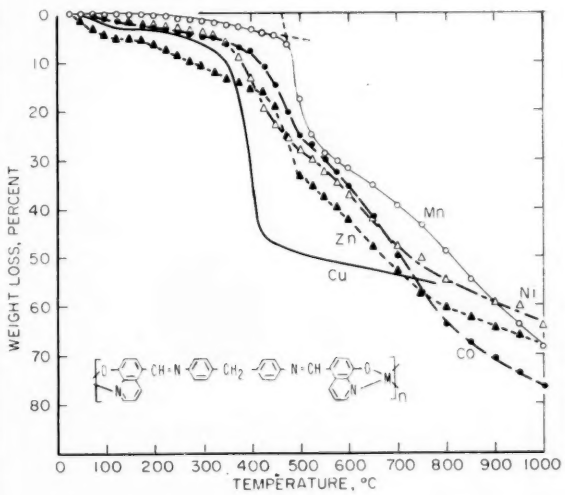

FIGURE 1. *Thermograms of* Mn(II), Co(II), Ni(II), Cu(II), *and* Zn(II) *5,5′-[methylene bis(p-phenylenenitrilomethylidyne) di-8-quinolinol coordination polymers.*

(Heating rate in vacuum, 2.5 °C/min.)

These values agree closely with the calculated 6 percent water content in these polymers based on $[MnL \cdot 2H_2O]_n$, where L represents the ligand. The weight loss of the Zn(II) polymer up to 425 °C amounted to about 17 percent, and these volatiles

may have contained solvent and low molecular weight compounds in addition to water.

After this initial weight loss a rather sharp break occurred in each of the thermograms, signifying the onset of a decomposition process accompanied by a rapid loss of volatile fragments. As a measure of thermal stability, the decomposition temperature of the polymers was determined by the procedure utilized earlier [1]. Briefly, as shown in figure 1 by the dashed lines on the thermogram for the Mn polymer, this involved the drawing of straight lines through the experimental points on the expanded thermogram, before and after the initial sharp break in the curve that occurred at moderately low weight losses. The intersection of these two lines was then projected to the temperature axis and this temperature was arbitrarily defined as the decomposition temperature. These temperatures, for each run, are listed in table 3 and are plotted in figure 2 as a function of the atomic number of metal incorporated in the backbone of the polymers.

TABLE 3. *Decomposition temperatures of coordination polymers*

Coordination polymer	Decomposition temperature, °C		
	Run 1	Run 2	Avg.
Mn	475	465	470
Co	410	420	415
Ni	375	385	380
Cu	345	355	350
Zn	430	430	430

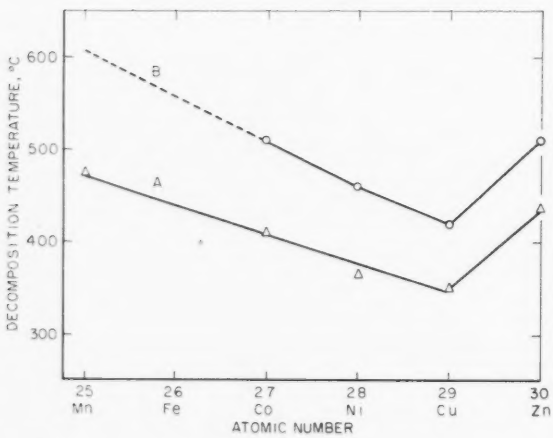

FIGURE 2. *Plot of decomposition temperatures of polymers versus atomic number of coordinated metal.*
A. 5,5′-[methylenebis(*p*-phenylenenitrilomethylidyne)] di-8-quinolinol polymers.
B. Bis(8-hydroxy-5-quinolyl)methane polymers.

It is interesting to note the marked similarity between the shapes of the plots for the polymers of 5,5′-[methylenebis(*p*-phenylenenitrilomethylidyne)] di-8-quinolinol (curve A) and bis(8-hydroxy-5-quinolyl)methane (curve B), reported earlier [1]. In curve A, a linear relationship is seen to exist between the decomposition temperature and the atomic number of the metal, for the polymers containing Mn(II), Co(II), Ni(II), or Cu(II), with the temperature decreasing from about 470 °C to approximately 350 °C. A rather sharp break occurs in the thermogram for the Mn-Schiff base polymer at about 470 °C, the critical temperature at which accelerated weight loss ensues. No such break was observed in the thermogram of the Mn-bis(8-hydroxy-5-quinolyl)-methane polymer, probably because the loss of water and other volatile constituents below the decomposition temperature obscured this point. However, the present work, as well as the thermal characteristics of the metal chelates of 8-hydroxyquinoline [1], tends to substantiate the extrapolation shown in curve B. The Zn(II) 5,5′-[methylenebis(*p*-phenylenenitrilomethylidyne)] di-8-quinolinol polymer shows a departure from the thermal stability trend established by the other first-row, divalent transition metals. In fact, its decomposition temperature is about 90 °C higher than that of the analogous Cu(II) polymer. The procedures developed by Doyle [9], and Horowitz and Metzger [10] for calculating activation energies and reaction order were found to be inapplicable to the coordination polymers of 8-hydroxyquinoline derivatives in the instances in which the data were tested. Obviously, the decomposition temperature alone is a crude measure of the thermal stability of the samples and more refined and sensitive criteria for evaluating the polymers are currently under examination.

A number of conclusions may be deduced from an examination of the curves shown in figure 2. First, the substitution of a large organic bridge for the CH_2 group in the 5,5′-position of the ligand lowers the apparent decomposition temperature of the polymers by 80 to 100 °C. Secondly, the decomposition mechanism, near the temperature at which accelerated weight loss occurs, appears to involve metal-ligand scissions in both polymer systems and is dependent on the nature of the metal which unites the ligands in the polymer. At this time there is little detailed information about the nature of decomposition over the entire temperature range used in this investigation but the mechanism does not appear to be a simple one.

It would be quite informative if values for the bond angles and bond distances were available for these polymers, particularly at the metal-ligand site, so that one could correlate these data with the thermal stability of the polymers. Unfortunately, only one definitive structural study of an 8-hydroxyquinolate system has been made. This was the work of Merritt and coworkers [11] on Zn-8-hydroxyquinolate. This paper reported the bond distances for Zn-O and Zn-N as 2.05 and 2.06 Å, respectively, and indicated that the 5-membered ring formed on chelation was under strain. Thus, the Zn-N-C_8 angle was found to be 111.8° rather than the anticipated 120° (fig. 3). For the divalent metal oxides, when the M-O interatomic distances are plotted versus the atomic numbers of the metals, the relationship depicted in figure 4 is obtained. Thus it is apparent that the

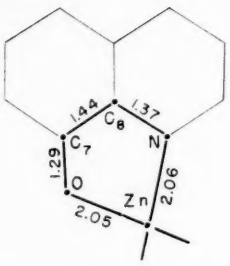

BONDS	ANGLE,°
O-Zn-N	79.8
Zn-N-C_8	111.8
N-C_8-C_7	116.1
C_8-C_7-O	117.4
C_7-O-Zn	114.3

FIGURE 3. *Bond distances (Å) and bond angles in 5-membered chelate ring.*

(Data from Merritt, Cady, and Mundy)

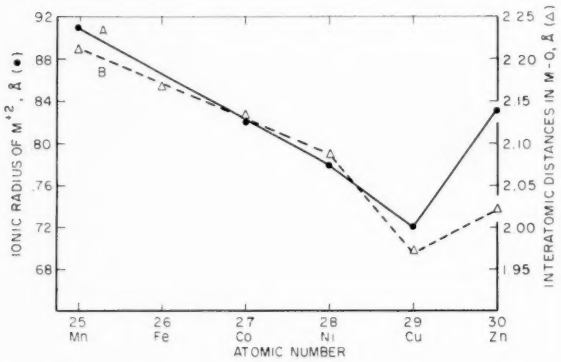

FIGURE 4. *Plot of ionic radius(●) and interatomic distances in metal oxides (Δ) versus atomic number of metal.*

Δ Wyckoff, R. W. G., Crystal Structure, Interscience Publishers, Inc., 1951; International Tables for X-ray Crystallography, The Kynoch Press, Birmingham, England (1962), table 4.1

● Ahrens, L. H., Geochim Cosm. Acta **2**, 155 (1952).

bond distances are related to the periodic properties of the metal. Also shown in figure 4 is the relationship between the ionic radii of the metals and their atomic number. The shape of these plots bears a striking resemblance to those shown in figure 2 (curves A and B) where the decomposition temperature has been related to the atomic numbers of the metals in the polymers.

Returning to table 2 it can be seen that by the time the temperature reached 1000 °C the Co polymer had lost about 75 percent of its original weight while the weight loss of the remaining polymers amounted to 65 to 68 percent. During the run, the furnace was maintained at 1000 °C for about 8 hr until the sample lost no additional weight. In table 4 the values obtained for the final residues and volatiles are compared with the calculated metal and C, H, N, O content of the original polymers. For the Cu, Ni, and Co samples, the residues differed from the calculated metal content in the original polymers by about 10 percent, on a relative basis. Some of the residues contained metal oxides, which may have been formed when the apparatus was opened to the air after the pyrolysis. This could, in part, account for the high results obtained for the residues from the Mn, Co, and Ni coordination polymers. There is some evidence to indicate that the metal oxides may not be formed during the decomposition of some of the polymers.

TABLE 4. *Comparison of final residues and volatiles with amount of metal and organic constitutents in original polymers*

Polymer	Found[a]		Calculated	
	Residue	Volatiles	Metal[b]	*C,H,N,O*
	%	%	%	%
Mn	12.8	87.2	9.2	90.8
Co	11.3	88.7	9.8	90.2
Ni	12.1	87.9	9.8	90.2
Cu	9.3	90.7	10.5	89.5
Zn	trace	100	10.8	89.2

[a] After pyrolysis at 1,000 °C until the residue reached constant weight.

[b] Based on $[ML{\cdot}2H_2O]$ where $L = C_{28}H_{22}O_2N_4$.

For the Zn-Schiff base polymer, only a trace of residue remained, indicating that essentially the entire sample volatilized under the conditions of the experiment. This finding is also in keeping with the proposed decomposition mechanism involving the rupture of metal-ligand bonds in that any metallic zinc or even zinc oxide formed during polymer degradation would have volatilized at 1000 °C in vacuum. Additional experiments are under way at the present time in which the decomposition products are being analyzed in the mass spectrometer. These experiments should provide more definitive information about the mechanism of decomposition for the coordination polymers of bis(8-hydroxyquinoline) derivatives.

6. References

[1] Horowitz, E., and Perros, T. P., J. Inorg. Nucl. Chem. **26,** 139 (1964).

[2] Friihof, E. J., Ph. D. Thesis, University of Illinois (1961).

[3] Marvel, C. S., Aspey, A. S., and Dudley, E. A., J. Am. Chem. Soc. **78,** 4905 (1956).

[4] Marvel, C. S., and Tarköy, N., J. Am. Chem. Soc. **79,** 6000 (1957).

[5] Martin, K. V., J. Am. Chem. Soc. **80,** 233 (1958).

[6] Bailar, J. C., Jr., and Goodwin, H. A., WADC Tech. Report 58–51, Part III, April 1960, pp. 66–73.

[7] Charles, R. G., J. Inorg. Nucl. Chem. **9,** 145 (1959).

[8] Clemo, G. R. and Howe, R., J. Chem. Soc. 3552 (1955).

[9] Doyle, C. D., J. Applied Poly. Sci. **5,** No. 15, 285 (1961).

[10] Horowitz, H. H. and Metzger, G., Anal. Chem. **35,** 1464 (1963).

[11] Merritt, L. L., Jr., Cady, R. T., and Mundy, B. W., Acta Cryst. **7,** 473 (1954).

(Paper 69A1–328)

JOURNAL OF RESEARCH of the National Bureau of Standards—A. Physics and Chemistry
Vol. 69A, No. 1, January–February 1965

Atomic Absorption Spectrum of Praseodymium (Pr I)

Romuald Zalubas and Michael Wilson*

(August 12, 1964)

Absorption lines of Pr I were observed using a King furnace. A list of 3532 lines in the region from 1741 to 5839 Å is presented.

An absorption spectrum is of great help in the analysis of a complex and line-rich spectrum. Therefore arrangements were made to obtain the absorption spectra of some rare earths at the Imperial College of Science and Technology in London. Absorption spectrograms of praseodymium, cerium, and erbium have been obtained. The plates were taken with a 3-m normal incidence vacuum spectrograph [1].[1] This instrument has a Bausch and Lomb aluminized replica grating of 30,000 lines per inch, blazed at 1500 Å in the first order. The plate factor is 2.7 Å/mm. Ilford Q2 and Astr. III plates were used. For the region above 2400 Å the spectrograph was not evacuated.

The absorption vessel used was a large King furnace [1] with the following modification: the praseodymium was vaporized in a 6 in. long, ½-in. bore tantalum tube clamped between the ends of the conventional graphite tubes. With a 40 KVA power supply feeding a current transformer capable of delivering 1300 A at 30 V, it was possible to heat the tantalum tube to any temperature up to its melting point at around 3000 °C. The advantage of the tantalum tube over graphite is that carbide formation is inhibited, thus enabling the vaporization of many materials which would otherwise react with hot graphite.

A constant flow of purified helium was maintained at about 8 mm Hg pressure to ensure clean conditions in the King furnace. The temperature was measured with an optical pyrometer suitably calibrated to allow for the difference in emissivity between the tube and a blackbody.

The following three sources for the production of continuum radiation were used: (1) a pointolite lamp (i.e., an incandescent strip of tungsten); (2) a 16 A xenon arc in a quartz envelope; and (3) a H_2 positive column discharge observed end-on. Quartz and quartz-lithium fluoride optical elements were employed in the system.

Absorption spectra at two different temperatures close to 1700 and 2000 °C, respectively, were photographed in each spectral region to assist in the classification of lines arising from the lower energy levels. An iron arc was superposed for standards in the region above 3000 Å while a copper hollow cathode was used in the region below 3000 Å.

These plates have been measured by Zalubas as part of the work on the description and analysis of Pr I being done at the National Bureau of Standards. A scanning comparator built at NBS [2] served for measuring the plates. The measurements were reduced by an electronic computer. In the region 1741 to 3000 Å the superposed standards were used for calculation of wavelengths of absorption lines. In the region above 3000 Å the superposed iron standards were used only for identification of those praseodymium absorption lines that had previously been observed in emission at NBS [3]. The wavelengths of absorption lines were then calculated using the accurately known Pr I emission wavelengths as internal standards. In the region 3000 to 5839 Å all absorption lines are easily identifiable with Pr I emission lines. In the shorter wavelength region absorption lines are more numerous than emission lines. Resonance lines of Er, Cr, Ca, Dy, Ho, Cu, Mg, Na, and Fe were found as impurities and eliminated.

The wavelengths are tabulated in table 1. The first column gives the wavelength in angstrom units. The second column contains intensities of lines estimated by eye on the absorption plates. The letter symbols are used to describe the character of the lines; c—complex, d—double, h—hazy, l—shaded to longer wavelength, s—shaded to shorter wavelength, w—wide, and bl—blended lines.

The wavelengths given in table 1 were obtained from one measurement of each line in absorption, at the 2000°C furnace temperature. Their values have been rounded off to two decimal places; in general they agree within ±0.02 Å with the values obtained from measurements of emission lines in the region above 3000 Å. Below 3000 Å, however, the wavelength accuracy is not exactly known, since shifts may occur when the copper standards are superposed; although an unlikely occurrence, this possibility could not be ruled out by a comparison with emission line wavelengths in the same region.

*Imperial College of Science and Technology, London, England.
[1] Figures in brackets indicate the literature references at the end of this paper.

Since iron and copper standards were superposed on absorption spectrograms, there are some regions where the lines were partly masked by iron and xenon emission lines or molecular bands, thus causing apparent wavelength shifts. Also, some lines which we observed in emission as self-reversed were completely masked on the absorption plates by superposed standards.

The above wavelength accuracy is sufficient for identification purposes in astronomical or spectrochemical analysis. For spectrum analysis, the emission line wavelengths derived from the plates taken with higher dispersion instruments are used. Using the absorption data, regularities in the spectrum of Pr I have already been discovered, and analysis of the Pr I spectrum is being continued at the National Bureau of Standards.

It is our pleasure to express our appreciation to C. H. Corliss for the generous assistance he has provided. We are indebted to W. R. S. Garton for suggesting the tantalum tube modification to the King furnace. We also thank Mrs. R. L. Peterson for her assistance in preparing table 1.

References

[1] W. R. S. Garton and K. Codling, Proc. Phys. Soc. (London) **75**, 87 (1960).
[2] M. L. Kuder, J. Res. NBS **65C** (Eng. and Instr.) No. 1, 1 (1961).
[3] R. Zalubas, unpublished data (1964).

TABLE 1.—*Wavelengths and intensities of absorption lines of* Pr

λ_{vac}	Int.	λ_{air}	Int.	λ_{air}	Int.	λ_{air}	Int.	λ_{air}	Int.	λ_{air}	Int.
1741.63	3	2005.10	5	2086.21	1	2141.41	2	2205.64	2	2277.97	3
1747.84	2	2024.03	1	2086.68	1	2142.40	2	2206.25	2	2278.23	2
1762.95	5	2024.39	3	2087.10	2	2142.77	1	2206.55	2 h	2278.41	3
1765.68	4	2025.87	5	2087.63	3	2143.99	3 wh	2207.01	2	2279.28	3
1766.44	8	2026.19	1	2090.71	1 s	2144.62	1	2207.42	1	2279.70	2
1769.19	5	2027.27	2 sh	2091.38	2	2144.92	2	2208.04	2	2280.27	1
1774.88	5	2038.37	4	2091.88	2	2147.83	1	2208.55	1	2280.56	8 s
1825.36	1	2039.08	5 s	2092.23	2	2150.78	3	2209.17	2	2282.44	2
1827.95	4	2039.86	3 d	2092.42	2	2152.02	2	2209.43	2	2282.89	2
1841.48	2	2039.86	3 d	2092.85	2	2155.77	1	2210.96	2	2283.26	1
1842.61	2	2040.90	2	2093.02	1	2156.56	3	2211.65	1	2283.87	2
1847.49	2	2042.80	2	2093.21	1	2157.20	1	2212.87	1	2284.14	3
1848.16	1	2043.07	2	2094.10	1	2157.86	1	2213.52	2	2284.62	3
1850.70	2	2045.37	5	2094.40	1	2158.59	1	2214.18	2	2284.93	8 s
1851.16	2	2046.60	3	2094.88	2	2159.49	1	2216.72	2	2285.51	1
1852.33	1	2047.27	2	2095.64	1 d	2160.08	2	2216.96	1	2285.90	2
1853.83	1	2047.89	1	2096.49	2 wh	2161.64	1	2218.97	1	2285.51	1
1854.37	1	2048.12	1	2099.62	1	2162.03	1	2219.28	3	2285.62	1
1855.29	1	2048.84	3 wd	2100.11	1	2162.44	1	2219.67	2	2285.90	2
1855.59	1	2049.25	3	2101.75	1	2163.20	2	2220.08	2 wh	2286.06	1
1856.39	1	2049.58	1	2102.40	1	2164.34	2	2220.67	3	2286.36	1
1857.36	1	2050.32	1	2102.62	1	2165.17	2 sh	2222.02	2	2286.86	2 wd
1857.84	2	2050.54	5	2103.12	3	2165.50	2	2223.97	1	2287.31	8
1865.33	1	2051.31	3	2103.12	2	2165.92	1	2225.09	2 wh	2287.91	5
1866.10	1	2052.96	6	2103.72	1	2166.68	1	2231.85	2 wh	2288.15	3
1869.26	1	2054.07	2 sh	2104.18	2	2168.09	1	2233.23	2	2289.40	1
1880.10	1	2056.57	1	2105.48	3	2168.61	2	2234.20	1	2289.59	5
1880.43	1	2057.29	2	2106.45	2	2168.89	2	2234.39	1	2290.35	4
1881.00	1	2057.63	4	2106.91	2	2170.05	2	2234.87	2	2291.72	4
1883.79	1	2058.33	3	2107.13	3	2172.49	1	2235.27	3	2291.98	1
1885.99	1	2059.50	2	2107.44	1	2173.14	2	2236.37	2	2292.48	4
1887.79	1	2060.29	3	2108.67	1	2173.45	2	2237.48	1	2294.39	1
1888.35	1	2060.61	1	2109.02	1	2173.65	2	2238.05	2	2295.13	1
1890.39	1	2061.60	4 d	2110.64	2	2174.13	3	2239.60	3	2295.59	2
1894.67	1 wh	2062.96	2	2111.51	3 sh	2174.63	2	2239.74	2	2295.78	5
1896.94	1	2064.21	3	2112.37	3	2179.03	3	2240.33	1	2296.70	4
1898.59	1	2064.58	2	2112.75	1	2181.80	2 sh	2240.85	2	2296.91	3
1900.96	1	2065.57	2	2113.54	3	2182.42	1	2241.09	2	2297.21	3
1901.44	1	2068.89	3	2113.98	2 lw	2182.62	1	2243.24	2	2297.43	2
1904.80	2	2069.42	2	2115.03	1	2184.19	2	2243.44	2	2300.15	3
1905.82	2 h	2071.24	1	2118.30	2	1991.22	1	2246.11	2	2300.60	3
1906.57	1	2071.49	5	2118.79	3	2185.07	1	2247.78	3	2301.11	1
1908.35	1	2072.35	3	2119.18	1	2185.54	2	2248.48	1	2301.22	4
1934.58	2	2072.65	2	2120.72	1	2185.90	1	2250.32	2 wh	2301.48	4
1935.83	1	2073.30	1	2121.07	3	2186.55	2 sh	2251.26	2 h	2302.10	2
1937.31	2	2073.48	3	2122.17	2 wh	2187.25	3	2253.37	3 hw	2302.34	4
1947.02	2	2074.13	2	2123.43	2	2187.99	3	2263.51	2	2302.53	3
1950.29	1	2074.63	2	2123.88	1	2188.81	2	2269.15	3	2302.67	3
1957.89	3	2075.41	1	2124.12	1	2190.26	1	2266.86	3 w	2303.48	3
1958.65	1	2075.50	2	2124.71	2	2191.14	2	2269.16	8	2303.59	2
1959.68	1	2075.78	2	2126.37	2	2193.00	3	2269.89	3	2303.83	4
1960.20	3	2076.00	3	2129.42	2	2194.17	1	2270.61	4	2304.25	1
1961.29	1	2076.19	1	2129.73	1 b l	2194.86	1	2270.98	4	2304.25	2
1962.17	2	2076.44	2	2130.68	1 b l	2196.89	2 w	2272.12	3 s	2304.53	1
1962.95	1	2077.51	3	2131.64	2	2197.72	2	2272.80	3	2304.80	2
1964.12	1	2078.11	3 s	2132.07	1	2198.81	1	2273.11	5	2305.02	2
1972.32	1	2078.87	2	2132.55	1	2199.05	1	2274.04	3	2305.10	3
1977.57	2 w	2079.56	3	2133.34	1	2200.05	1	2274.68	8	2305.30	3
1983.28	1	2080.80	1	2134.77	2 d	2200.20	1	2275.19	5	2305.48	3
1991.06	2 h	2081.36	3	2135.27	2	2200.78	2	2275.52	2	2305.82	3
1986.05	1 w	2082.24	2	2137.70	2	2202.96	1	2277.04	3	2306.17	4
1993.11	1	2082.47	1	2138.35	2 sh	2203.59	2	2277.31	1	2306.66	2
1993.64	1	2082.83	3	2139.20	2 h	2204.06	2	2277.65	1	2306.91	1
		2083.42	3	2139.76	1	2204.72	3	2277.97	3	2307.13	4
		2085.81	1	2140.95	2	2205.07	1	2277.64	2	2307.91	3

TABLE 1.—*Wavelengths and intensities of absorption lines of* Pr—Continued

λ_{air}	Int.	λ_{air}	Int.	λ_{air}	Int.	λ_{air}	Int.	λ_{air}	Int.	λ_{air}	Int.
2308.07	2	2333.86	1	2358.91	3	2382.60	1	2405.08	3	2432.13	2
2308.21	2	2334.14	8	2359.17	3	2382.83	1	2405.22	3	2432.44	2 d
2308.72	2	2336.79	3	2359.69	1	2383.62	3	2405.40	1	2433.06	2
2309.12	3	2338.27	2	2360.73	3	2383.83	2	2405.72	3	2433.44	2
2309.79	2	2338.46	2	2360.88	2	2384.34	3	2407.23	2	2433.71	2
2310.14	3 h	2339.02	4	2361.85	2	2384.51	2	2407.34	2	2434.20	2
2309.98	3	2339.14	1	2362.11	2	2384.73	5	2407.59	4	2434.34	2
2310.72	5	2339.51	1	2362.32	3	2385.26	2 lc	2408.00	3	2434.83	2
2311.01	3	2340.01	3	2362.62	8	2385.73	2 lc	2408.37	3	2435.20	5
2311.01	3 w	2340.23	4	2362.78	2	2386.50	3	2408.84	3	2435.68	2
2311.81	8	2341.11	2	2363.05	2	2386.65	2	2409.27	3	2435.86	1
2312.52	3	2341.12	2	2363.24	2	2386.91	3	2409.83	8	2436.09	4
2313.17	3	2341.39	1	2363.98	2	2387.05	2	2409.99	2	2436.33	3
2313.39	2	2343.03	2	2364.28	3	2387.14	2	2411.22	3	2436.81	3
2313.54	1	2343.36	5 sh	2364.42	1	2387.63	4	2411.57	2	2439.19	3 s
2313.71	1	2344.10	4	2364.55	2	2387.74	3	2412.13	2	2439.56	3
2314.06	1	2344.34	2	2364.92	1	2388.39	2	2412.29	2	2439.74	1
2314.24	3	2344.83	2	2365.00	1	2388.54	3	2412.55	2	2440.57	3
2314.67	1	2345.02	3	2365.13	4	2388.86	3	2412.90	1 d	2440.88	2
2315.05	2	2345.34	4	2365.71	3	2389.39	2	2413.22	2	2441.96	8
2315.38	5	2345.61	1	2365.94	3	2389.51	2	2413.76	2	2442.62	2
2315.80	3	2346.12	2	2366.65	3	2389.68	3	2413.88	2	2442.89	1
2316.44	2	2346.33	2	2366.93	8	2390.02	3	2414.75	2	2443.12	1
2316.89	2	2346.54	8	2367.11	5	2390.37	2	2414.92	2	2443.60	2
2317.29	3	2347.01	5	2368.56	1	2390.89	2	2415.07	2	2443.81	2
2317.84	3	2347.30	6	2368.75	3	2391.04	4	2415.48	2	2444.63	2
2318.38	3	2347.58	1	2368.98	3	2391.43	4	2415.75	2	2444.78	2
2318.86	3	2347.98	3	2369.22	3	2391.60	2	2416.24	2	2444.95	2
2319.11	5	2348.46	2	2369.61	3	2391.97	2	2416.81	8	2445.38	2
2319.96	1	2348.67	2	2370.41	2	2392.50	4	2416.99	4	2445.48	4
2320.08	2	2349.03	3	2370.86	3	2392.81	2	2417.07	5	2446.27	3
2320.32	2 l	2349.37	3	2371.15	3	2393.15	3	2419.74	3 d	2446.37	2
2320.79	4	2349.72	8	2371.28	3	2393.26	4	2420.04	3	2446.53	3
2321.18	6	2350.19	3	2372.15	8	2393.57	4	2420.41	2	2446.70	2
2321.34	2	2350.35	3	2372.42	1	2393.71	3	2420.78	1	2446.93	2
2321.78	1	2350.48	5	2372.83	2	2393.96	2	2421.05	8	2447.02	5
2322.28	2	2351.18	4	2372.95	2	2394.02	2	2421.42	2	2447.09	2
2322.50	2	2351.50	2	2373.19	3	2394.36	3	2421.88	3	2447.61	2
2322.71	3	2351.75	5 l	2373.32	2	2394.82	2	2422.26	2	2448.45	1
2323.70	3	2352.15	5	2373.42	2	2394.95	1	2422.38	2	2448.78	1
2324.33	4	2352.56	3	2373.88	2	2395.20	3	2422.60	4	2449.70	3
2324.50		2353.00	1	2374.16	5	2395.35	3	2423.24	8	2449.83	2
2324.81	3	2353.12	2	2374.43	2	2395.73	2	2423.84	3	2450.33	2
2325.04	1	2353.24	2	2374.97	1	2396.26	4	2424.25	2	2450.48	3
2325.16	1	2353.42	1	2375.07	5 h	2396.84	3	2425.00	1	2450.60	2
2325.40	3	2353.79	2	2375.50	2	2397.08	2	2425.29	1	2451.09	1
2325.58	2 w	2354.24	3	2375.64	4	2397.28	2	2425.45	3	2451.35	1
2325.85	2	2354.33	2	2376.00	3	2397.40	1	2425.75	1	2451.79	3
2325.92	2	2354.59	2	2376.20	2	2398.02	3	2426.04	3	2452.00	3
2326.07	4	2354.79	4	2376.66	4 s	2398.21	4	2426.26	2	2452.12	3
2326.86	3	2355.25	2	2377.17	4	2398.57	3	2426.44	1	2452.77	3
2327.43	3	2355.26	2	2377.51	3	2398.98	2	2426.73	2	2453.21	3
2327.97	2	2355.47	3	2378.08	1	2399.33	1	2427.46	3	2453.28	3
2328.13	3	2355.47	3	2378.47	8	2399.42	2	2427.72	1	2453.52	3
2328.59	3	2355.90	2	2378.90	2 d	2400.51	2	2428.27	1	2453.82	2
2328.76	2	2356.04	2	2379.34	3	2401.36	3	2428.46	2 h	2454.11	1
2329.02	3	2356.20	3	2379.58	2	2401.54	3	2428.81	2	2454.40	3
2329.87	3 w	2356.54	3	2379.88	2	2401.71	2	2428.98	2	2454.60	2
2330.34	1	2356.85	8	2380.11	3	2401.94	2	2429.11	1	2454.87	2
2330.79	4	2357.13	2	2380.50	2	2402.52	2	2429.72	2	2455.18	3
2332.01	5	2357.58	1	2380.57	2	2402.64	1	2429.84	3	2455.26	2
2332.40	3	2357.97	2	2380.89	2	2403.89	3	2430.40	2	2455.50	2
2332.52	4	2358.24	1	2381.07	2 d	2404.14	5	2430.57	3	2455.98	1
2333.04	1	2358.69	2	2381.44	2	2404.30	1	2430.76	2	2456.36	2
2333.36	2	2358.77	1	2381.72	2	2404.50	1	2431.35	5	2456.85	2

TABLE 1.—*Wavelengths and intensities of absorption lines of* Pr—Continued

λ_{air}	Int.	λ_{air}	Int.	λ_{air}	Int.	λ_{air}	Int.	λ_{air}	Int.	λ_{air}	Int.
2457.06	2	2478.87	3	2523.25	2	2552.15	8	2578.37	4	2598.08	4
2457.27	2	2479.41	2	2523.78	3	2552.93	2	2578.96	2	2598.17	1
2457.37	2	2480.07	2	2524.40	2	2553.21	2	2579.68	2 b l	2599.10	3
2457.76	3	2480.35	3	2525.24	1	2553.75	3	2580.28	2	2599.61	3
2457.85	3	2480.64	2	2525.49	1	2553.86	2	2580.36	4	2599.74	4
2458.21	4	2481.26	4	2525.72	1	2554.08	2	2580.47	2	2599.85	8
2458.69	2	2481.41	3	2525.83	1	2554.42	1	2580.78	1	2599.85	8
2458.98	2	2482.45	3	2526.66	1 b l	2554.83	1	2581.05	2	2600.72	8
2459.12	2	2482.79	3	2526.99	8	2555.01	1	2581.42	3	2600.86	4
2459.49	3	2484.01	2	2527.20	2	2555.18	1	2581.58	3	2601.65	1
2459.73	2	2484.72	2	2527.65	1	2555.26	3	2581.86	1	2602.24	1
2460.29	5	2485.16	3	2528.41	5	2555.50	1	2581.95	1	2602.32	1
2460.69	3	2485.43	1 b l	2528.92	2	2555.76	1	2583.16	2	2602.68	3
2460.77	2	2485.52	1	2529.39	5	2556.47	2	2583.36	5	2602.84	3
2461.21	5	2485.73	2	2529.71	3	2556.97	1	2583.61	3	2602.94	1
2461.63	3	2487.37	3	2530.06	1	2557.05	2	2584.00	3	2603.44	8
2462.07	3	2489.99	3 b l	2530.17	1	2557.30	2	2584.35	3	2603.67	2
2462.37	5	2491.04	3	2530.98	5	2557.54	3	2585.62	2	2603.89	1
2462.37	3	2491.42	1	2531.12	2	2558.77	1	2586.16	1	2604.09	2
2463.05	3	2491.64	2	2531.48	2	2558.98	2	2586.66	1	2604.91	5
2463.77	2	2491.87	1	2531.82	5	2559.35	1	2586.79	1	2605.93	3
2463.87	4	2492.49	8	2532.28	2	2559.53	2	2586.86	1	2606.05	1
2463.97	1	2492.83	4	2532.38	1	2560.21	3	2586.96	1	2606.90	8
2464.79	4	2494.53	3	2532.49	2	2560.48	3	2587.43	3	2607.22	2
2465.40	4	2495.07	2	2533.33	2	2560.61	2	2587.55	1	2607.33	2
2465.57	1	2496.12	5	2534.17	1	2561.20	3	2587.76	3	2607.59	3
2465.77	8	2496.29	1	2534.47	3	2561.86	2	2587.88	3	2607.90	4
2466.06	4	2496.52	1	2534.73	2	2562.94	2	2588.04	3	2608.18	2
2466.72	8	2496.92	1	2535.51	2	2563.09	2	2588.43	2	2608.34	1
2466.91	1	2497.08	6	2536.18	1	2563.51	1	2588.81	3	2609.12	3 s
2467.17	8	2497.92	2 b l	2536.29	2	2563.93	1	2589.00	1	2609.66	3
2467.51	1	2497.99	2 b l	2536.39	1	2564.06	1	2589.08	3	2609.76	1
2467.74	1	2499.70	3	2539.09	3	2564.18	1	2589.22	1	2610.93	2
2467.87	2	2499.97	2	2540.10	3	2564.30	3	2589.93	1	2611.68	3 b l
2467.98	3	2501.00	2	2540.63	3	2564.52	2	2590.31	2	2613.74	4
2468.29	4	2501.24	3	2541.14	3	2564.63	5	2590.45	3	2613.91	4
2468.46	3	2502.59	1	2541.80	2	2565.12	1	2590.56	5	2614.73	2
2468.81	3	2502.90	1	2541.94	1	2566.15	2	2590.96	2	2615.40	2
2468.94	2	2503.13	1	2542.16	1	2566.44	2	2591.20	2	2616.01	1
2469.17	3	2505.77	3	2542.28	1	2566.61	1	2591.30	3	2616.10	1
2469.60	6	2505.96	2	2542.71	1	2567.21	1	2591.58	3	2616.22	1
2469.73	8	2506.72	1	2543.01	1	2567.76	2	2591.93	2	2616.60	1
2470.04	1	2507.24	1	2543.44	2	2567.99	1	2592.11	2	2616.90	1
2470.13	2	2509.32	1	2543.83	2	2568.11	1	2592.46	2	2617.43	1
2470.74	2	2509.59	3	2544.09	3	2568.62	4	2593.12	2 b l	2618.72	8
2470.82	2	2510.83	3 t r	2545.30	2	2568.89	4	2593.23	8	2619.79	2
2471.50	2	2512.10	1	2545.65	1	2569.05	1	2593.45	5	2623.16	1
2471.69	5	2512.46	1	2545.83	3	2569.32	1	2593.82	2	2623.48	1
2472.13	2	2513.57	1	2546.22	1	2569.76	2	2594.05	1	2625.07	2
2472.28	4	2513.77	1	2546.47	1	2569.92	2	2594.48	2	2625.33	3 s
2472.44	2	2513.93	1	2547.20	1	2570.11	2	2594.58	1	2626.60	2
2472.70	1	2514.81	1	2547.48	2	2570.84	5	2594.87	1	2626.94	4
2472.95	2	2515.09	1	2548.40	1	2571.40	2	2595.03	1	2627.55	4
2473.10	2	2517.21	1	2548.86	1	2572.47	1	2595.25	2	2627.72	1
2473.48	5 sh	2517.96	4	2549.03	3	2572.63	2	2595.41	1	2628.66	1
2474.01	5	2518.03	1 b l	2549.18	1	2573.16	1	2595.76	2	2629.00	1
2474.39	1	2518.41	1	2549.35	1	2573.39	1	2595.85	3	2629.16	1
2474.72	3	2518.66	1	2549.79	1	2573.70	2	2596.16	3	2629.46	1
2475.19	3	2518.82	2	2550.00	3	2574.10	2	2596.30	4	2630.09	1
2475.49	2	2519.91	1	2550.15	1	2574.19	2	2596.47	1	2630.45	3
2475.84	1	2519.99	1	2550.28	1	2574.55	5	2596.57	2	2631.10	5
2476.03	4	2521.13	1	2550.54	1	2574.81	4	2596.82	1	2631.20	4
2477.18	2	2521.37	2	2550.82	1	2576.89	2	2597.09	2	2631.39	2 b l
2478.18	2	2522.44	1 b l	2551.32	1	2577.19	2	2597.59	5	2631.82	3
2478.68	3	2522.94	1	2551.81	1	2577.65	2	2597.78	1	2631.93	1

TABLE 1.—*Wavelengths and intensities of absorption lines of* Pr—Continued

λ_{air}	Int.	λ_{air}	Int.	λ_{air}	Int.	λ_{air}	Int.	λ_{air}	Int.	λ_{air}	Int.
2632.44	5	2674.22	3 b l	2719.96	2	2765.37	3	2795.69	5	2826.90	2
2632.74	6	2677.22	1	2720.18	1	2765.81	1	2796.13	3	2827.01	1
2633.09	12	2677.56	1	2720.49	1	2765.92	3	2796.83	5	2827.09	5
2633.80	1	2677.95	1	2720.60	1	2766.13	1	2797.27	2	2827.87	1
2634.05	1	2678.48	3	2721.05	3	2766.27	3	2797.79	1	2828.03	3
2634.70	1 b l	2678.67	3	2721.54	3	2766.27	2	2797.91	5	2828.55	1
2634.78	1 b l	2679.36	1	2721.82	2	2767.32	3	2798.13	8	2829.84	8
2634.91	2	2679.96	1	2722.42	1	2767.73	1	2798.32	1	2830.31	3
2635.12	3	2682.55	1	2725.39	2	2768.09	5	2798.94	2	2831.50	8
2636.24	2	2683.04	2	2725.63	2	2768.43	8	2799.52	3	2831.98	3
2636.33	3	2683.60	1	2727.02	1	2769.85	5	2800.10	3	2832.62	5
2636.54	8	2684.54	1	2727.95	2	2770.02	5	2800.56	2	2833.17	5
2637.04	1	2684.80	2	2728.58	5	2770.38	2	2800.93	3	2833.82	2
2737.32	3	2685.31	1	2728.76	1	2771.01	5	2802.09	8	2833.98	1
2637.40	1	2685.43	1	2729.39	1	2772.56	3	2802.50	5	2834.25	4
2637.75	2	2685.68	1	2729.74	2	2772.90	2	2802.88	2	2834.60	2
2639.63	1	2686.19	1	2729.86	1	2773.61	1	2803.65	1	2835.38	8
2640.36	2	2687.54	1	2730.01	1	2773.76	1	2804.18	8	2835.48	6
2640.82	1	2687.69	2	2730.35	2	2774.78	3	2804.92	3	2835.97	8
2641.23	5	2688.38	1	2730.59	2	2775.27	3	2805.24	5	2836.12	2
2641.55	1	2688.51	1	2731.01	1	2775.73	3	2805.37	2	2837.06	8
2641.98	1	2688.82	2	2731.91	1	2776.48	1	2805.63	8	2837.23	3
2642.16	5	2690.46	1	2733.19	5	2776.91	3	2806.02	4	2837.64	8
2642.69	2	2692.42	1	2736.67	1	2777.53	1	2806.76	4	2838.60	2
2643.63	5	2695.04	1	2736.84	1	2777.73	3	2807.61	1	2838.71	3
2644.05	1	2696.09	1	2737.27	1	2777.84	1 b l	2808.23	3	2839.37	8
2644.43	1	2696.35	2	2737.90	2	2778.31	1	2809.04	3	2840.29	8
2646.25	1	2698.04	1	2738.76	5	2778.67	8	2809.50	1	2840.78	1
2646.39	2	2698.53	3	2739.22	3	2779.42	2	2809.66	1 b l	2841.07	2
2648.15	3	2699.18	1	2740.62	1	2779.88	2	2809.74	2 b l	2841.83	8
2648.55	3	2699.44	1	2741.29	1	2780.10	3	2810.09	3	2842.26	2
2648.82	1	2700.11	1	2741.50	2	2780.38	2	2810.64	2	2842.47	2
2650.01	2	2700.21	1	2741.95	3	2780.55	1	2810.98	1	2843.02	8
2650.54	1	2701.26	1	2742.81	3	2780.66	3	2813.94	10 1	2843.28	8
2652.62	3	2702.07	3	2746.06	2	2780.94	1	2814.14	1	2843.88	4
2653.60	3	2702.28	3	2746.05	2 b l	2781.32	2	2814.44	8	2844.07	8
2653.96	1	2704.49	5	2746.38	1	2782.05	2	2814.51	4 b l	2844.50	2
2654.33	1	2706.04	2	2747.75	1	2782.29	1	2814.96	5	2845.29	8
2654.86	1	2706.37	1	2748.23	2	2782.56	3 b l	2815.47	8	2845.58	6
2655.08	2	2707.14	1	2748.58	3	2782.63	2 b l	2816.35	3	2847.13	3
2655.24	2	2707.84	1	2748.81	1	2783.03	1	2816.88	3	2847.48	8
2655.37	3	2708.54	1	2749.69	1	2783.14	3	2817.13	2	2847.93	5
2655.54	1	2708.92	5	2750.81	8	2783.56	8	2817.30	8	2848.97	3
2656.15	3	2709.11	8	2751.22	2	2783.74	2	2817.93	2	2849.16	4
2656.64	1	2709.98	3	2751.41	1	2784.84	8	2818.23	3	2849.98	1
2657.23	2	2710.95	1	2751.53	5	2785.18	1	2818.77	2	2850.36	4 s
2658.29	1	2711.06	1	2752.46	1	2785.50	2	2819.33	8	2850.68	5
2658.88	1	2711.16	3	2753.12	2	2785.78	8	2819.68	8	2851.87	2
2661.10	2	2711.34	8	2753.72	3	2786.46	5	2819.78	3	2852.79	2
2661.71	1	2712.73	1	2754.64	2	2786.89	5	2819.93	1	2852.97	1
2661.89	1	2713.09	1	2754.96	1 b l	2787.99	2	2820.68	3	2853.15	2
2663.04	2	2714.04	3	2755.02	2	2788.60	3	2820.98	3	2853.23	1
2663.36	5	2714.36	1	2755.63	8	2789.79	1	2821.16	3	2855.45	1
2663.64	1	2714.50	4	2758.45	1	2789.95	2	2821.26	3	2856.48	3
2664.60	2	2714.75	1	2758.92	1	2790.16	8	2821.68	6	2857.17	8
2667.57	1	2714.94	1	2760.42	2	2791.13	3	2821.83	8	2858.05	3
2668.50	5	2715.17	1	2760.82	2	2792.36	2	2822.00	8	2858.74	2
2669.27	1	2715.62	1	2761.70	3	2792.63	3	2823.41	1	2858.83	3
2669.66	1	2715.77	2	2762.16	5	2792.76	3	2823.78	1	2859.06	5
2669.93	1	2716.25	2	2762.29	5 1	2793.07	1	2824.01	4	2859.41	4
2670.51	1	2716.38	1	2764.22	1	2793.30	1	2824.24	5 b l	2859.91	5
2671.09	1	2717.89	1	2764.38	1	2794.00	4 b l	2824.78	8	2860.76	5 1
2671.35	1	2718.32	2	2764.73	2	2794.88	1	2825.87	4	2860.91	3
2672.17	1	2718.42	8	2764.73	3	2795.20	5	2826.20	5	2861.65	4
2673.09	2	2719.15	2	2765.01	1	2795.47	4	2826.67	5	2862.00	1

TABLE 1.—*Wavelengths and intensities of absorption lines of* Pr—Continued

λ_{air}	Int.	λ_{air}	Int.	λ_{air}	Int.	λ_{air}	Int.	λ_{air}	Int.	λ_{air}	Int.
2862.27	5	2902.09	1	2955.99	1	3132.25	8	3228.41	3	3340.45	4
2862.43	5	2902.51	8	2956.67	1	3133.23	3	3228.62	4	3343.91	4
2863.24	3	2903.40	1	2957.03	2	3134.79	4	3228.90	2	3346.58	1
2863.59	1	2903.61	2	2959.12	2	3136.09	2	3231.28	2	3347.41	5
2864.20	8	2904.03	1	2962.65	2	3142.06	4	3231.51	1	3348.24	5
2864.93	8	2904.33	2	2963.64	10	3142.88	1 b l	3231.70	1	3349.58	2
2865.72	4	2905.11	3	2964.92	1	3144.03	1 b l	3232.58	3	3351.34	2
2866.15	4	2905.21	1	2967.03	2	3146.92	4 b l	3233.25	4	3353.44	3
2866.45	8	2906.09	2	2974.16	3	3147.92	2 b l	3235.02	4	3357.40	2
2867.23	2	2906.16	1	2975.54	2	3148.35	3	3235.25	1	3358.51	2
2868.30	1	2907.23	1	2985.43	1 b l	3150.86	1	3235.84	1	3358.94	1
2868.68	2	2907.39	5	2985.54	5	3151.53	1 b l	3238.52	3 h	3359.13	1
2869.43	8	2907.85	2	2986.79	2	3155.90	3	3240.60	3	3363.96	8
2869.88	3	2908.02	1	2987.42	2	3157.20	2 b l	3242.41	2	3365.27	4
2871.02	3	2909.29	2	2992.38	2	3158.33	1 b l	3244.29	8	3366.06	1
2872.76	4	2910.03	4	2994.71	1	3158.88	3 b l	3244.61	3	3366.37	2
2873.63	2	2910.58	5	2997.63	1	3159.75	3 b l	3245.49	2	3369.12	5
2873.93	8	2911.65	12	3000.70	1	3160.02	2	3246.08	2	3372.86	1
2874.23	6	2912.35	1	3001.42	1	3160.34	1 b l	3246.49	4	3373.33	1
2874.47	1	2912.80	1	3006.28	2 w	3161.65	1	3248.72	4	3374.99	3
2874.87	1	2913.89	2	3008.30	3	3163.79	2	3253.15	8	3375.20	2
2875.11	2	2914.55	5	3008.92	1	3167.15	2	3254.62	2	3375.52	1
2875.52	5	2914.70	3	3011.90	1	3167.64	1	3257.18	1	3378.34	8
2877.07	8	2915.01	10	3013.04	4	3169.78	2 b l	3258.02	2	3379.25	1
2877.41	2	2915.63	1	3014.12	2	3170.57	3	3258.97	3	3380.06	4
2877.67	2 b l	2916.03	10	3014.75	1 w	3170.92	1	3259.41	1	3381.42	8
2878.82	3	2916.58	3	3014.83	1 b l	3171.42	1	3259.80	1	3386.04	10
2879.52	8	2916.81	2	3014.96	2	3171.73	1	3260.08	1	3386.63	3
2879.71	10 l	2918.78	3	3017.14	3	3173.09	5	3260.87	4	3391.48	1
2880.36	3	2919.83	1	3017.67	1	3174.05	1	3261.24	4	3393.67	2
2880.95	3	2920.35	2	3018.63	4	3174.39	3	3262.22	3	3393.95	2
2881.27	5	2920.54	1	3019.79	1	3175.61	2	3262.40	2	3394.24	2
2881.56	2	2920.61	3	3021.87	1	3176.21	1	3263.91	2	3395.02	1
2882.35	1	2920.89	1	3022.19	1	3178.85	2	3264.32	8	3395.45	3
2882.63	1	2921.32	1	3022.81	1	3179.97	2	3265.87	1	3395.89	2
2883.67	4	2921.72	1	3026.00	3 b l	3181.02	4	3276.29	1	3396.36	2
2883.94	8	2922.26	3	3027.39	1	3184.13	8	3277.10	1	3393.52	1
2885.87	10	2923.34	8	3028.24	1	3187.03	6	3283.05	2	3393.67	2
2886.83	4	2923.89	3	3033.32	2	3188.41	4	3283.41	5	3393.95	2
2887.36	4	2925.92	2	3034.78	2	3188.88	2	3289.03	1	3394.24	2
2887.56	2	2927.11	2	3035.24	2	3190.70	3	3289.63	3	3395.00	1
2888.41	2	2928.77	1	3047.14	1	3198.60	4	3293.59	3	3395.45	4
2888.56	3	2929.00	1	3047.53	2	3198.74	3	3297.10	2	3395.91	3
2888.82	2	2930.80	2	3052.59	1	3199.26	2	3297.50	3	3396.32	2
2890.54	3	2930.99	1	3054.75	2	3199.64	3	3298.41	1	3397.20	1
2890.73	3	2931.68	2	3055.65	1	3199.95	1	3299.38	1	3397.48	1
2891.27	4	2932.47	1	3056.17	2	3200.35	1	3303.01	3	3398.91	1
2891.62	4	2933.47	2	3056.70	2	3201.14	1	3303.24	2	3399.77	1
2891.99	12	2935.22	2	3059.81	3	3201.60	1	3303.44	3	3400.14	1
2893.44	10	2936.34	1	3063.61	3 b l	3203.12	3	3306.76	5	3402.87	2
2894.21	8	2938.53	2	3066.03	1	3206.04	1	3308.39	3	3402.95	4
2894.64	6	2939.38	1	3071.57	2	3206.33	2	3314.86	3	3403.76	5
2895.47	2	2940.05	2	3101.95	2 b l	3206.61	1	3316.45	3	3404.60	3
2895.91	8	2940.71	5	3102.65	2 b l	3207.16	2	3317.42	2	3404.99	3
2896.54	1	2941.14	1	3103.80	3	3212.49	5	3319.62	3	3405.70	3
2896.65	3	2942.72	1	3105.11	3 b l	3216.24	5	3327.08	2	3406.70	1
2896.73	2	2944.93	5	3113.63	1	3216.80	2	3328.89	2	3408.74	3
2896.92	3	2945.78	2	3118.03	3	3218.26	5	3330.05	2	3409.25	5
2897.65	4	2947.24	2	3119.36	8	3219.91	2	3331.61	3	3409.69	2
2898.22	8	2948.11	2	3122.96	8	3221.83	5	3332.77	1	3410.13	3
2899.24	3	2948.11	2	3124.28	1	3222.47	3	3333.30	1	3411.67	1
2899.37	12	2949.61	2	3125.45	5	3223.82	3	3333.86	2	3414.75	3
2899.92	4	2951.01	3	3126.07	4	3225.19	5	3334.69	3	3415.66	4
2900.52	8	2951.20	1	3126.33	4	3225.55	3	3337.28	2	3417.81	4
2901.81	6	2955.15	1	3127.79	8	3228.13	3	3339.34	1	3417.98	5

748-345—65——5

TABLE 1.—*Wavelengths and intensities of absorption lines of* Pr—Continued

λ_{air}	Int.	λ_{air}	Int.	λ_{air}	Int.	λ_{air}	Int.	λ_{air}	Int.	λ_{air}	Int.
3418.66	1	3516.33	1	3644.70	1	3738.94	2	3832.31	3	3961.70	8
3420.83	1	3517.17	1	3649.08	2	3739.59	1	3833.07	2	3961.85	2
3421.94	1	3518.49	10	3650.73	4	3739.80	1	3833.23	2	3962.85	2
3422.43	1	3519.65	3	3651.46	1	3744.80	5	3834.35	3	3963.24	3
3423.26	2	3521.32	2	3651.98	1	3748.98	3	3834.69	4	3964.90	1
3425.20	3	3522.97	3	3653.37	1	3750.38	5	3836.10	5	3965.26	2
3426.08	2	3523.19	3	3654.13	1	3756.13	2	3836.30	2	3966.28	8
3426.72	1	3527.86	1	3654.63	5	3757.06	1	3838.77	2	3966.55	1
3432.04	10	3529.61	1	3657.09	3	3758.35	1	3844.10	2	3966.88	1
3432.63	2	3529.84	2	3658.04	2	3758.84	1	3848.10	3	3969.30	2
3434.47	4	3530.66	1	3659.20	1	3760.22	4	3850.38	4	3971.63	1
3436.89	1	3532.29	1	3661.48	3	3760.69	1	3858.02	4	3972.70	2
3437.60	4	3532.82	8	3662.47	3	3760.96	3	3859.11	2	3973.71	1
3438.85	2	3542.08	2	3664.38	1	3761.37	1	3861.78	1	3974.32	1
3440.06	1	3543.74	5	3665.07	2	3763.11	1	3864.10	1	3974.67	2
3440.59	1	3544.59	1	3665.46	1	3763.97	1	3866.59	4	3976.94	1
3440.97	1	3549.26	1	3666.38	2	3764.90	8	3870.72	1	3977.32	8
3441.57	2	3550.65	3 h	3668.47	5	3766.02	1	3872.64	2	3977.69	1
3442.40	2	3551.41	3	3668.88	1	3766.75	5	3874.83	1	3978.17	1
3443.24	2	3551.65	2	3671.11	4	3768.42	5	3877.29	4 h	3978.60	1
3444.30	4	3555.26	2	3675.50	3	3768.95	3	3878.21	4	3979.66	1
3445.83	1	3558.81	2	3676.08	4	3769.93	1	3878.80	2	3979.88	3
3447.83	5	3563.50	8	3677.59	3	3770.80	2	3881.69	1	3980.23	1
3450.10	5	3564.13	5	3678.30	5	3773.47	5	3883.30	5	3980.48	1
3450.66	2	3564.76	1	3679.91	2 h	3776.07	6	3883.98	3	3980.87	2
3453.80	5	3572.30	9 s	3681.69	5	3779.29	4	3884.28	1	3981.39	1
3454.86	1	3573.09	1	3683.52	2	3779.73	1	3886.30	1	3981.68	1
3458.06	2	3575.62	2	3685.76	3	3780.29	2	3892.40	2	3982.07	1
3459.44	1	3577.16	1	3687.67	5	3780.94	2	3895.63	3	3982.46	3
3459.86	2	3578.68	5	3687.86	1	3782.82	3	3898.41	4	3982.70	1
3461.20	3	3582.97	3	3693.61	8 s	3783.81	1	3899.36	3	3983.36	5
3466.24	3	3586.64	1	3695.46	4	3785.07	3 s	3900.67	2	3983.52	1
3467.02	3	3590.84	2	3698.74	3	3786.11	1	3901.29	1	3983.84	5
3468.55	1	3591.21	3	3700.24	3	3787.90	4	3901.81	1	3984.42	6
3468.66	2	3591.90	2	3701.59	2	3788.19	1	3906.82	1	3985.04	1
3469.05	5	3593.50	5	3702.89	1	3789.73	5	3909.22	1	3985.65	1
3470.06	1	3599.03	1	3703.33	3	3791 21	1	3910.57	5	3986.10	1
3470.33	3	3603.65	2	3705.14	1	3791.42	1	3912.29	1	3986.75	2
3471.68	1	3604.48	1	3706.05	3 h	3792.52	4	3913.03	1	3987.04	1
3474.46	4	3605.31	4	3707.63	2	3792.95	4	3913.53	2	3987.18	2
3475.51	5	3605.79	3	3708.37	2	3793.61	1	3916.62	1	3987.61	2
3478.36	3	3606.20	3	3708.66	2	3794.17	3	3921.08	2	3990.07	1
3479.25	3	3609.61	1	3711.17	4	3794.77	3	3922.86	2	3990.59	1
3479.84	2	3612.33	1	3713.44	1	3795.30	2	3923.62	3	3991.47	2
3482.09	3	3616.23	2	3715.62	4	3796.16	2	3924.49	8	3992.31	1
3482.61	2	3617.39	3	3716.47	1	3797.34	2	3934.09	4	3992.99	2
3483.31	3	3617.62	8 s	3719.92	3	3797.69	2	3934.69	1	3994.33	8
3485.75	2	3620.78	1	3721.68	4	3800.43	2	3935.02	5	3995.95	2
3487.55	1	3621.24	1	3723.78	1	3801.49	3	3935.90	1	3997.78	5
3489.31	1	3622.20	5	3724.15	5	3803.18	5	3936.21	1	3998.09	1
3489.62	1	3625.58	1	3724.37	5	3806.26	2	3937.20	3	3999.38	5
3490.99	2	3626.41	1	3725.52	1	3807.31	2	3937.37	3	4000.15	2
3491.36	1 b l	3627.42	2	3726.45	1	3807.61	1	3938.11	1	4000.81	1
3491.51	2 b l	3629.25	5	3728.78	1	3811.17	4	3941.26	1	4001.07	1
3494.83	5	3629.96	1	3729.95	2	3811.70	3	3941.41	1	4001.98	8
3495.83	1	3631.99	1	3729.92	2	3812.47	4	3942.44	5	4002.68	2
3500.32	10 s	3632.45	1	3730.71	1	3814.95	2	3943.90	6	4005.73	1
3503.75	3	3633.16	5	3732.49	5	3817.61	3 s	3945.41	5	4007.27	1
3506.99	3	3634.39	1	3733.74	1	3820.16	5	3946.22	8	4008.33	1
3509.57	2	3634.91	1	3734.02	4	3822.63	1	3948.59	3	4009.37	1
3510.07	2	3642.23	1	3734.77	1	3822.79	2	3951.99	2	4010.17	1
3510.21	1	3642.49	1	3736.05	3	3823.32	3	3953.67	2	4010.87	2
3511.18	1	3643.06	3	3736.57	2	3824.10	4	3954.72	5	4011.18	2
3512.04	1	3643.64	2	3737.14	1	3824.57	2	3955.23	5	4011.50	5
3512.99	1	3644.00	2	3738.67	1	3830.94	2	3956.35	2	4013.55	1

TABLE 1.—*Wavelengths and intensities of absorption lines of* Pr—Continued

λ_{air}	Int.	λ_{air}	Int.	λ_{air}	Int.	λ_{air}	Int.	λ_{air}	Int.	λ_{air}	Int.
4014.23	1	4099.57	1	4182.47	4	4265.66	3	4339.40	3	4402.47	1
4014.99	1	4100.08	1	4183.21	1	4267.19	5	4339.65	1	4403.02	1
4020.59	1	4101.08	1	4184.41	8	4268.64	2	4341.18	1	4403.58	1
4022.82	1	4102.71	2	4188.42	3	4270.37	1	4342.64	1	4404.69	2
4023.71	5	4103.37	4	4188.89	1	4270.79	1	4343.41	2	4405.10	3
4024.11	3	4108.34	2	4189.04	1	4273.11	2	4343.50	2	4405.78	1
4025.54	2	4109.13	1	4189.32	3	4274.96	1	4343.77	2	4406.00	2
4027.64	5	4110.39	1	4192.17	1	4276.78	2	4344.68	1	4408.15	3
4028.50	1	4111.68	2	4192.58	1	4277.60	2	4346.93	2	4408.83	1
4029.75	1	4112.02	8	4194.72	1	4278.23	1	4347.27	4	4410.23	1
4030.08	1	4112.80	3	4196.42	1	4285.15	2	4347.87	1	4410.86	2
4033.65	1	4113.36	3	4197.23	4	4285.54	1	4349.15	2	4411.83	1
4034.34	1	4115.06	1	4198.99	8	4286.17	1	4349.66	3	4413.36	1
4035.02	1	4116.35	2	4200.16	2	4286.17	1	4350.72	1	4416.92	1
4036.93	1	4119.84	1	4205.09	1	4288.23	1	4351.18	1	4417.19	1
4038.18	5	4120.17	1	4205.44	2	4288.76	1	4352.16	1	4417.39	1
4039.81	8	4121.26	3	4207.18	1	4290.25	1	4354.75	2	4417.80	1
4042.43	8	4122.28	2	4207.77	2	4290.53	5	4355.20	1	4420.29	1
4044.05	8	4122.99	1	4210.64	2	4294.84	1 b l	4355.97	1	4421.87	1
4044.86	1	4123.72	1	4214.22	1	4294.96	3 b l	4356.49	2	4422.44	1
4046.65	1	4123.98	3	4214.47	8	4295.26	1	4358.46	2	4423.65	1
4047.26	1	4125.13	1	4215.30	1	4295.75	3	4358.74	2	4424.66	1
4047.94	8	4125.57	5	4216.78	3	4297.94	2	4358.99	2	4426.94	1
4048.82	1	4125.88	2	4217.68	5	4299.43	8	4359.69	2	4428.45	1
4049.16	3	4126.33	1	4218.65	1	4301.34	5	4360.95	8	4428.94	2
4051.17	5	4127.25	2	4219.82	2	4301.92	1	4361.52	4	4430.13	8
4051.98	2	4129.14	3	4220.70	1	4303.23	3	4362.84	2	4431.57	2
4052.36	1	4132.86	1	4221.17	1	4303.52	3	4363.64	1	4431.91	2
4053.25	2	4133.16	1	4221.78	3	4303.99	1	4366.49	1	4432.43	2
4053.51	1	4133.46	1	4222.11	1	4304.66	1	4367.28	2	4432.59	2
4054.77	2	4134.49	1	4223.20	3	4305.82	1	4368.54	2	4433.08	1
4055.20	1	4137.38	1	4224.30	2	4305.82	1	4369.45	1	4433.79	1
4057.31	4	4138.19	1	4225.54	3	4308.45	1	4369.63	1	4435.33	1
4059.90	2	4140.04	1	4228.46	1	4310.42	1	4369.84	4	4435.82	1
4061.12	1	4140.54	2	4229.77	1	4311.28	1	4370.22	1	4436.85	1
4062.50	5	4141.18	1	4230.11	1	4311.73	1	4370.39	2	4437.48	4
4062.89	1	4141.91	1	4230.68	3	4312.60	1	4370.94	1	4437.94	2
4064.19	3	4142.40	4	4231.16	1	4313.17	4	4372.83	2	4439.90	2
4065.42	8	4144.38	2	4232.31	1	4313.46	3	4375.24	1	4441.36	8
4065.95	3	4144.67	2	4236.99	6	4313.85	1	4375.86	1	4442.10	2
4066.84	1	4146.14	3	4237.88	2	4314.37	1	4376.78	1	4442.88	2
4067.60	2	4150.00	1	4239.17	1	4314.69	4	4376.99	1	4445.00	2
4068.83	1	4150.59	2	4240.58	2	4315.42	2	4377.62	5	4445.31	2
4069.96	2	4150.85	1	4241.38	1	4315.60	1	4377.86	2	4445.81	4
4072.80	3	4152.03	5	4242.67	2	4316.51	1	4379.83	5	4446.52	1
4074.34	1	4153.43	4	4245.40	2	4318.42	2	4380.74	1	4447.87	3
4075.86	1	4158.47	3	4245.64	1	4320.38	4	4381.58	3	4448.18	2
4077.19	2	4161.56	1	4246.29	2	4320.55	2	4382.01	5	4450.09	3
4079.80	2	4161.77	3	4247.09	1	4321.80	1	4384.01	1	4450.33	3
4081.46	1	4162.19	1	4247.86	1	4322.04	1	4385.50	5	4450.43	1 b l
4082.00	1	4163.87	1	4251.83	1	4323.08	2	4386.00	1	4452.49	8
4082.31	5	4165.79	2	4252.05	2	4324.41	1	4386.66	1	4456.13	2
4083.89	3	4166.93	1	4252.63	3	4324.69	1	4386.82	1	4456.60	1
4084.44	2	4168.75	2	4253.03	3	4324.83	2	4387.58	4	4458.07	1
4085.77	4	4168.84	1	4253.29	1	4325.30	2	4388.25	2	4458.43	2
4086.56	5	4169.65	8	4254.83	3	4325.41	1	4389.26	2	4459.39	8
4089.33	1	4170.60	1	4256.47	2	4328.92	4	4392.08	5	4460.62	2
4090.20	5	4172.15	1	4257.43	2	4329.65	1	4392.46	5	4461.92	2
4091.10	3	4172.96	3	4258.08	1	4330.49	1	4394.11	1	4462.21	1
4091.25	2	4173.19	2	4259.46	1	4331.84	2	4394.54	1	4463.71	8
4091.34	8	4174.22	1	4262.99	1	4332.87	1	4395.81	8	4464.62	1
4092.07	1	4175.29	1	4263.74	1	4333.95	5	4396.27	1	4466.01	2
4095.24	5	4177.44	5	4264.06	1	4334.34	1	4397.17	4	4466.74	2
4095.84	4	4177.80	2	4264.91	1	4337.96	2	4398.29	2	4468.91	1
4096.83	1	4181.61	3	4265.49	3	4338.79	1	4402.15	1	4470.40	2

TABLE 1.—*Wavelengths and intensities of absorption lines of* Pr—Continued

λ_{air}	Int.	λ_{air}	Int.	λ_{air}	Int.	λ_{air}	Int.	λ_{air}	Int.	λ_{air}	Int.
4470.61	1	4531.85	3	4597.69	4	4659.51	2	4728.60	1	4840.78	2
4472.94	1	4532.33	10	4598.95	5	4659.76	1	4730.66	3	4842.55	5
4474.07	5	4533.92	3	4600.75	4	4660.91	8	4733.37	3	4846.85	2
4474.44	4	4534.34	1	4602.58	8	4661.56	1	4736.67	5	4848.11	8
4475.83	1	4534.89	1	4603.86	1	4662.08	1	4740.92	2	4848.58	1
4476.15	1	4535.48	2	4605.24	4	4662.20	1	4741.44	2	4848.92	1
4476.67	1	4537.14	1	4606.95	1	4663.30	1	4743.55	2	4849.30	1
4477.31	1	4538.54	2	4607.99	1	4664.74	1	4744.08	5	4850.11	1
4478.01	1	4540.61	1	4609.87	2	4665.96	1	4745.22	2 w	4850.60	2
4478.60	2	4541.26	10	4611.15	2	4667.15	1	4748.58	2	4851.49	4
4480.11	4	4542.04	1	4611.70	3	4668.14	1	4749.71	2	4853.71	3
4480.97	1	4542.67	1	4611.88	3	4669.71	1	4750.51	3	4855.36	2
4481.37	1	4546.68	2	4612.77	4	4670.54	8	4751.55	2	4856.08	8
4481.89	2	4547.23	1	4613.08	1	4671.10	1	4752.80	1	4856.92	2
4482.35	2	4547.90	1	4615.40	1	4671.25	1	4757.11	1 w	4857.41	5
4482.96	1	4548.23	1	4616.43	1	4673.38	2	4758.51	2	4858.87	1
4484.04	1	4549.36	2	4617.11	1	4673.58	1	4759.28	2	4861.98	1
4484.68	4	4550.01	1	4617.34	2	4674.11	1	4760.99	1	4862.35	1
4484.78	3 b l	4551.23	1	4617.73	8	4674.79	8	4763.67	1	4863.11	1
4485.30	3	4551.69	2	4618.28	2	4675.06	3	4764.45	3	4863.48	1
4485.98	8	4552.25	10	4621.94	2	4675.51	1	4767.81	8 l	4866.00	1
4486.81	1	4552.83	3	4622.74	5	4677.76	1	4770.46	5	4869.33	2
4487.05	2	4553.50	2	4624.07	3	4679.02	5	4772.33	2	4870.13	2
4487.42	1	4554.12	2	4625.01	1	4680.46	5	4773.46	2	4875.00	3
4487.99	2	4556.27	1	4625.29	2	4682.02	3	4774.56	5	4876.56	2
4488.58	8	4556.66	1	4625.64	8	4682.19	2	4775.46	3	4880.61	2
4489.54	1	4559.34	1	4626.50	1	4682.70	5	4779.27	2	4882.26	4
4490.78	1	4559.67	2	4627.08	1	4683.23	1	4788.32	8	4883.81	1
4492.18	1	4560.42	1	4627.66	1	4683.45	3	4791.97	2	4884.46	2
4492.90	8	4560.95	2	4628.00	1	4684.04	2	4795.39	2	4886.71	2 h
4493.96	1	4561.85	1	4628.16	1	4687.80	10	4797.54	1	4889.65	2
4494.53	1	4563.32	2	4628.49	1	4688.50	1	4798.75	3	4894.90	2
4496.00	1	4563.84	2	4629.50	1	4689.54	8	4801.50	5	4895.68	1
4496.71	1	4564.34	2	4630.12	1	4690.33	3	4802.69	2	4896.10	4
4497.01	1	4565.05	2	4631.62	1	4690.56	3	4808.25	10	4896.90	1
4497.38	1	4565.81	3	4632.27	5	4691.77	3	4811.10	3	4897.24	1
4500.38	1	4566.85	2	4634.24	2	4692.65	8	4813.58	1	4897.93	1
4500.71	1	4567.34	1	4635.05	2	4694.52	8	4813.91	1	4898.71	1
4500.89	1	4567.63	1	4635.68	8	4695.75	8	4814.38	2	4899.46	2
4501.97	2	4568.31	1	4636.28	2	4696.44	2	4815.73	1	4900.00	1
4502.86	5	4568.70	1	4637.20	2	4697.17	5 w	4816.18	1	4901.81	2
4503.93	1	4569.38	2	4639.14	2	4698.00	2	4816.75	1	4904.38	2
4504.43	1	4569.63	3	4639.54	8	4698.86	2	4817.18	1	4905.37	2
4506.45	1	4570.36	4	4639.88	2	4699.57	8	4817.62	2	4906.16	1
4506.97	1	4570.82	2	4640.19	6	4700.62	2	4818.09	1	4906.96	8
4508.44	1	4570.98	2	4641.10	2	4701.50	1	4818.96	1	4907.90	4
4511.36	3 b l	4571.12	1	4646.39	1	4706.20	8	4820.81	2	4909.71	3 b l
4511.44	4 b l	4572.14	9	4646.98	8	4706.96	3	4821.18	2	4911.43	1
4512.15	3	4574.24	1	4648.15	5	4709.51	8	4822.13	2	4911.92	4
4514.96	2	4574.93	3	4649.43	1	4709.97	2	4824.03	2	4913.37	1
4515.24	1	4577.02	2	4649.66	1	4711.83	5	4825.16	1	4914.00	8
4516.93	1	4581.39	2 w	4649.87	2	4712.05	1	4825.85	3	4914.65	3
4517.77	1	4582.08	1	4651.01	1	4713.07	8	4827.53	4	4915.36	4
4519.13	1	4583.46	1	4651.20	1	4714.15	8	4828.10	3	4921.70	2
4519.62	6	4585.94	1	4651.66	2	4714.53	1	4830.11	3	4924.51	10
4521.48	1	4586.63	1	4652.38	2	4714.87	2	4832.49	1	4925.29	2
4522.40	1	4586.89	5	4652.69	5	4715.23	5	4833.25	2	4927.02	1
4523.20	1	4587.20	1	4653.38	4	4717.03	2	4834.33	1	4928.37	1
4523.98	1	4587.98	8	4653.79	2	4717.47	2	4834.78	3	4932.10	8
4524.53	1	4590.89	1	4654.72	2	4718.49	2	4835.65	1	4933.03	1
4528.05	3	4591.93	1	4655.98	5	4719.03	2	4836.25	1	4935.08	2
4528.92	2	4593.25	5	4656.78	3	4722.36	1	4837.17	1	4935.95	4
4529.93	1	4594.69	2	4657.90	1	4722.61	2	4838.34	1	4938.40	4
4530.37	1	4595.27	4	4658.36	3	4724.75	2	4839.33	4	4939.73	5
4531.49	2	4596.83	2	4658.73	4	4725.50	1	4840.51	5	4940.25	3

TABLE 1.—*Wavelengths and intensities of absorption lines of* Pr—Continued

λ_{air}	Int.	λ_{air}	Int.	λ_{air}	Int.	λ_{air}	Int.	λ_{air}	Int.	λ_{air}	Int.
4942.70	1	5061.33	2	5291.60	1	5400.92	3	5522.40	8 b l	5678.69	1
4944.00	2	5062.10	3	5292.28	8	5402.58	3	5522.65	3 w	5681.05	1 b l
4944.79	2	5062.89	3	5295.93	5	5403.02	1	5523.32	2 h	5687.42	10 b l
4947.13	2	5063.40	4	5297.70	5	5408.19	3	5523.89	10	5691.05	2 b l
4947.81	1	5067.45	2 h	5298.75	5 b l	5409.42	2	5524.29	1	5695.46	4
4948.15	1	5069.56	1	5298.92	3	5410.49	2	5527.90	1	5696.36	1
4949.30	1	5072.41	1	5299.77	3	5412.95	1	5528.48	2	5697.17	1
4951.31	8	5075.88	2 wh	5300.43	3	5413.31	2	5530.21	10	5697.96	1
4954.76	2	5076.72	2 wh	5301.68	1	5416.51	3	5531.18	4	5698.60	1
4955.22	1	5084.49	1	5303.60	2	5416.98	1	5532.16	2	5700.57	1 w
4955.98	6	5086.47	2	5304.17	4	5418.75	3 b l	5536.27	1	5701.10	1
4960.17	5	5087.10	4	5304.54	1	5419.00	3 b l	5538.35	5	5701.54	5
4960.97	2	5093.93	2	5305.88	4	5420.27	2	5544.33	1	5702.19	1
4961.54	1	5095.42	3	5306.36	2	5422.36	2	5545.23	1	5704.36	1
4962.17	1	5096.35	2	5307.18	3 b l	5423.16	1 b l	5546.20	1	5705.38	1
4964.50	2	5098.94	3	5309.06	4	5424.50	3	5549.17	8	5705.85	1
4965.06	1	5108.57	2	5312.55	3	5425.82	1	5549.79	4	5707.59	2 w
4970.97	2	5109.24	3	5313.62	8	5427.25	3	5551.06	2 wh	5708.29	3
4971.17	1	5113.92	1	5314.30	2	5427.72	1	5551.83	3 w	5710.02	1
4971.55	1	5114.74	1	5314.64	1	5432.50	1	5555.56	2	5710.44	1
4971.99	3	5115.25	2	5315.17	3 h	5432.89	10	5558.07	1	5710.95	1
4972.58	1	5116.29	2	5316.56	12 w	5437.28	5	5558.82	1	5713.61	3 vw
4974.94	5	5117.32	2	5319.03	3	5438.13	2	5560.05	4	5714.62	2
4975.79	5	5118.36	1	5320.32	1	5438.74	2	5561.13	3	5715.96	1
4976.41	5	5118.88	1	5322.63	8	5439.43	3	5562.30	2	5716.29	2
4977.49	1	5120.59	2	5324.99	2	5441.85	2	5563.47	1	5717.03	1
4978.36	2	5121.26	2	5334.66	1 b l	5442.52	2	5563.94	1	5717.63	1
4979.14	3	5128.45	3	5334.85	1 b l	5443.09	2	5564.80	1 w	5718.12	8
4986.54	1	5129.15	1	5336.52	1	5443.88	1	5565.52	2 h	5721.49	2
4987.42	1	5129.88	1	5337.42	2	5446.42	2	5569.02	5	5722.23	8
4992.34	2	5133.44	10	5342.00	3	5448.91	2	5577.37	3	5724.12	1
4995.35	3	5139.82	5	5342.85	2	5449.60	3	5578.79	4	5724.54	4
4997.47	2	5147.48	3	5343.65	3	5450.74	3	5581.91	3	5724.95	1
4998.80	1	5149.92	2	5344.31	1	5452.26	2	5582.36	2	5726.35	1
4999.74	1	5156.80	1	5344.94	1	5452.89	1	5588.28	3	5726.76	2 hw
5000.63	2	5168.32	2	5345.24	2	5453.22	2	5588.80	1	5727.00	3
5003.20	3	5173.14	2	5345.53	2	5453.74	1	5589.26	1	5727.55	1
5007.65	5 b l	5173.90	2	5347.10	2	5457.05	2	5589.66	2	5729.26	1
5009.43	2	5176.41	1	5348.80	3	5457.98	1	5591.48	2	5729.54	1
5015.73	1	5177.37	3	5351.45	2	5459.06	3	5592.71	3	5731.12	1
5018.17	2	5178.38	2	5352.05	2	5459.85	1	5594.88	3 w	5731.76	4
5018.62	6	5179.79	1	5353.64	5	5460.26	10	5599.75	2 w	5738.83	4 b l
5018.97	4	5183.45	3	5358.98	8	5462.34	3	5608.76	1	5740.59	1
5019.78	4	5184.50	2	5363.40	2	5462.82	3	5611.17	1	5743.71	4
5024.76	2	5185.83	1	5364.37	3	5467.86	2	5611.80	1	5744.92	2
5026.92	4 b l	5187.53	1	5365.31	2	5469.49	4	5612.01	2 h	5746.51	2
5029.02	5 b l	5194.42	8	5366.70	1	5469.90	2	5617.62	2	5751.85	1
5029.45	2	5195.50	8	5372.43	3	5479.86	12	5620.59	1	5760.19	1
5029.77	1	5212.46	2	5374.24	4	5481.76	8	5624.03	1	5768.49	1
5031.05	3	5227.95	3	5375.44	1	5486.67	5	5624.93	2	5779.27	2
5033.11	2	5246.08	2	5376.76	1	5487.57	5	5627.26	1	5780.05	1
5033.39	4	5249.28	1	5377.71	3	5488.91	3	5630.92	1	5792.25	1
5034.57	1	5249.84	2	5378.57	1	5489.41	1	5633.14	2	5803.50	1
5037.78	2	5253.13	1	5381.13	5	5490.54	1 b l	5634.90	1	5804.57	2
5043.34	1	5255.84	1	5381.60	3 w	5490.77	1 b l	5635.24	2	5805.90	4
5043.85	5	5256.76	1	5385.25	2	5491.66	1	5636.94	3	5807.21	2
5045.56	5	5258.68	1	5385.84	2	5496.22	8	5642.06	1 w	5807.92	1
5046.13	1	5259.24	2	5386.08	1	5504.69	3	5645.65	2	5808.48	1
5046.64	1	5262.19	2	5386.63	1	5505.88	1	5653.01	5	5809.52	2
5053.44	4	5283.03	2	5388.83	8	5509.61	5	5653.88	2	5810.35	1
5055.09	2	5284.40	1	5389.82	3 w	5511.26	3 b l	5656.61	1	5811.19	1
5055.73	2	5285.64	10	5390.73	3	5514.48	1	5663.44	2	5811.78	3
5056.59	2	5287.60	2 wh	5392.76	3	5516.19	4	5672.22	3	5812.67	3
5058.32	3	5288.68	2	5395.83	12	5517.71	4	5673.41	1	5813.73	1
5059.71	1	5289.33	8	5398.87	2 h	5520.30	2 w	5678.20	2	5818.06	1

TABLE 1.—*Wavelengths and intensities of absorption lines of* Pr—Continued

λ_{air}	Int.	λ_{air}	Int.	λ_{air}	Int.	λ_{air}	Int.	λ_{air}	Int.	λ_{air}	Int.
5818.93	1	5820.79	6 s	5823.23	1	5828.93	1	5831.81	1	5834.51	2
5819.95	1	5821.33	4 w	5824.14	2	5829.32	1	5832.25	2	5835.12	8
5820.10	1	5822.43	2 w	5824.65	3	5830.05	1	5832.98	1	5837.71	5
5820.34	2 w	5822.97	1	5825.14	1	5831.45	3	5833.73	2	5839.03	1

(Paper 69A1–329)

JOURNAL OF RESEARCH of the National Bureau of Standards—A. Physics and Chemistry
Vol. 69A, No. 1, January–February 1965

Publications of the National Bureau of Standards*

Selected Abstracts

Hydrodynamic fluctuations and Stokes' law friction, R. Zwanzig, *J. Res.* **68B** (*Math. and Math. Phys.*), *No. 4, 143–145 (Oct.–Dec. 1964).*

The frictional force on a Brownian motion particle can be expressed by means of the time-correlation of the fluctuating force on the particle. We show that this method, applied to a spherical particle in a viscous incompressible fluid, leads to Stokes' Law. The calculation is based on the theory of hydrodynamic fluctuations due to Landau and Lifshitz, and on a hydrodynamic theorem due to Faxen.

Tables of electron radial functions and tangents of phase shifts for light nuclei (Z–1 through 10), C. P. Bhalla, *NBS Mono. 81, (Aug. 6, 1964), $3.25.*

To facilitate the theoretical analyses of beta-decay experiments in light nuclei electronic radial wave functions, evaluated at the nuclear radius, and tangents of phase-shifts are tabulated for total angular momentum equal to 1/2 and 3/2. Separate tables for electrons and positrons are given for ten values of Z, starting from Z equal to one, in steps of unity and for beta momentum values from 0.1 mc to 42.0 mc in steps of 0.1 mc. The nucleus is represented as a sphere with uniform charge distribution. The nuclear radius, p, is taken to be $1.2A^{1/3}10^{-13}$ cm in the major body of these tables. However, additional tables for $Z=6$ and $Z=7$ are given for $p=1.1A^{1/3}10^{-13}$ cm and $p=1.3A^{1/3}10^{-13}$ cm.

Project FIST. Fault isolation by semi-automatic techniques, G. Shapiro, O. B. Laug, G. J. Rogers, and P. M. Fulcomer, Jr., *NBS Mono. 83, (Sept. 17, 1964), 55 Cents.*

The method of Fault Isolation by Semi-automatic Techniques developed at the National Bureau of Srandards, to which the acronym FIST has been applied, creates a new field of metrology which permits the measurement of the dynamic performance of electronic circuits by unskilled personnel under field operating conditions. It is a diagnostic tool for rapidly isolating faults in modularized, non-computer type electronic equipment without removing the modules from the prime equipment.

The system consists of test points and associated circuitry which are built into the prime equipment, and a small, hand-carried, general-purpose test instrument. The test points are located on an easily accessible test panel and are arranged in an order which permits rapid checking of the modules in a logical sequence.

Fault isolation is accomplished by testing the dynamic performance of each module with a test instrument which is basically a device for comparing the peak-to-peak amplitudes of two periodic voltage waveforms. Since many circuit properties other than voltage must be measured, transformation networks are provided to convert the characteristic being measured to a periodic voltage which is within the range of the test instrument.

The tests are usually made while the module under test is performing its normal function with the normal inputs to the module providing the stimuli for the tests when this is not possible, a stimulus generator is used to furnish the necessary signal or signals.

These techniques have been reduced to practice. This report describes the hardware required and discusses practical ways in which the necessary circuitry can be built into the prime equipment. The simplicity of the programming and the speed with which a complex piece of electronic equipment can be checked are demonstrated. Finally, a prototype test instrument capable of simultaneously testing four characteristics of the module or of its stimuli is described in detail.

United States standard for the colors of signal lights, F. C. Breckenridge, *NBS Handb. 95 (Aug. 21, 1964), 25 cents.*

The standard provides in part I basic chromaticity definitions defining the chromaticities that are considered safe for use as representing the named colors. These are the basis for the selection of the national standard filters and for the tolerances given in part II for duplicating them. The procurement requirements of parts III and IV are based primarily on sets of these filters in combination with prescribed sources although provision is also made for procurement under the basic chromaticity definitions in cases in which it is impracticable to base the procurement on filters. Part V provides guidance in selecting signal colors for new uses, and part VI provides methods for special laboratory tests and serves as a technical interpretation of the practical tests prescribed in parts III and IV.

Studies of photodissociation of molecular ions, G. H. Dunn, *Book, Atomic Collision Processes, pp. 997–1005 (North-Holland Publ. Co., Amsterdam, The Netherlands, 1964).*

Preliminary results are reported on the measurement of the photodissociation cross section of H_2^+. Measurements have been made at a number of wavelengths between 3000 Å and 9000 A, and a comparison is made with available theory. Disagreement of the measurements with theory suggest that improvement of the theory is justified for detailed comparisons with experiment.

A linear decrease with ion source pressure of the photodissociation cross section at 5500 Å is observed. This dependence yields a lower limit of 10^{-15} cm^2 on the collision cross section for depopulating vibrational states of H_2^+ participating in photodissociation at 5500 Å.

White light was also used to observe photodissociation of H_2^+ and N_2^+, and an average cross section was calculated from the data and the spectral distribution of the lamp used.

An effort to observe photodissociation of H_3^+ yielded no results except to place an upper limit of 10^{-20} cm^2 on the average cross section.

Mechanical and dielectric relaxation of crystalline polymers in relation to degree of crystallinity and morphology, E. Passaglia, *Soc. Plastic Engrs., pp. 169–177 (July 1964).*

Mechanical and dielectric relaxation as related to the morphology of crystalline polymers is reviewed. The behavior with temperature of the imaginary part of the complex dielectric constant and the mechanical loss factor, tan δ, at constant frequency is discussed in detail for two typical crystalline polymers: poly(chlorotrifluoroethylene) and polypropylene. Three relaxations are typically observed: a low temperature relaxation occurring at temperatures below the dilotometric glass transition temperature; a glass temperature relaxation occurring near the glass transition temperature, and a high temperature relaxation occurring between the glass temperature and the melting point. The activation parameters are given for these relaxations, and the influence of morphology on them is discussed along with possible molecular interpretations.

Unitary symmetry in photoproduction and other electromagnetic interactions, C. A. Levinson, H. J. Lipkin, and S. Meshkov, *Physics Letters* **7,** *No. 1, 81–84 (Oct. 15, 1963).*

U-spin is rigorously conserved to all orders in the electromagnetic interaction and in the strong interactions which are

invariant under SU_3. Predictions which follow from U-spin conservation are given for 1) photoproduction, 2) meson photoproduction, 3) electromagnetic decays of baryon resonances, 4) static electromagnetic properties for the baryon octet, 5) photoproduction of two mesons, and 6) photoproduction of Z^-.

Initial preparation and metastable transitions in mass spectra, H. M. Rosenstock, V. H. Dibeler, and F. N. Harllee, *J. Chem. Phys.* **40,** *No. 2, 591–594 (Jan. 15, 1964).*

Variation of initial preparation to search for non-equilibrium kinetic effects (Frey) is discussed in connection with the kinetics of unimolecular ionic decomposition processes occurring in the mass spectrometer. A particular example, dependence of the rates of competing metastable transitions of hexyl ions on mode of preparation is studied in detail. The hexyl ions were prepared by electron impact ionization and decomposition of a variety of normal alkanes, *n*-hexyl bromide and di-*n*-hexyl ether. At low electron energies (30 ev) the ratio of the competing metastable transitions is constant within experimental error. This supports the applicability of the quasi-equilibrium theory of mass spectra to such processes. At higher electron energies there is a slight dependence of the ratio on parent ion mass.

Inelastic electron scattering from rare gases, determination of oscillator strengths in the continuum, C. E. Kuyatt and J. A. Simpson, *Proc. Third Intern. Conf. Physics of Electronic and Atomic Collisions, London, England, 1963, pp. 191–200 (North Holland Publ. Co., Amsterdam, The Netherlands, 1964).*

The inelastic scattering of 500–1000 eV electrons from the rare gases has been measured for small angle collisions and energy losses to 106 eV. Approximate relative oscillator strengths for continuum excitations of helium and neon have been derived from the forward scattering intensities. The results in helium are in good agreement with the latest uv measurements and with calculations. In the case of neon, previous experiments and calculations differ considerably. The present results agree well with the most recent uv measurements, except that the electron measurements do not show a sharp L ionization edge. This difference can probably be attributed to the effect of preionization lines with a resonance shape which have recently been observed.

The characterization of large single crystals by high-voltage X-ray Laue photographs, H. S. Peiser and E. P. Levine, *(Proc. 11th Ann. Conf. Applications of X-ray Analysis, Aug. 1962), Book, Advances in X-ray Analysis* **6,** *158–163 (Plenum Press Inc., New York, N.Y., 1963).*

Large single crystals can be examined by conventional X-ray diffraction procedures only at their surface or by destructive sectioning. With the limitations inherent in polychromatic X-ray photography, high-voltage Laue pictures are shown to give some information on the internal quality of large crystals. Asterism in conventional Laue photographs is contrasted with streaks due to geometric effects in Laue patterns of large crystals. Detail within the streaks reveals sub-grain structure. A primary extinction effect can be used as striking proof of good crystals being capable of scattering coherently over large distances.

The calculations of autoionization probabilities, J. W. Cooper, *Proc. Third Intern. Conf. Physics of Electronic and Atomic Collisions, London, England, 1963, pp. 595–599 (North Holland Publ. Co., Amsterdam, The Netherlands, 1964).*

Calculations have been carried out for the autoionization probabilities and level widths of the doubly excited states $(2snp)^{1,3}P$ and $(ns^2p)^{1,3}P^{n=2,3,4}$ in He. Although the model used for the calculations was crude, the level widths computed agree order of magnitude-wise with recent experimental observations. The probable effect of the strong coupling between levels of the above series for $n>2$ and of additional configuration mixing is discussed. The calculations point up the fact that the important region for the autoionization process corresponds to small radial distances from the nucleus. It was also found that the results were relatively insensitive to the exact form of the wave functions and for the calculations.

The basis of the functional assumption in the theory of the Boltzmann equation, M. S. Green and R. A. Piccirelli, *Phys. Rev. 132, No. 3, 1388 (Nov. 1963).*

The long-time behavior of the *n*-particle probability densities for a large, dilute system of point particles interacting with short-range forces is studied. The main result is an exact series for the *n*-particle density which consists of two parts. The first part is a time-independent functional of the singlet density which is expressed as a funtional power series and which is a direct analog of the equilibrium density series. The second part is also a functional power series in the singlet density but the coefficients depend on time and on the initial correlations. The coefficients of both series are given explicitly in terms of operators which are determined by the dynamics of isolated groups of particles. It is demonstrated that these operators vanish for phase points corresponding to motions during which there are two or more groups of particles which either are statistically and dynamically independent or are such that each of them is dynamically connected to the rest by no more than one particle. It is argued that all the terms of the exact series are finite and that the terms of second part (the error) decrease with increasing time so that the first part is the asymptotic form proposed by Bogoliubov. The relevance of the results for the Boltzmann equation is indicated.

Energy dependence for the photodetachment of I^- near threshold, B. Steiner, M. L. Seman, and L. M. Branscomb, *Proc. Third Intern. Conf. Physics of Electronic and Atomic Collisions, London, England, 1963, pp. 537–542 (North Holland Publ. Co., Amsterdam, The Netherlands, 1964).*

The photodetachment of atomic iodine negative ions has been observed in a crossed beam experiment with much higher spectral resolution than previously used in this laboratory. The iodine negative ions were formed in a discharge through an ammonia-iodine vapor mixture and mass analyzed in the apparatus used in previous experiments. The photon beam originated in a high pressure xenon lamp and was resolved in an F/1.5 monochromator. The threshold region near 4040 Å has been scanned with a photon beam half width of 18 Å, and the region down to 3000 Å with a half width of 33 Å. Transitions ascribed to $^1S_0 \rightarrow {}^2P^o_{3/2}$ and $^1S_0 \rightarrow {}^2P^o_{1/2}$ were observed. The experimental slit function has been unfolded from the first threshold region to reveal the "true" threshold behavior. The derived radiative attachment cross section in region of the threshold will be presented.

Nuclear magnetic resonances of ^{69}Ga and ^{71}Ga in gallium-substituted yttrium iron garnet, R. L. Streever and G. A. Uriano, *Phys. Rev. Letters* **12,** *No. 22, J516 1–3—J516 3–3 (June 1, 1964).*

We have recently observed the nuclear magnetic resonance of ^{69}Ga and ^{71}Ga in the mixed garnet system $3Y_2O_3 \cdot (5-x)Fe_2O_3 \cdot xGa_2O_3$. The resonance has been observed at 77 °K over a concentration range from x=.25 to x=2.6 and at room temperature over a smaller concentration range. The resonance frequency for ^{71}Ga at 77 °K reaches a maximum at about x=1.5 of 30.0 MHZ (in zero applied field) corresponding to a hyperfine field of about 2.3 tesla (23 kilogauss). The resonance is from nuclei of ions on (d) sites and the hyperfine field is believed to arise from an unpaired spin density on the gallium ion which is coupled strongly with nearest neighbor iron ions. Gallium ions on (d) sites have eight nearest neighbors (4 neighbors on (a) sites and 4 on (d) sites) and the resonance is particularly interesting because the concentration dependence allows us to separate out the sign and magnitude of the contribution to the field from iron ions on (a) and (d) sites.

Polymorphism of ABO_3-type rare earth borate solid solutions, R.S. Roth, J. L. Waring, and E.M. Levin, *(Proc. Third Rare Earth Research Conf., Apr. 2-24, 1963), Book, Rare Earth Research, Chapter on Structure of Rare Earth Compounds, pp. 1030–1055 (Gordon and Breach Science Publ., Inc., New York, N.Y., 1964).*

Polymorphic relations of solid solutions of the ABO_3-type rare earth borates have been studied by means of quenching techniques and high temperature X-ray diffraction. It has

been found that the polymorph reported as the high temperature form of $MdBO_3$ (Levin, Roth, and Martin, 1961) is only metastable and is formed, on cooling, from a phase isostructural with H-$LaBO_3$. The similar polymorph of $SmBO_3$ is apparently stable from room temperature to about 1065 °C. The high vaterite form of $SmBO_3$ is stable from about 1065° to 1285° and the H-$LaBO_3$ type from 1285° to the melting point. Phase equilibrium diagrams have been constructed for the systems involving $LaBO_3$ with many of the other RBO_3 compounds and for $NdBO_3$-$SmBO_3$. The aragonite and vaterite type structures are not stable in the central portion of most of these systems. Instead, the H-$LaBO_3$ and L-$SmBO_3$-type phases appear as the stable polymorphs. The H-$LaBO_3$-type polymorph is a low symmetry distortion of a calcite type structure. As smaller ions are added in solid solution to $LaBO_3$ the distortion becomes less until with $LaLo(BO_3)_2$ an hexagonal phase is formed which may have a dolomite type structure, although the super-structure peaks are not evident. However, this phase apparently disorders to a H-$LaBO_3$ type solid solution rather than to the true calcite type structure. Although the temperature of the high-low inversion of the vaterite-type structures is lowered by the addition of $LaBO_3$ in solid solution, in no case has the high-vaterite structure been obtained at room temperature.

Optically pumped magnetometers and related experiments in high magnetic fields, P. L. Bender, *Book, Quantum Electronics, Ed. P. Grivet and N. Bloembergen, III.* **I,** *263–273 (Columbia University Press, New York, N.Y., 1964).*
Some considerations on optically pumped magnetometers are given. Related experiments in high magnetic fields giving alkali nuclear moments and departures from the Breit-Rabi formula are suggested.

Hydrogen atom addition to solid four-carbon olefins, R. Klein and M. D. Scheer, *J. Phys. Chem.* **67,** *1874–1877 (Sept. 1963).*
An investigation of the hydrogen atom addition to condensed, solid, four-carbon olefins in the 77° K region has shown that the general reaction is terminal hydrogen atom addition to terminal double bonds followed by disproportionation and recombination of the resulting radicals. H atoms also react with the hydrocarbon radical in a similar manner. All of the butene-2 formed from butene-1 and from butadiene-1,3 is *trans*, but that formed from butadiene-1,2 is both *cis* and *trans*. Butadiene-1,3 produces nine eight-carbon dimers, butadiene-1,2, three, and isobutene, none. One of the major products of the H atom addition reaction with butadiene-1,2 is butyne-2.

Anomalous transmission of rare gases for electrons of subexcitation energies, J. A. Simpson, *Proc. Third Intern. Conf. Physics of Electronic and Atomic Collisions, London, England, 1963, pp. 128–134 (North Holland Publ. Co., Amsterdam, The Netherlands, 1964).*
Electrons of variable energy ($\Delta E_{1/2} \sim 0.05$ eV) are passed through a chamber containing rare gas at a pressure of some microns. Electrons which are deflected less than 40 mr are energy analyzed (resolution ~ 0.05 eV) and collected. Two types of transmission anomalies, with energy widths essentially instrumental, are observed at energies below those necessary to excite the atom. The first, in He at 19.1 ± 0.1 eV, is an enhanced transmission followed by a decrease in a typical dispersion line shape. The second anomaly in Ne at 15.9 ± 0.15 eV, is not so strong and has a more complicated structure consisting of a doublet (~ 0.1 eV separation). Both components are sharp decreases in transmission without dispersion line shape. A brief description of the apparatus is included.

Electron microscopy and diffraction of aluminum oxide whiskers, D. J. Barber, *Phil. Mag.* **10,** *No. 103, 75–94 (July 1964).*
Whiskers of α-Al_2O_3 have been grown by the condensation and oxidation of aluminium on an alumina substrate, and examined by transmission electron microscopy and diffraction. Unbroken whiskers invariably terminate in a small globule of aluminium and have a 'drumstick' form. The most perfect whiskers are ribbons with their principal surfaces parallel to the (0001) planes; the majority of these have a $<1\bar{1}20>$ growth direction. With intense heating in the electron beam, such ribbons can be thermally etch pitted. Many drumsticks are tubular rather than ribbonlike and drumsticks containing axial dislocations have also been seen. The effect of intense heating on these whiskers has been investigated. Occasionally, the aluminium globules melt and react with the carbon support film in the microscope to give crystalline Al_4C_3. Alternatively, a globule may explode to form many small globules that immediately develop stems; thus, new whiskers are formed in the microscope. The relevance of these observations to proposed mechanisms for the growth of drumstick whiskers is discussed.

The crystal structure of 1-ethyldecaborane, A. Perloff, *Acta Cryst.* **17,** *332 (1964).*
Direct evidence for the existence of 1-ethyldecaborane has been established by a single crystal X-ray structure analysis using, in part, the method of direct phase determination developed by Karle and Hauptman. The compound crystallizes in the orthorhombic system with $a = 10.11 \pm 0.01$, $b = 14.40 \pm 0.01$, and $c = 7.28 \pm 0.01$ Å. The space group is $P2_12_12_1$ and the unit cell contains four molecules of $B_{10}H_{13}C_2H_5$. The compound is a simple substitution derivative of decaborane and no significant distortion of the decaborane molecule is induced by the substitution.

Optically observed inner shell electron excitation in neutral Kr and Xe, K. Codling and R. P. Madden, *Phys. Rev. Letters* **12,** *No. 4, 106–107 (Jan. 1964).*
The far ultraviolet continuum radiation emitted by the N.B.S. 180 Mev electron synchrotron has been used for the study of the absorption spectra of Kr and Xe in the 120–200A spectral region. Structure involving transitions to neutral atom energy levels has been observed for the first time at energies in excess of 50 ev above the 1st ionization limits of Kr and Xe. These transitions involve the excitation of inner shell d electrons and result in two series for each element, namely $3d^{10}4s^24p^6\ {}^1S_0 - 3d^94s^24p^6\ ({}^2D_{3/2,\ 5/2})\ np\ {}^1P^\circ_1$ in Kr, and $4d^{10}5s^25p^6\ {}^1S_0 - 4d^95s^25p^6\ ({}^2D_{3/2,\ 5/2})\ np\ {}^1P^\circ_1$ in Xe.

Dielectric polarizability of fluid parahydrogen, J. W. Stewart, *J. Chem. Phys.* **40,** *3297-3306 (June 1964).*
The dielectric constant of liquid and gaseous para-hydrogen has been measured by the capacitance ratio method between 24°K–100°K and 2–326 atmospheres. This encompasses the density range 0.002–0.080 gm/cm³. These data have been combined with recently available PVT results in order to calculate the Clausius-Mosotti function to 0.05% precision. In the range considered, the C–M function, or polarizability, instead of being constant, initially rises with density to a maximum 0.2% above the low density value of 1.00427 cm³/gm, and then falls. The data in this range can be represented to within experimental error by a quadratic function of density. The deviation from constancy is too small for detailed correlation with existing theories of polarizability to be feasible. The results are presented in tabular form. Also the dielectric constant at any desired density can easily be calculated to an accuracy better than 0.1% in $\epsilon - 1$ from the function fitting the polarizability.

Standard potential of the Ag–AgCl electrode in 5% aqueous mannitol, R. Gary and R. A. Robinson, *J. Chem. Eng. Data* **9,** *No. 3, 376–378 (July 1964).*
The standard potential of the Ag–AgCl electrode from 0° to 60° has been determined by e.m.f. measurements on the cell: Pt/H_2:HCl(m) in 5% mannitol; AgCl/Ag. From these data and from data on the same cell containing no mannitol, the relative partial molal quantities $\Delta\bar{G}°$, $\Delta\bar{H}°$ and $\Delta\bar{S}°$ for the change in solvent are calculated. The value of $\Delta\bar{G}°$ for HCl in 5% mannitol at 25° is found to be 54.0 j. mole^{-1}. There is a small but significant change in the e.m.f. of the cell if mannitol is replaced by its diastereoisomer, sorbitol.

Optical investigations of film formation and removal on gold anodes in acidic oxalate solutions, W. E. Reid and J. Kruger, *Nature* **203,** *No. 4943, 402 (July 25, 1964).*
Evidence has been obtained for film formation on gold anodes in acidic oxalate solutions using ellipsometry. The thickness

of the film increases linearly with the potential above 1.1 V (NHE) in 1 M H_2SO_4 and solutions of low oxalate content (4 g/l) to give a thickness of about 20A. The film is reduced at potentials below 1.1 V and also by acidic oxalate solutions. Optical evidence indicates that this film is more likely to be an oxide film rather than chemisorbed oxygen.

Recently discovered autoionizing states of krypton and xenon in the λ 380–600A, R. P. Madden and K. Codling, *J. Opt. Soc. Am.* **54,** *No. 2, 268–269 (Feb. 1964).*

The far ultra-violet continuum radiated by the NBS 180 Mev electron synchrotron has been utilized for the study of the absorption spectra of krypton and xenon in the wavelength region 380–600Å. Many new autoionizing states in both elements, lying 10–40 ev above the first ionization limit, have been discovered. The following series have been identified: $4s^24p^6\ ^1S_0 - 4g4p^6\ np\ ^1P_1^0$ and $4s^24p^6\ ^1S_0 - 4s^24p^45s\ np\ ^1P_1^0$ in krypton, $5s^25p^6\ ^1S_0 - 5s5p^6\ np\ ^1P_1$ in xenon.

"U-spin equalities" and octet symmetry breaking, S. Meshkov, G. A. Snow, and G. B. Yodh, *Phys. Rev. Letters* **13,** *No. 6, 212–217 (Aug. 10, 1964).*

The "U-Spin equalities" are compared with experiment, in order to see to what extent the SU_3 predictions are obeyed. Deviations from pure SU_3 symmetry by an order of magnitude are found. The role of symmetry breaking in the interaction matrix elements is investigated and correlated with the possible appearance of superresonances.

Electrode potentials in fused systems. VII. Effect of ion size on membrane potentials, K. H. Stern and J. A. Stiff, *J. Electrochem. Soc.* **III,** *No. 8, 893–897 (Aug. 1964).*

Concentration cells exhibiting glass membrane potentials have been measured for the AgBr–NaBr, AgCl – KCl, and AgCl – CsCl systems. Only for the first of these can the bulk composition be used to calculate cation transport numbers in the membrane. For the latter two the sodium ion impurities in the melt appear to be potential determining. In the sodium-containing systems the anions appear to be transported as part of a cationic silver complex.

On the identity of three generalized master equations, R. Zwanzig, *Physica* **30,** *1109–1123 (1964).*

Three apparently different quantum mechanical master equations, derived by Prigogine and Resibois, by Montroll, and independently by Nakajima and by Zwanzig, are shown to be identical. The derivation by Zwanzig, based on projection operator and Liouville operator techniques, is repeated in greater detail than in previous articles. The results of Prigogine and Resibois, and of Montroll, are found by making changes in notation.

The oxide films formed on copper single crystal surfaces in water. III. Effect of light, J. Kruger and J. P. Calvert, *J. Electrochem. Soc.* **III,** *No. 9, 1038–1041 (Sept. 1964).*

Studies of the effect of illumination on the growth of oxide films on copper single crystal surfaces immersed in water containing different amounts of dissolved oxygen reveal that while illumination has little effect on the oxidation process when the water is in equilibrium with a 100% oxygen atmosphere, it does lower the rate of film formation when the water is in equilibrium with 1% oxygen. For both the (111) and (100) illumination causes a departure from the rate law observed for oxidation in the dark. At intensities of 290 μw/cm² or higher the film formed on the (111) never grows beyond a limiting thickness of 100 Å. The behavior observed can be explained on the basis of a competition between growth and dissolution reactions, the dissolution reaction being promoted by illumination.

Thermodynamics of aqueous solutions of hydriodic acid from electromotive force measurements of hydrogen-silver iodide cells, H. B. Hetzer, R. A. Robinson, and R. G. Bates, *J. Phys. Chem.* **68,** *No. 7, 1929–1933 (1964).*

Electromotive force measurements of the cell $Pt;H_2(g)$, HI(m), AgI;Ag have been made at 11 temperatures from 0 to 50°. The standard e.m.f. ($E°$) is given within 0.05 mv. by the equation $E° = -0.15242 - 3.19 \times 10^{-4}(t-25) - 2.84 \times 10^{-6}(t-25)^2$, where t is the temperature in degrees Celsius. These values are in excellent agreement with those obtained by Owen from studies of borax-buffered KI solutions at 5, 10, 30, 35, and 40° but differ by 0.14 to 0.17 mv. at 15, 20, and 25°. The activity coefficient ($\gamma_\pm$) of HI at molalities (m) from 0.005 to 0.9 has been derived. The relative partial molal enthalpy (L_2) of HI at 25° was calculated and compared with that for HCl and HBr. At 25° and $m = 0.1$, $\gamma_\pm$ is 0.811 and L_2 is 130 cal. $mole^{-1}$.

Other NBS Publications

J. Res. NBS 68B (Math. and Math. Phys.), No. 4 (Oct.–Dec. 1964), 75 cents.

Hydrodynamic fluctuations and Stokes' Law friction. R. Zwanzig. (See above abstracts.)

Equivalence of certain inequalities complementing those of Cauchy-Schwarz and Hölder. J. B. Diaz, A. J. Goldman, and F. T. Metcalf.

Weak generalized inverses and minimum variance linear unbiased estimation. M. Zelen and A. J. Goldman.

Improvement of bounds to eigenvalues of operators of the form $T.*T$. N. W. Bazley and D. Fox.

The greatest crossnorm. R. Schatten.

Radio Sci. J. Res. NBS/USNC–URSI, 69D, No. 1 (Jan. 1965), $1.00

Some problems of ionospheric nonlinearities. D. H. Menzel.

Some nonlinear phenomena in the ionosphere. V. A. Bailey.

An experimental study of gyro interaction in the ionosphere, at oblique incidence. F. H. Hibberd.

On some nonlinear phenomena in the ionospheric plasma. P. Caldirola and O. De Barbieri.

Ionospheric cross modulation: a microscopic theory. D. Layzer and D. H. Menzel.

VLF noise bands observed by the Alouette I satellite. J. S. Belrose and R. E. Barrington.

Excitation of optical radiation by high power density radio beams. L. R. Megill.

Alteration of the electron density of the lower ionosphere with ground-based transmitters. P. P. Lombardini.

Collision effects in hydromagneto-ionic theory. H. K. Sen and A. A. Wyller.

Electromagnetic wave reflection from an oscillating, collision-free magneto-ionic medium. O. E. H. Rydbeck.

Nonlinear propagation of electromagnetic waves in magneto-plasmas. II. (An invited abstract) M. S. Sodha and C. J. Palumbo.

Standard X-ray diffraction powder patterns, H. E. Swanson, M. C. Morris, E. H. Evans, and L. Ulmer, NBS Mono. 25-Sec. 3 (July 31, 1964), 40 cents.

Hydraulic Research in the United States 1964, Ed. H. K. Middleton, NBS Misc. Publ. 261 (Aug. 14, 1964), $1.25.

Water-repellent preservative non-pressure treatment for millwork, CS262–63 (Dec. 31, 1963), 10 cents.

Quarterly radio noise data March, April, May 1963, W. Q. Crichlow, R. T. Disney, and M. A. Jenkins, NBS Tech. Note 18–18 (July 25, 1964), 50 cents.

A helicopter battery service simulator, W. G. Eicke, Jr., NBS Tech. Note 244 (Aug. 28, 1964), 20 cents.

Factors influencing the design of original-document scanners for input to computers, NBS Tech. Note 245 (Aug. 19, 1964), 35 cents.

Radiochemical analysis: Activation analysis, instrumentation, radiation techniques, and radioisotope techniques, Ed. J. R. DeVoe, NBS Tech. Note 248 (Aug. 21, 1964), 50 cents.

Tooth fluorometer, A. F. Forziati, J. Kumpula, and J. J. Barone, J. Am. Dental Assoc. **67,** No. 5, 663–669 (Nov. 1963).

Thermodynamic representation of high-pressure vapor-liquid equilibria, J. M. Prausnitz, Chem. Eng. Sci. **18,** 613–630 (1963).

Nuclear magnetic relaxation of the impurity nucleus in dilute

ferromagnetic alloys, R. L. Streever, Phys. Rev. **134,** No. 6A, A1612–A1617 (June 15, 1964).

NBS microcopy resolution test chart, B. H. Fouquet, Proc. Natl. Microfilm Association Meeting, San Francisco, Calif., Apr. 30–May 13, 1963, pp. 67–74 (1963).

Metastable transitions in mass spectra of methane and the deuteromethanes, V. H. Diebeler and H. M. Rosenstock, J. Chem. Phys. **39,** 1326 (1963).

Electron distribution in the ionosphere, J. W. Wright, Proc. URSI XIVth General Assembly, Sept. 1963, Tokyo, Japan XIII, 206–222 (1964).

Studies at NBS of the platinum-6% rhodium vs. platinum-30% rhodium thermocouple—A preliminary report, G. W. Burns, Proc. SAE Meeting, Sept. 23–27, 1963, Los Angeles, Calif., Preprint 750B, (1963).

Spread-*F* observations by the Alouette topside sounder satellite, W. Calvert and C. W. Schmid, J. Geophys. Res. **69,** No. 9, 1839–1852 (May 1, 1964).

Spectral distribution of typical daylight as a function of correlated color temperature, D. B. Judd, D. L. MacAdam, and G. Wyszecki, J. Opt. Soc. Am **54,** No. 8, 1031–1040 (Aug. 1964).

Medical applications of refrigeration, E. F. G. Brentari and R. V. Smith, ASHRAE Guide and Data Book, ch. 68, 773–778 (Am. Soc. Heating, Refrig. Air Conditioning Engrs., Inc., New York, N.Y., 1964).

Measuring the directivity of a directional coupler using a sliding short-circuit and an adjustable sliding termination, R. W. Beatty, IEEE Trans. Microwave Theory Tech. **MTT–12,** No. 3,283 (May 1964).

Mass spectrometric study of the photoionization of acetylene and acetylene-d_2, V. H. Dibeler and R. M. Reese, J. Chem. Phys. **40,** No. 7, 2034–2035 (Apr. 1, 1964).

Magnetically retained evaporation mask, F. E. Jones and A. B. Castle, Sr., Rev. Sci. Instr. **34,** No. 9, 1055 (Sept. 1963).

Low-temperature infrared studies of the chemistry of free radicals, M. E. Jacox and D. E. Milligan, Appl. Opt. 3, 873 (July 1964).

Characteristics of energy losses of electrons in solids, L. Marton, Book, Actions Chimiques et Biologiques Des Radiations, ch. IV, pp. 260–281 (Masson et Cie Editeurs, Paris, France, 1964).

Isotopic fractionation of uranium related to roll features in sandstone, Shirley Basin, Wyoming, J. N. Rosholt, E. N. Harshman, W. R. Shields, and E. L. Garner, Econ. Geology **59,** 570 (1964).

Book, Thermal Degradation of Organic Polymers, S. L. Madorsky (Interscience Publ. Inc., New York, N.Y., 1964).

Solid state detector for beta-ray spectroscopy below 4.2°, K. J. Chin, A. T. Hirshfeld, and D. D. Hoppes, Rev. Sci. Instr. **34,** No. 12, 1258–1259 (Nov. 1963).

Simple derivation of the Faxen solution to the Lamm equation, G. H. Weiss, J. Math, Phys. **5,** No. 5, 675–676 (May 1964).

Should the convention definition of mismatch loss be abandoned? K. A. Norton, Proc. IEEE **52,** 710 (June 1964).

Frequency and time standards, G. E. Hudson, Electronics World **72,** 20–23 (Aug. 1964).

Recognition of clauses in machine translation of languages, F. L. Alt, Proc. Intern. Conf. Machine Translation of Languages and Applied Language Analysis, Teddington, England Symp. No. 13, pp. 126–142 (Her Majesty's Stationery Office, London, England, Sept. 1961).

X-ray study of a cadmium borate glass, S. Block, J. Molin, and J. Piermarini, J. Am. Ceram. Soc. **46,** 557 (1963).

World days program, A. H. Shapley, IQSY Notes **5,** 27–30 (Dec. 1963); **6,** 27–32 (Mar. 1964); 7, 13–15, (May 1964).

Weights and measures and aerosols, M. W. Jensen, Proc. 50th Annual Meeting of Chemical Specialties Manufactures Association, pp. 33–35 (Dec. 9–12, 1963).

Transequatorial reception of a very-low-frequency transmission, C. J. Chilton, A. Diede, and S. Radicells, J. Geophys Res. **69,** No. 7, 1319–1328 (Apr. 1, 1964).

Tomorrow's facilities for standards and measurement, H. F. Wollin, Scale J. **50,** No. 6, 2 (Mar. 1964).

Review of recent developments of high temperature thermocouples, P. D. Freeze, Am. Soc. Mech. Engrs., Paper No. 63–Wa, 212, 16 (Nov. 1963).

Effects of magnetic disturbance as noted on oblique incidence ionograms, V. Agy and K. Davies, AGARDograph **59,** The effect of disturbances of solar origin on communications, Ed. G. J. Gassmann, pp. 167–176 (Pergamon Pres, Inc., London, England, 1963).

Editorial, R. W. Beatty, IEEE Trans. Microwave Theory Tech. **MTT–12,** No. 3, 274 (May 1964).

Comparison calibration of inductive voltage dividers, R. V. Lisle and T. L. Zapf, ISA 1963 Proc. Paper 7.1.63 (1963).

Correction to a method for measuring the directivity of directional couplers, G. E. Schafer and R. W. Beatty, IEEE Trans. Microwave Theory Tech. **MTT–12,** No. 3, 361 (May 1964).

Ionospheric absorption in conjugate regions and possible oscillation of the ionosphere, H. J. A. Chivers, and J. K. Hargreaves, Nature **202,** 891–893 (May 30, 1964).

Inline waveguide attenuator, W. Larson, IEEE Trans. Microwave Theory Tech. Corres. Sec. **MTT–12,** No. 3, 367–368 (May 1964).

Infrared spectroscopy of weak charge-transfer absorption spectra of NO in Kr and CH_3OH solutions, E. E. Ferguson and H. P. Broida, J. Chem. Phys. **40,** 3715 (1964).

Index to Journal of Association for Computing Machines, W. W. Youden, J. Assoc. Comp. Mach. **10,** No. 4, 583–646 (Oct. 1963).

Improved transducer for external recording of arterial pulse waves, M. Davis, B. Gilmore, and E. Freis, IEEE Trans. Bio-Med. Elec. **BME–10,** No. 4, 173–175 (Oct. 1963).

Physical properties of cements, based on zinc oxide hydrogenated rosin, *o*-ethoxybenzoic acid and eugenol, S. Civijan and G. M. Brauer, J. Dental Res. **43,** No. 2, 281–299 (Mar.–Apr. 1964).

A study of geomagnetic effects associated with auroral zone electron precipitation observed by balloons, W. H. Campbell, J. Geomagnetism and Geoelectricity **11,** No. 1, 37–57 (June 1964).

On the constitution of the topside ionosphere, R. W. Knecht, H. Rishbeth, and T. E. VanZandt, (Proc. of NATO Advanced Study Inst., April 17–26, 1963, Skeikampen, Norway), Book Electron Density Distribution in Ionosphere and Exoshere, pp. 348–350 (North Holland Publ. Co., Amsterdam, The Netherlands, 1964).

On a problem of G. Sansone, M. Newman, Ann. Mat. **LXV,** 27–34 (1964).

A time-varying model of the ionospheric *F2* layer, H. Rishbeth, J. Atmospheric Terrest. Phys. **26,** No. 6, 657–685 (June 1964).

The anomaly in the response of semiconductor detectors at low temperatures, W. R. Dodge, S. Domen, D. Hopper, and A. Hirshfeld, IEEE Trans. Nucl. Sci. **NS–11,** 1–14, (June 1964).

A theoretical study of the Martian ionosphere, R. B. Norton, Book, Advances in the Astronautical Science Exploration of Mars **15,** 533–542 (Western Periodicals, California, 1963).

A new high voltage calibration facility at the National Bureau of Standards, Boulder, W. W. Scott, ISA 1963 Proc. Paper No. 7.2.63 (1963).

A low input VSWR coaxial diode switch for the UHF band, W. L. Ecklund, IEEE Trans. Microwave Theory Tech. Corres. Sec. **MTT–12,** No. 3, 359 (May 1964).

Suggested practices for establishing sampling and sample preparation techniques in spectrochemical analysis, R. E. Michaelis, Book, Methods for Emission of Spectrochemical Analysis, 4th Edition, pp. 256–259 (American Society for Testing Materials, Phila., Pa., Feb. 1964).

S-wave hyperon-nucleon interactions and SU_3 symmetry, P. D. DeSouza, G. A. Snow, and S. Meshkov, Phys. Rev. **135,** p. 565 (1964).

Synthesis of higher ketoses by aldol reactions, II. Unsubstituted heptuloses, R. Schaffer, J. Org. Chem. **29,** 1471–1475 (June 1964).

Excess entropy at glass transformation, A. B. Bestul and S. S. Chang. J. Chem. Phys. **40,** 3731 (1964).

The large 50 Mc/s dipole array at Jicamarca Radio Observatory, G. R. Ochs, Digest of the 1963 IEEE Professional Groupon Antennas and Propagation p. 237 (July 1963).

The ionosphere and radio propagation in the lower frequencies (a report of an AGU session by the same title) T. N. Gautier, Science **143,** No. 3611, 1197–1199 (Mar. 13, 1964).

Numerical analysis of the thermal environment of occupied underground spaces with finite cover using a digital computer, T. Kusuda and P. R. Achenbach, ASHRAE Trans. **6,** No. 6, 99–105 (June 1964).

A diffusive model for the initial phase of a solar proton event, G. C. Reid, J. Geophys. Res. **69,** 2659–2667 (June 1964).

Emission spectrometry, B. F. Scribner and M. Margoshes, Anal. Chem. **36,** No. 5, 329–343R (1964).

Elementary derivation of time-correlation formulas for transport coefficients, R. Zwanzig, J. Chem. Phys. **40,** No. 9, 2527–2533 (May 1964).

A complete description of the normal subgroups of genus one of the modular group, M. Newman, Am. J. Math, **86,** 17–24 (1964).

Abbreviated Calendar record, January–February 1964, A. H. Shapley, IQSY Notes **7,** 19–25 (May 1964).

Evidence for a cooperative intramolecular transition in poly-L-proline, F. Gornick, L. Mandelkern, A. F. Diorio, and D. E. Roberts, Am. Chem. Soc. **86,** No. 13, 2549–2555 (July 1964).

The isomerization of D-manno-3-heptulose by alkali, R. Schaffer, J. Org. Chem. **29,** 1471–1475 (June 1964).

Insertion loss concepts, R.-W. Beatty, Proc. IEEE **52,** 663–671 (June 1964).

Reaction rates for the formation of He_2+ and Ne_2+, E. C. Beaty and P. L. Patterson, Book, Comptes Rendus de la VI^e Conference Internationale sur les Phenomenes D'Ionisation dans les Gaz, Ed. P. Hubert and E. Cremieu-Alcan III, pp. 289–293 (S.E.R.M.A. Publ. Co., Paris, France, 1963).

Ranking laboratories and evaluating methods of measurement in round-robin tests, T. W. Lashof, Mater. Res. Std. **4,** No. 8, 397–407 (Aug. 1964).

Projection X-ray microscopy of roofing materials, S. B. Newman and S. H. Greenfeld, Mater. Res. Std. **3,** No. 11, 893–898 (Nov. 1963).

Polarography as an analytical tool, J. K. Taylor, J. Assoc. Offic. Agri. Chem. **47,** No. 1, 21–27 (Jan. 1964).

Polar-cap absorption, D. K. Dailey, Planetary Space Sci. **12,** 495–541 (May 1964).

Polymorphism in isopropyl alcohol, G. S. Ross, H. L. Dixon, L. Frolen, and D. J. Termini, Science **141,** No. 3585, 1043–1044 (Sept. 1963).

Changes in relation between refractive index and Young's modulus as the result of successive heat treatment, E. H. Hamilton, J. Am. Ceram. Soc. **47,** No. 4, 167–170 (Apr. 1964).

Characteristics of programs for KWIC and other computer-produced indexes, W. W. Youden, (Proc. American Documentation Institute Annual Meeting, Oct. 1963) Book, Automation & Scientific Communication, pp. 331–332 (H. T. Luhn, Am. Documentation Inst., 1963).

Plastics, G. M. Klein, The 1964 Americana Annual, p. 532 (Americana Corp., Chicago, Ill., 1964).

Oxygen atom reactions with condensed olefins, M. D. Scheer and R. Klein, Science **144,** No. 3623, 1214 (Apr. 1964).

Bound states in a Debye-Hueckel potential, C. R. Smith, Phys. Rev. **134,** A1235–A1237 (June 1964).

The units and standards of electrical measure, F. K. Harris, Electron World **72,** No. 2, 29–32 (Aug. 1964.)

Tetragonal phases of the general type $10M_2O_5{\cdot}90M_2O_5$ apparently isostructural with $Ta_2O_5{\cdot}2Nb_2O_5$, J. L. Waring and R. S. Roth, Acta Cryst. **17,** 455–456 (1964).

Ionizing radiation and constitution of the atmosphere, T. E. VanZandt, Proc. URSI XIVth General Assembly, Sept. 1963 Tokyo, Japan **XIII,** 158–164 (1964).

Interpretation of frequency shifts due to electron exchange collisions, P. L. Bender, Phys. Rev. **134,** No. 5A, A1174–A1180 (June 1, 1964).

International Geophysical Calendar for the years of the Quiet Sun 1964–1965, A. H. Shapley and J. V. Lincoln, J. Radio Res. Lab., Japan **10,** 185–192 (Mar. 1963); IUGG Chronicle **50,** 171–174 (July 1963); URSI Inform. Bull. **139,** 64–71 (July–Aug. 1963); IGY Bull. **74,** 15–18 (Aug. 1963); Weatherwise **16,** 160–161 (Aug. 1963); J. Geophys Res. **68,** 5318–5323 (Sept. 1963); Trans. Am. Geophys. Union **44,** 821–824 (Sept. 1963); J. Atmospheric Terrest. Phys. **26,** No. 1, 151–157 (Jan. 1964); Nature **201,** 11–13 (Jan. 4, 1964).

International Geophysical calendar 1963, A. H. Shapley and J. V. Lincoln, IQSY Notes **4,** 34 (Sept. 1963).

Internal friction in rutile containing point defects, J. B. Wachtman, Jr., and L. R. Doyle, Phys. Rev. **135A,** 276, (1964).

Instant color correction, C. S. McCamy, Modern Photo. **28,** No. 1, 66–67 (Jan. 1964).

Review of static seals for cryogenic systems, R. F. Robbins and P. R. Ludtke, J. Spacecraft Rts **1,** No. 3, 253–259 (May–June 1964).

Resurgence of solar and geomagnetic activity in September and October 1963, A. H. Shapley, IQSY Notes **5,** 10, (Dec. 1963).

Dose fields from plane sources using point source data, J. H. Hubbell, Nucleonics **21,** No. 8, 144–148 (Aug. 1963).

Diurnal and seasonal variations of the atmosphere near the 100-kilometer level, J. W. Wright, J. Geophys. Res. **69,** 2851–2853 (June 1964).

D-region electron density profiles during auroras, G. M. Lerfald, C. G. Little, and R. Parthasarathy, J. Geophys. Res. **69,** 2857–2860 (June 1964).

Binary error probability due to an adaptable fading model, M. Nesenbergs, IEEE Trans. Comm. Systems **CS–12,** No. 1, 64–73 (Mar. 1964).

An X-ray determination of the Debye temperature of silver iodide, G. Burley, J. Phys. Chem. Solids **25,** 629 (1964).

HF propagation characteristics in equatorial latitudes, A. Barghausen, G. Jacobs, and D. Lillie, Program & Digest of IEEE Trans. Ant. Prop. Intern. Symp. July 9–11, 1963, Boulder, Colo., pp. 37–42 (IEEE, New York, N.Y. 1963).

Hall generators: what, why, and how much?, S. Rubin, 1964 IEEE Intern Convention Record, Part 8, p. 74 (Mar. 1964).

The half-life of carbon-14: Comments on the mass-spectrometric method E. E. Hughes and W. B. Mann, Intern. J. Appl. Rad. Isotopes **15,** No. 1, 97–100 (Jan. 1964).

A unitary symmetry selection rule and its application to new resonances, C. A. Levinson, H. J. Lipkin, and S. Meshkov, Il Nuovo Cimento **32,** Ser. X, 1376–1379 (1964).

A recalibration of the National Bureau of Standards tritiated water standards by gas counting, W. B. Mann, R. W. Medlock, and O. Yura, Intern. J. Appl. Rad. Isotopes **15,** No. 6, 351–361 (1964).

The guided propagation of ELF and VLF radio waves between the earth and the ionosphere, D. D. Crombie and A. G. Jean, Proc. URSI XIVth General Assembly, Sept, 1963, Tokyo, Japan XIII, 195–206 (1964).

Electronic scanning for large radiotelescopes, T. A. Clark, Digest of 1963 IEEE Professional Group on Antennas and Propagation, pp. 242–246 (July 1963).

The excitation of the 2P state of hydrogen by electrons of near-threshold energy, G. E. Chamberlain, S. J. Smith, and D. W. O. Heddle, Phys. Rev. Letters **12,** No. 23, 647–649 (June 8, 1964).

Theory of operation of the rotary positive displacement meter, C. T. Collett (Proc. 23d Annual Gas Measurement Short Course, Aug. 20, 1963), West Virginia Univ. Tech. Bull. **70,** 48–53 (1963).

The zeros of infrapolynomials with prescribed values at given points, J. L. Walsh and O. Shisha, J. Math. Anal. Appl. **7,** No. 2, 176–182 (Oct. 1963).

The establishment and maintenance of the unit of voltage at the NBS Boulder Laboratories, B. A. Wickoff, ISA 1963 Proc. Paper No. 28.2.63 (1963).

On the production of the $Z^-(\Omega^-)$ Baryon, H. J. Lipkin, C. A. Levinson, and S. Meshkov, Phys. Letters **7,** No. 2, 159–161 (Nov. 1, 1963).

On the implication of diurnal, seasonal and geographical variations in composition of the high atmosphere from *F*-region measurements, J. W. Wright, J. Geophys. Res. **68,** No. 19, 5413–1520 (Oct. 1, 1963); Book, Electron Density Distribution in Ionosphere and Exosphere (Proc. of NATO Advances Study Institute, April 17–26, Sheikampen, Norway), pp. 105–115 (North Holland Publ. Co., Amsterdam, The Netherlands, 1963).

On the effect of heterogeneity in molecular weight on the sedimentation equilibrium second virial coefficient of polymers

in good solvents, I. H. Billick, J. Phys. Chem. **68,** No. 7, 1798–1800 (July 1964).

A symmetry group containing both the Lorentz group and SU_3, A. O. Brant, Il Nuovo Cimento **32,** 234–236 (Apr. 1964).

Four-point probe measurement of non-uniformities in semiconductor sheet resistivity, L. H. Swartzendruber, Solid State Electronics **7,** 413–422 (1964).

The use of dual-polarized broad beam antennas to determine the extraterrestrial intensity of the cosmic radio noise at high frequencies, C. G. Little, G. M. Lerfald, and R. Parthasarathy, Digest of the 1963 IRE Professional Group on Antennas and Proagation, pp. 9–15 (July 1963).

The solid state of rare gases, G. L. Pollack, Rev. Mod. Phys. **36,** No. 3, 748–792 (July 1964).

The present and future of astrophysics and its effects on industry in Colorado, L. M. Branscomb, Book, Colorado and the New Technological Revolution: Proceedings of the University-Industry Liaison Conference 1963, Ed. W. H. Miernyk, pp. 55–64 (Bureau of Economic Research, Institute of Behavioral Science, Univ. of Colorado, Boulder, 1964).

A simplified freezing point apparatus, G. S. Ross and A. R. Glasgow, Jr., Anal. Chem. **36,** No. 3, 700 (Mar. 1964).

Autoionization in helium using a synchrotron light source, R. P. Madden, and K. Codling Proc. VIth Intern'l Conf. of Ionization Phenomena in Gases, Paris, France 1963, V. **1,** 139–143 (1963).

Radiowave scattering in the ionosphere, K. L. Bowles, Book, Advances in Electrons and Electron Physics **19,** 55–176 (1964).

Radio, the ionosphere, and IQSY, R. W. Knecht, Proc. URSI XIVth General Assembly, Sept. 1963, Tokyo, Japan XIII, 169–180 (1964).

Pseudopentagonal twins in electrodeposited copper dendrites, F. Ogburn, B. Paretzkin, and H. S. Peiser, Acta Cryst. **17,** 774–775 (1964).

Conduction-cooled, concentric sphere glass trap, S. Ruthberg, J. Vacuum **14,** No. 1, 11 (Jan. 1964).

Conductance of potassium chloride in highly purified *n*-methylpropionamide from 20 to 40°, T. B. Hoover, J. Phys. Chem. **68,** No. 14, 876–879 (Apr. 1964).

Field measurements of air infiltration in ten electrically heated houses, C. W. Coblentz, and P. R. Achenbach, ASHRAE J. **5,** No. 7, 69 (July 1963).

Discrepancy in conversion of early melting-point temperatures, S. J. Schneider, J. Am. Ceram. Soc. **46,** No. 7, 354–355 (1963).

Relation of solar active regions at central meridian passage to ionospheric disturbance, C. S. Warwick and J. V. Lincoln, AGARDograph **59,** The Effect of Disturbances of Solar Origin on Communications, Ed. G. J. Gassmann, pp. 229–233 (Pergamon Press Inc., London, England, 1963).

Report of committee E-2 on emission spectroscopy, R. E. Michaelis, Am. Soc. Testing Mater. Proc. **63,** 456 (1963).

The relationship between intensity of carbon arc and asphalt oxidation, J. R. Wright, P. G. Campbell, and T. L. Fridinger, ASTM Spec. Tech. Publ. No. 347, pp. 3–20 (May 1964).

Evidence for field-aligned ionization irregularities between 400 and 1000 km above the earth surface, T. E. VanZandt, W. Calvert, R. W. Knecht, and G. B. Goe, Book, Space Research, Ed. W. Priester, III, 271–273 (North Holland Publ. Co., Amsterdam, The Netherlands, 1963).

Experimental predictions from unitary symmetry (SU_3), C. A. Levinson, H. V. Lipkin, and S. Meshkev, (Proc. 1963 Intern. Conf. Nucleon Structure, Stanford Univ., Calif.), Book, Nucleon Structure, p. 309 (University Press, Stanford, Calif., Aug. 1963).

Summary of symposium on recent research on bituminous materials, S. H. Greenfeld, ASTM Spec. Tech. Publ. No. 347, pp. 108–111 (May 1964).

First results in NASA topside sounder satellite, R. W. Knecht, S. Russell, and J. E. Jackson, Book, Advances in Astronautical Sciences **11,** 61–85 (Western Periodicals Co., Calif., 1963).

Reaction rates for the formation of He_2^+ and N_e^+, E. C. Beaty and P. L. Patterson, Book, Comptes Rendus de la VI^e Conf. Intern. sur les Phenomenes d'Ionisation dans les Gaz, Ed. P. Hubert and E. Cremieu-Alcan III, pp. 289–293 (S.E.R.M.A. Publ. Co., Paris, France, 1963).

Comparisons of experimental reaction cross sections with various relations obtained from SU_3, S. Meshkob, Proc. Conf. Symmetry Principles at High Energy, Coral Gables, Fla., Jan. 1964, pp. 104–126 (1964).

Very-low-frequency radio waves and the ionosphere, D. D. Crombie, Science **142,** No. 3591, 508–510 (Oct. 25, 1963).

Standardization of dimensions of packages for self-service selling, A. T. McPherson and A. S. Best, THE PACKET, Packaging Professional **2,** No. 3, 4–5 (Packaging Inst., 1964).

Response characteristics of a 4π neutron detector, H. Gerstenberg, Bull. Am. Phys. Soc. **9,** Pt. 2, 421 (Apr. 28, 1964).

Geomagnetic and solar data, J. V. Lincoln, J. Geophys. Res. **69,** No. 13, 2841 (July 1, 1964).

Spectroscopic investigations of fluorescence and chemiluminescence in gases, (collection of papers), T. Carrington, Aero-Space Research Laboratory Report No. 64–51 (Mar. 1964).

Fractionation of uranium isotopes and daughter products in weathered granite and uranium-bearing-sandstone, Wind River basin region, Wyoming, J. N. Rosholt, E. L. Garner, and W. R. Shields, U.S. Geol. Surv. Prof. Paper 501-B, pp. 884–887 (1964).

Some results of a new method for obtaining ionospheric N(h) profiles with a bearing on the structure of the lower *F* region, J. W. Wright and A. K. Paul, J. Geophys. Res. **68,** No. 19, 5413–5420 (Oct. 1, 1963); Proc. NATA Advanced Study Institute, Skeikampen, Norway, (Apr. 17–26, 1963), Book, Electron Density Distribution in the Ionosphere and Exosphere, pp. 105–115 (North Holland Publ. Co., Amsterdam, The Netherlands, 1963).

Error analysis of Miller's recurrence algorithm, R. W. J. Olver, Math. Comp. **18,** No. 85, 65–74 (Jan. 1964).

Sr^{87}/Sr^{86} ratios in Hawaiian lavas, P. Lessing and E. J. Catanzaro, J. Geophys. Res. **69,** No. 8, 1599–1601 (Apr. 15, 1964).

The spheroidal method for satellite orbits, J. P. Vinti, Proc. Intern. Symp. Use of Artificial Satellites for Geodesy, pp. 12–16 (North Holland Publ. Co., Amsterdam, The Netherlands, 1963).

Opening angles of electron-positron pairs, H. Olsen, Phys. Rev. **131,** No. 1, 406–415 (July 1, 1963).

Some impulse sparkover voltages for a 200 cm sphere gap, H. N. Cones, IEEE Component Parts Conf. Paper No. CP 63–929 (June 1963).

Determination of optical thickness gradients from a far distance, J. R. Meyer-Arendt, R. B. Herrick and C. B. Emmanuel, J. Opt. Soc. Am. **53,** 1344 (1963).

Solar particles and interplanetary fields, C. S. Warwick, Book, Advances in the Astronautical Sciences **13,** 666–681 (Western Periodicals, Calif., 1963).

Vaporization of uranium monophosphide, K. A. Gingerick, P. K. Lee, and J. E. Efimenko, Nature **200,** No. 4908, 774–776 (1963).

A radio-meteorological study, B. R. Bean, E. J. Dutton, V. R. Frank, J. A. Lane, and W. B. Sweezy, Program and Digest 1963 IEE Prof. Group Antennas and Propagation Symp. Space Telecommunications, July 9–11, 1963, Boulder, Colo., pp. 56–60 (1963).

The interaction of 350 keV polarized neutrons with oriented Ho^{165} nuclei, H. Marshak, R. Wagner, P. P. Miller, and T. Tamura, Physics Letters **10,** No. 3, 316 (June 15, 1964).

Systematic atmospheric refraction errors of baseline type radio tracking systems and methods of their correction, G. D. Thayer and B. R. Bean, Proc. First Space Congress, Cocoa Beach, Florida (Apr. 1964).

Error bounds for asymptotic expansions in turning-point problems, F. W. J. Oliver, Soc. Ind. Appl. Math. **1,** No. 1, 200–214 (Mar. 1964).

Summary of session I and II of the symposium on X-ray and electron probe analysis, R. E. Michaelis, ASTM Spec. Tech. Publ. No. 349 (Dec. 1963).

Prebunching in electron linacs, J. E. Leiss, Proc. Conf. Proton Linear Accelerators, Yale Univ., New Haven, Conn., pp. 267–273 (Oct. 1963).

Report on standard samples, reference samples and high-purity material for spectrochemical analysis, R. E. Michaelis, ASTM Spec. Tech. Publ. No. 58–E (1963).

Phase diagrams for ceramists, Book, E. M. Levin, C. R. Robbins, and H. F. McMurdie, American Ceramic Society Inc., Columbus, Ohio (1964).

Transverse propagation of electromagnetic waves in a cylindrically stratified plasma, J. R. Wait, Proc. Radio Physics Symp., University of California, Los Angeles, Aug. 7–9, 1963, Ed. J. Brandstatter (Holden-Day, Inc., San Francisco, Calif., 1964).

Variations in phase path of man-made one-hop whistler mode signals at 18.6 kilocycles per second, D. D. Crombie, F. A. McNeill, and G. M. Allcock, J. Geophys. Res. **68,** No. 23, 6229–6325 (Dec. 1, 1963).

Fluorometric demonstration of tryptophan in dentin and bone protein, K. C. Hoerman and S. A. Mancewicz, J. Dental Res. **43,** No. 2, 276–280 (Mar.-Apr. 1964).

The calibration of inductive voltage dividers and analysis of their operational characteristics, T. L. Zapf, ISA Trans. **2,** No. 3, 195–200 (July 1963).

Nighttime variations of *F*-region electron density profiles at Puerto Rico, T. Shimazaki, J. Geophys. Res. **69,** No. 13, 2781–2797 (July 1, 1964).

Obscurities of oscillator noise, L. Fey, W. R. Atkinson, and J. Newman, Proc. IEEE Letter **52,** 104–105 (Jan. 1964).

Standard electromotive force of the hydrogen-silver chloride cell and the thermodynamics of solutions of hydrochloric acid in 50 wt. % methanol from 10 to 40°C, M. Paabo, R. A. Robinson, and R. G. Bates, J. Chem. Eng. Data **9** No. 3, 374 –6 (July 1964).

The *F*-region : asonal anomaly, J. W. Wright, J. Geophys. Res. **68**, No. 14, 4379–4381 (July 15, 1963).

Coherent Raman effect in the off-axis Raman resonator, H. Takuma and D. A. Jennings, Appl. Phys. Letters **4,** No. 11, 185–186 (June 1964).

Effects of composition and irradiation on the glass transition temperature of methyl methacrylate-styrene copolymers, M. S. Parker, V. J. Krasnansky, and B. G. Acchammer, J. Appl. Polymer Sci. **8,** 1825–1838 (1964).

The scope of electrochemistry, W. J. Hamer, J. Electrochem. Soc. **110,** No. 6, 115C (June 1963).

Report on sugars and sugar products, E. J. McDonalds, J. Assoc. Official Agri. Chem. **46,** 35 (1963).

Thermal conductivity and viscosity of simple fluids, J. V. Sengers, Am. Chem. Soc. **9,** No. 4, C-57-C-70 (Sept. 1964).

Some recent developments in mobile metal thermocouples. L. O. Olsen, Am. Soc. Auto. Engrs. Paper No. 750A, p. 10 (Sept. 1963).

Gallium-palladium alloys as dental filling material, R. M. Waterstrat and R. W. Longton, Public Health Rept. **79,** No. 7, pp. 638–642 (July 1964).

Minutes of the meeting at the Ohio State University, Columbus, Ohio, of the Triple Commission for Spectroscopy, June 13, 1963, C. E. Moore, J. Opt. Soc. Am. **54**, No. 3, 425–432 (Mar. 1964).

High frequency microvolt measurements, F. X. Ries, ISA Preprint, pp. 37.2.63–1—37.2.63–5 (Sept. 1963).

Comparison of a new SU_3 prediction with experiment, S. Meshkov, G. A. Snow, and G. B. Yodh, Phys. Rev. Letters **12,** No. 3, 87–92 (Jan. 20, 1964).

Measurement of photochemical degradation in certain plastics by color reactions with phenylenediamines, V. E. Gray and J. R. Wright, J. Appl. Polymer Sci. **8,** No. 4, 1505–1519 (1964).

On Rayleigh's non-linear vibration equation, A. Ghaffari, Proc. Intern. Symp. Non-Linear Vibration II, 130–133 (Sept. 1961).

An unmodulated twin channel microwave attenuation measurement system, D. H. Russell, ISA Preprint, pp. 37.3.63–1—37.3.63–17 (Sept. 1963).

Beam loading and beam blowup in electron linacs, J. E. Leiss, Proc. Conf. Proton Linear Accelerators, Yale Univ., New Haven, Conn., pp. 74–95 (Oct. 1963).

Residual range and range rate errors due to the troposphere, E. C. Barrows, Proc. Conf. Tropospheric Refraction (Dec. 1963).

Tropospheric refraction and attenuation of radio waves, B. R. Bean, Book, Advances of Radio Research, p. 53–155 (Academic Press Inc., New York, N.Y., June 1964).

Kikuchi pattern from a silicon wedge, H. A. Fowler, Acta Cryst. 17, No. 7, 869–871 (July 1964).

On line data handling system for the National Bureau of Standards LINAC, J. Leiss, J. Broberg, R. Schrack, and J. M. Wyckoff, IEEE Trans. Nuclear Sci. NS–11, No. 3, 331–337 (June 1964).

Long-term characteristic for air-ground propagation in band nine, R. S. Kirby, Program and Digest 1963 IEEE Prof. Group Antennas and Propagation Symp. Space Telecommunications, July 9–11, 1963, Boulder, Colo., p. 43–47 (1963).

Measurement of effective temperatures of microwave noise sources, J. S. Wells, W. C. Daywitt, and C. K. S. Miller, IEEE Trans. Instr. Meas. IM–13, No. 1, 17–28 (Mar. 1964).

The turbulent characteristics of the radio refractive index near the ground, B. R. Bean and R. E. McGavin, Program and Digest 1963 IEE Prof. Group Antennas and Propagation Symp. Space Telecommunications, July 9–11, 1963, Boulder, Colo., pp. 60–64 (1963).

Use of high-strength ceramics in vibration transducers, E. Jones, J. Acoust. Soc. **36,** No. 6, 1215–1216 (June 1964).

Phase instability in a tropospheric relay link, E. C. Barrows, Program and Digest 1963 IEEE Prof. Group. Antennas and Propagation Symp. Space Telecommunications, July 9–11, 1963, Boulder, Colo., pp. 52–55 (1963).

Analysis of rotation errors of a waveguide rotary-vane attenuator, W. Larson, IEEE Trans. Instr. Meas. **IM–12,** No. 2, 50–55 (Sept. 1963).

The radio thermal noise properties of the lower atmosphere, B. R. Bean, Program and Digest 1963 IEEE Prof. Group. Antennas and Propagation Symp. Space Telecommunications, July 9–11, 1963, Boulder, Colo., pp. 30–31 (1963).

**Publications for which a price is indicated are available by purchase from the Superintendent of Documents, U.S. Government Printing Office, Washington, D.C. 20402 (foreign postage, one-fourth additional). Reprints from outside journals and the NBS Journal of Research may often be obtained directly from the authors.*

UNIVERSITY MICROFILMS
313 NORTH FIRST STREET
ANN ARBOR, MICHIGAN
SJR-A-OCT

UNI
GOVERNMEN
DIVISION OF
WASHINGTON, D.
OFFICIAL BUSINESS

PENALTY FOR PRIVATE USE TO AVOID
PAYMENT OF POSTAGE, $300

JOURNAL OF RESEARCH of the National Bureau of Standards Vol. 69A, No. 1 January-February 1965
A. Physics and Chemistry

Contents

	Page
Heat of decomposition of sodium and potassium chlorate. Alexis A. Gilliland and Donald D. Wagman.	1
Application of precise heat-capacity data to the analysis of the temperature intervals of the NBS–1955 and the International Practical Temperature Scales in the region of 90 °K. George T. Furukawa and Martin L. Reilly.	5
Heat capacity and thermodynamic properties of beryllium aluminate (chrysoberyl), $BeO \cdot Al_2O_3$, from 16 to 380 °K. George T. Furukawa and William G. Saba.	13
Thermodynamics of the ternary system: water-sodium chloride-barium chloride at 25 °C. R. A. Robinson and V. E. Bower.	19
Compressibility of eleven inorganic materials. C. E. Weir.	29
Determination of the intermolecular entanglement coupling spacings in polyisoprene by viscosity measurements. Lewis J. Fetters.	33
Electrical conductivity of dilute solutions of "sea water" from 5 to 120 °C. Cyrus G. Malmberg.	39
Preparation of a carbonate-free complex calcium aluminate. H. A. Berman.	45
Synthesis and thermal stability of bis(8-hydroxyquinoline)-Schiff base coordination polymers. Emanuel Horowitz and Theodore P. Perros.	53
Atomic absorption spectrum of praseodymium (Pr I). Romuald Zalubas and Michael Wilson.	59
Publications of the National Bureau of Standards.	71

Library of Congress Catalog Card Number: 62–37039

For sale by the Superintendent of Documents, U.S. Government Printing Office, Washington, D.C., 20402. Price 70 cents (single copy). Subscription price $4 a year; 75 cents additional for foreign mailing.
UNITED STATES GOVERNMENT PRINTING OFFICE, WASHINGTON : 1965